# 机器学习在强子物理中的应用

Qian Wang (王倩)

qianwang@m.scnu.edu.cn

2025年强子物理与有效场论前沿讲习班

郑州大学 郑州 2025年8月17日-9月2日

# AI 百年发展

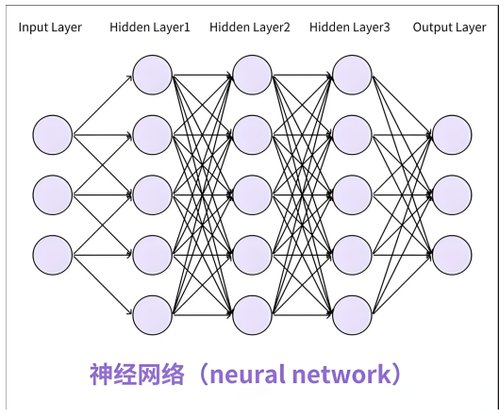

神经网络（neural network）

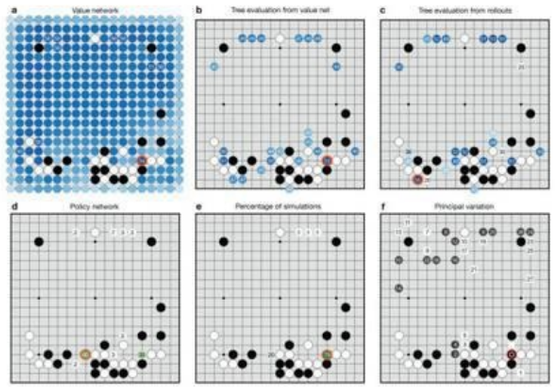

AlphaGo

科学大模型?

2022


人工智能大模型

ChatGPT 问世

AlphaGo 2018

围棋

2016 AlphaFold

蛋白质结构预测

1941-1974

早期人工智能

1980-1987

“专家系统”

2005-今

飞速发展

T1037 / 6vr4
90.7 GDT
(RNA polymerase domain)

T1049 / 6y4f
93.3 GDT
(adhesin tip)

AI 技术飞速发展，正在掀起一场新的科技革命

参考 段文辉 院士 2025年 彭桓武讲座 报告

# AI 分类与工作逻辑

## AI 分类

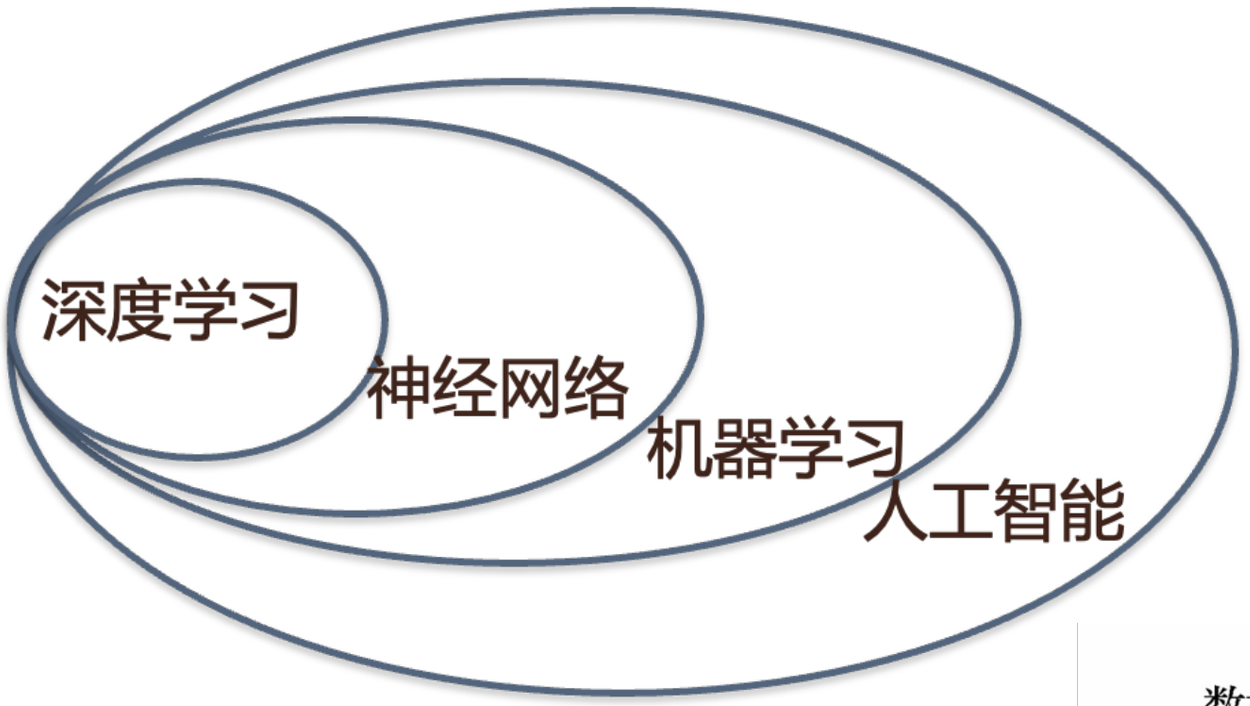


## AI 工作逻辑

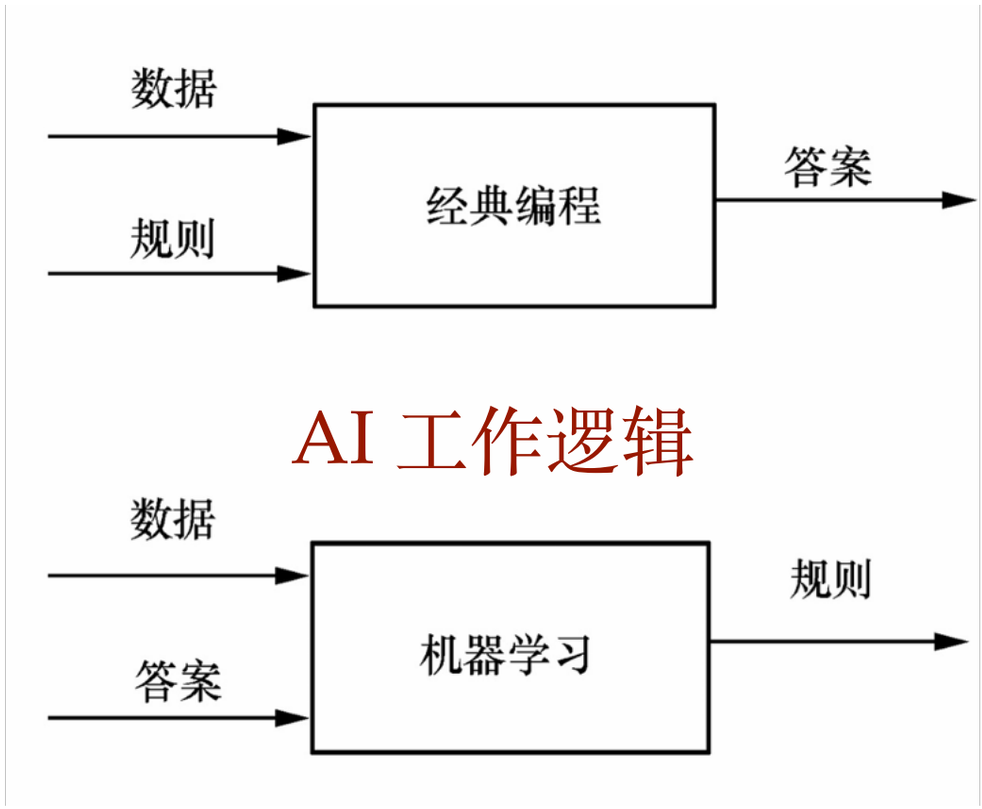

# 神经网络

- 基于近似定理，神经网络具有极强的表达能力

K. Hornik, et.al, Neural Networks 2 (1989)359

神经元

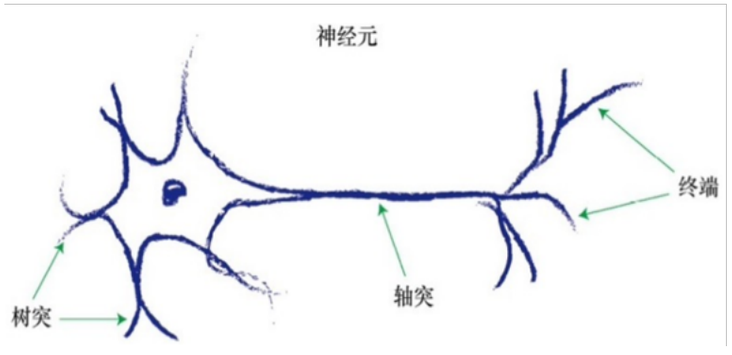


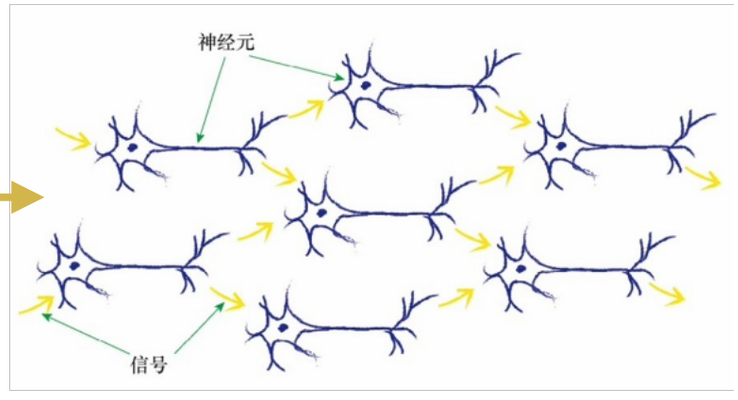


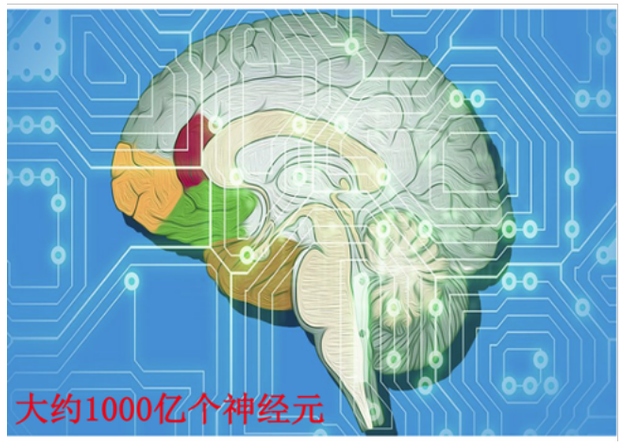


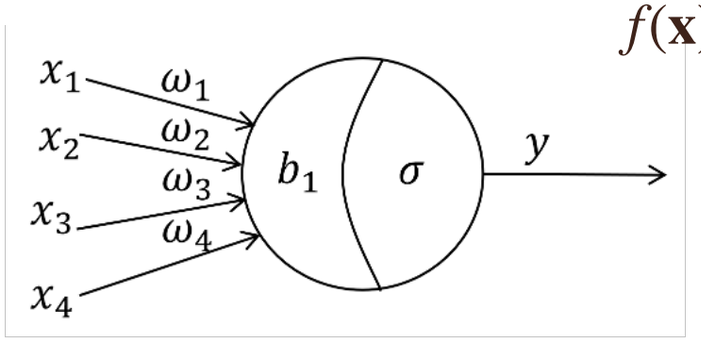


$$f(\mathbf{x}) \approx \sum_{i=1}^{N(e)} a_i \sigma\left(\mathbf{w}_i \cdot \mathbf{x} + b_i\right)$$

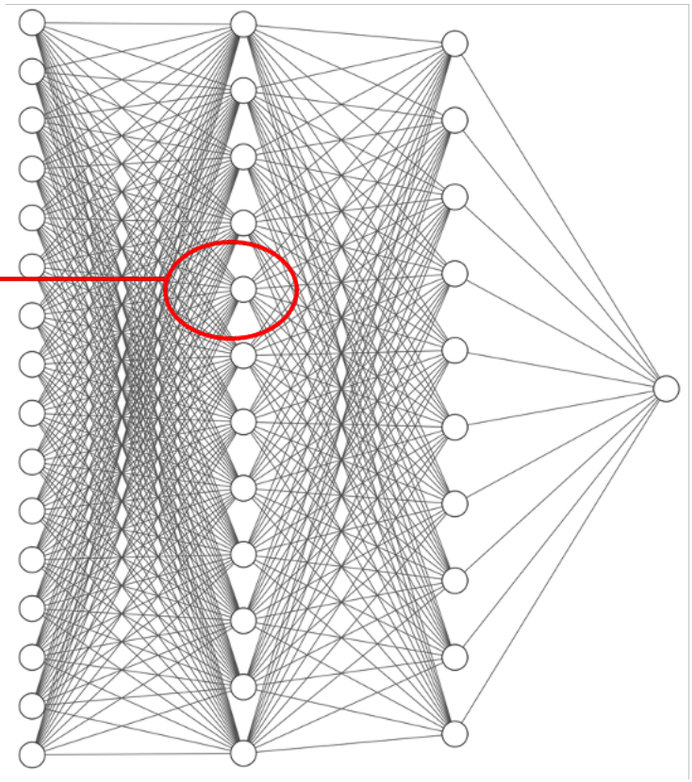

线性变换 + 非线性变换 ≈ 任意函数

输入层　隐藏层　输出层

# 激活函数

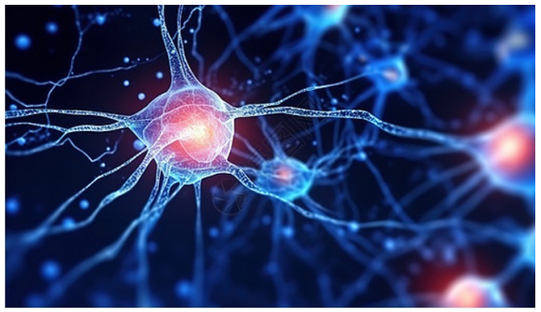

- 只有满足一定条件的信号才能传递到下一个神经元

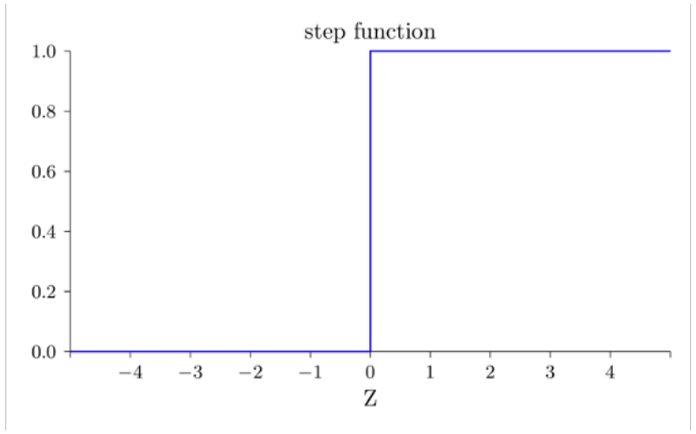


平滑后

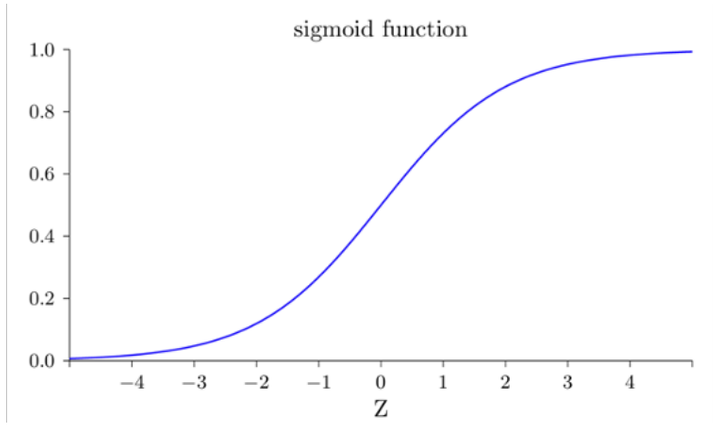


- 深度学习

ReLu function

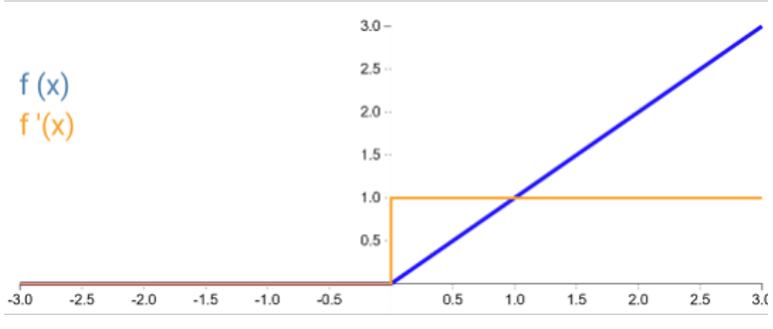


Leaky ReLu function

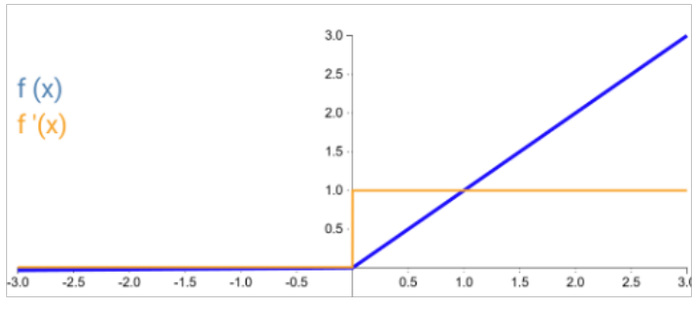


RReLu function

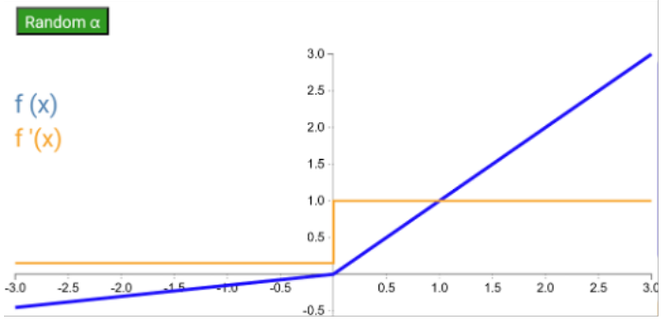


解决梯度消失的问题

# 损失函数

- 为了网络输出接近真实值，定义损失函数描述网络输出与真实值的差异

均方差损失函数（解决回归问题）

$$L(Y \mid f(x)) = \frac{1}{n}\sum_{i=1}^{N}\left(Y_i - f\left(x_i\right)\right)^2$$

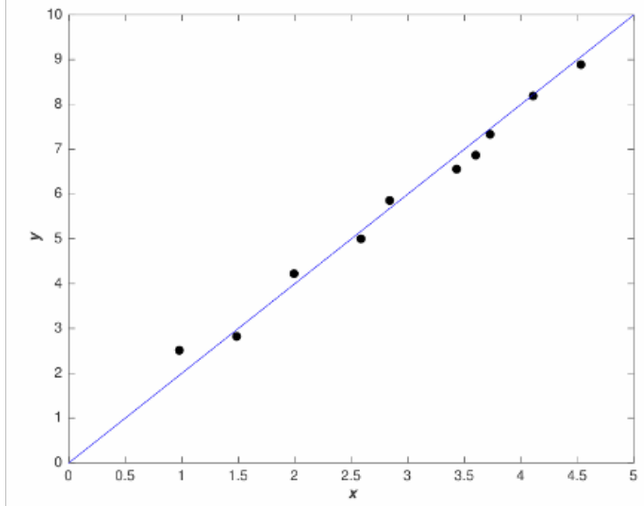


交叉熵损失函数（解决分类问题）

$$L(Y \mid f(x)) = \sum_{i=1}^{n} Y_i \times \log\left(\frac{Y_i}{f\left(x_i\right)}\right)$$

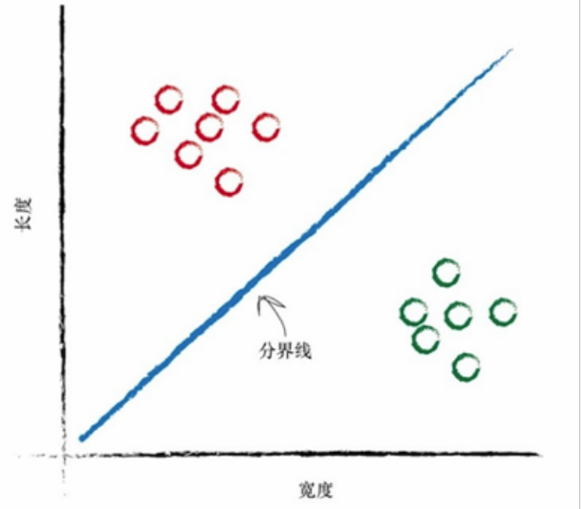

# 损失函数

- 损失函数的设置往往与待解决的问题直接相关，例如PINN物理信息神经网络，在解决偏微分问题时，将偏微分方程定义在损失函数中

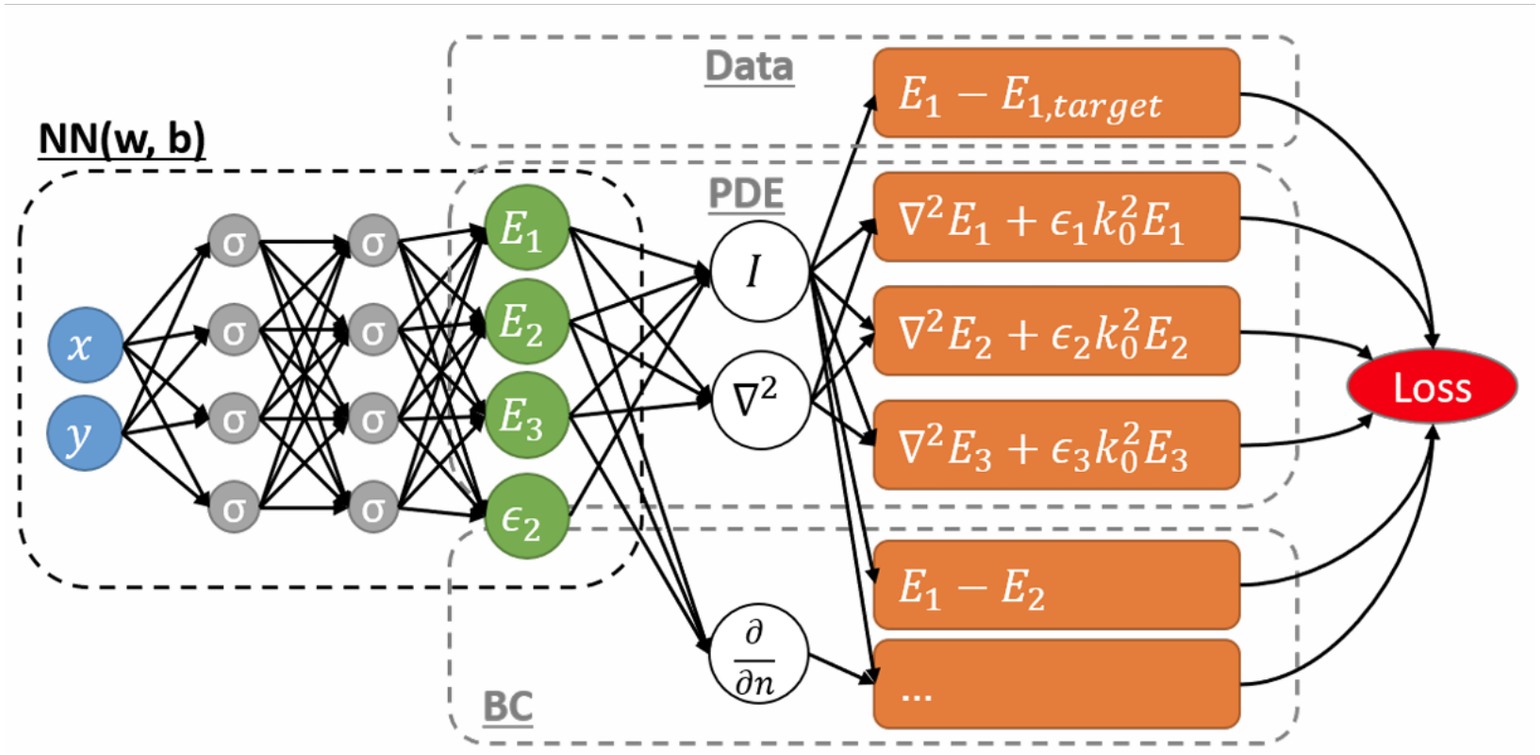

# 梯度下降

- 通过更新网络中的参数寻找损失函数的最小值

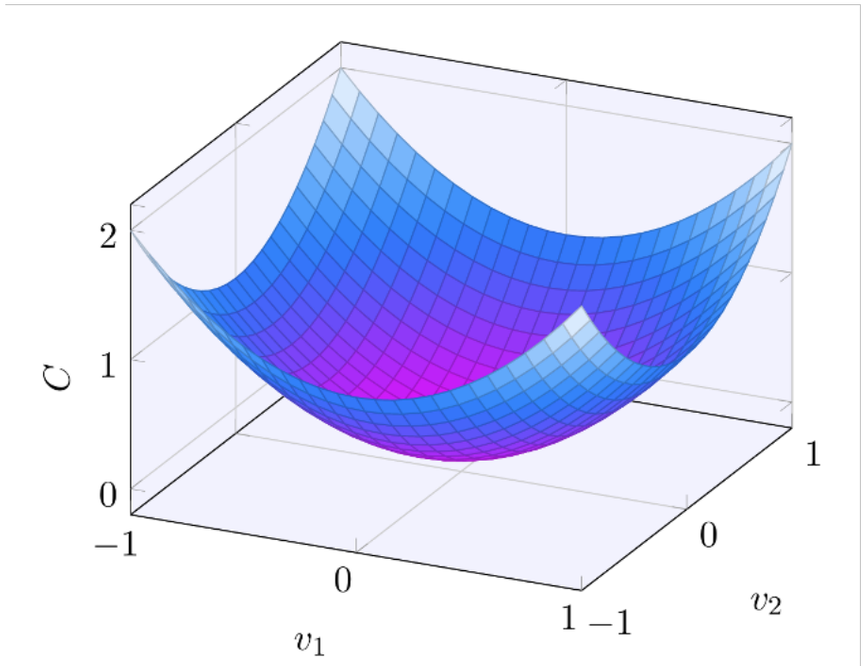


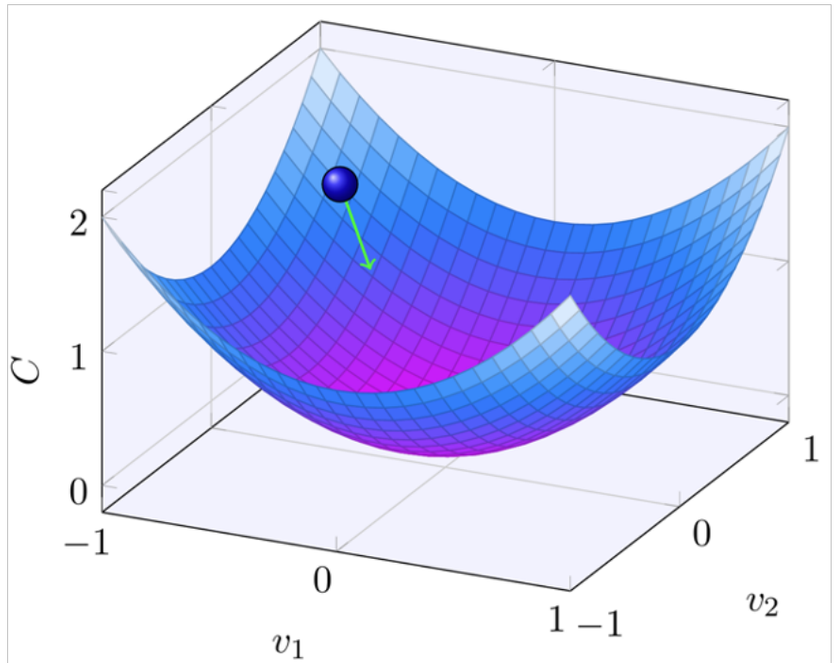


损失函数的导数可以揭示局部的形状，沿梯度的方向改变参数值，重复该过程，损失函数逐渐减小至最小值

$$\nabla C \equiv \left(\frac{\partial C}{\partial v_1}, \frac{\partial C}{\partial v_2}\right)^T \qquad v \to v' = v - \eta \nabla C$$

# 神经网络的正向和反向传播

- 正向传播，计算从输入层穿过隐藏层至输出层，得到神经网络输出结果。

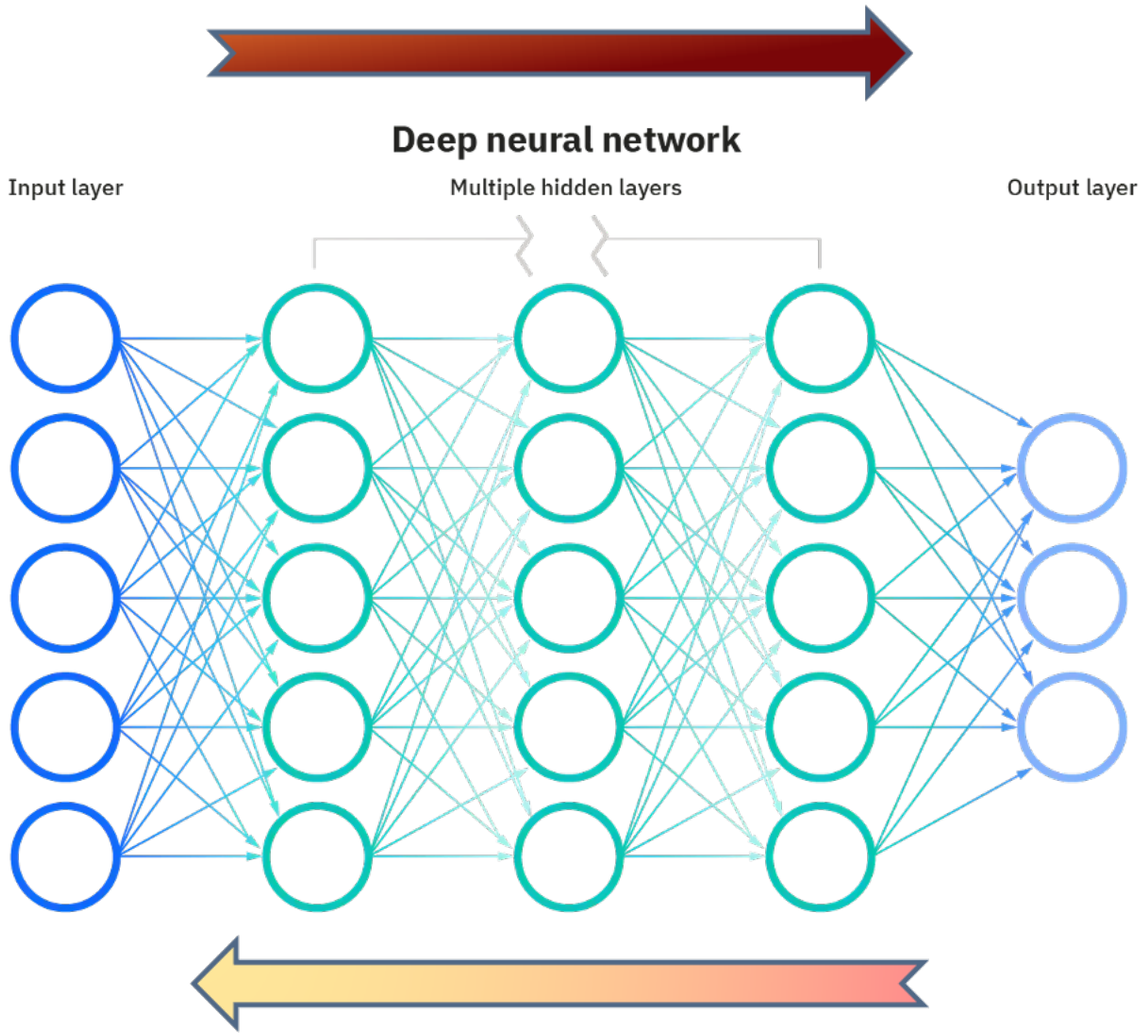


- 反向传播，计算从输出层穿过隐藏层至输入层，得到神经网络参数。

神经网络的训练就是正向传播和反向传播的循环

# 机器学习发展历史


图灵测试
多层感知器
卷积神经网络
1943
1950
1957
1969
1981
1986
1989
1995
2005
神经元模型
感知器
异或问题
反向传播算法
梯度问题
深度学习
Weights
Bias
Output
Inputs (outputs from previous layer)
Weighted sum
Activation function
AlexNet
残差神经网络
AlphaGo
2009
2012
2014
2015
2016
2019
2024
ImageNet
生成对抗网络
ChatGPT
诺贝尔物理学奖
IMAGENET
ChatGPT
THE NOBEL PRIZE IN PHYSICS 2024
John J. Hopfield
Geoffrey E. Hinton
"for foundational discoveries and inventions that enable machine learning with artificial neural networks"
THE ROYAL SWEDISH ACADEMY OF SCIENCES

# 机器学习发展历史

© Nobel Prize Outreach.
Photo: Nanaka Adachi

John J. Hopfield
Nobel Prize in Physics 2024

Born: 15 July 1933, Chicago, IL, USA

Affiliation at the time of the award: Princeton University, Princeton, NJ, USA

Prize motivation: “for foundational discoveries and inventions that enable machine learning with artificial neural networks”

Prize share: 1/2

## Work

When we talk about artificial intelligence, we often mean machine learning using artificial neural networks. This technology was originally inspired by the structure of the brain. In an artificial neural network, the brain’s neurons are represented by nodes that have different values. In 1982, John Hopfield invented a network that uses a method for saving and recreating patterns. He found inspiration in physics' models of how many small parts in a system affect the system as a whole. The invention became important in, for example, image analysis.

# 机器学习发展历史

1943

神经元

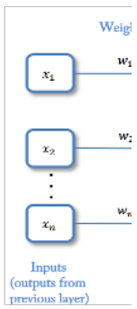


© Nobel Prize Outreach.
Photo: Clément Morin

Geoffrey Hinton
Nobel Prize in Physics 2024

Born: 6 December 1947, London, United Kingdom

Affiliation at the time of the award: University of Toronto, Toronto, Canada

Prize motivation: “for foundational discoveries and inventions that enable machine learning with artificial neural networks”

Prize share: 1/2

200

Image

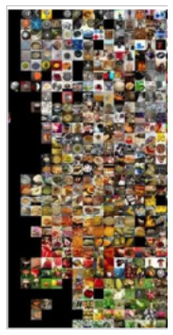

## Work

When we talk about artificial intelligence, we often mean machine learning using artificial neural networks. This technology was originally inspired by the structure of the brain. In an artificial neural network, the brain’s neurons are represented by nodes that have different values. In 1983–1985, Geoffrey Hinton used tools from statistical physics to create the Boltzmann machine, which can learn to recognise characteristic elements in a set of data. The invention became significant, for example, for classifying and creating images.

学奖

# 机器学习发展历史

- 卷积神经网络、残差网络、生成对抗网络的性能对比

| | CNN | ResNet | GAN |
|---|---|---|---|
| 特征提取能力 | ⭐⭐⭐⭐ (优秀局部特征提取) | ⭐⭐⭐⭐⭐ (深层全局特征) | ❌ (不直接用于特征提取) |
| 生成逼真数据 | ❌ | ❌ | ⭐⭐⭐⭐⭐ (图像/视频/音频生成) |
| 训练稳定性 | ⭐⭐⭐⭐ (20层内稳定) | ⭐⭐⭐⭐⭐ (千层可训) | ⭐⭐ (模式崩溃风险高) |
| 参数量效率 | ⭐⭐⭐ (VGG参数量大) | ⭐⭐⭐⭐ (残差结构减少冗余) | ⭐⭐ (双网络复杂度高) |

# 机器学习在物理中的应用

- 高能实验数据分析

- 基于无监督机器学习聚类算法检测反常信息 Ameli F., et al., arXiv:2104.11388v1
- 基于卷积神经网络去除背景噪声 Komiske, J. High Energy Phys. 12, 051.

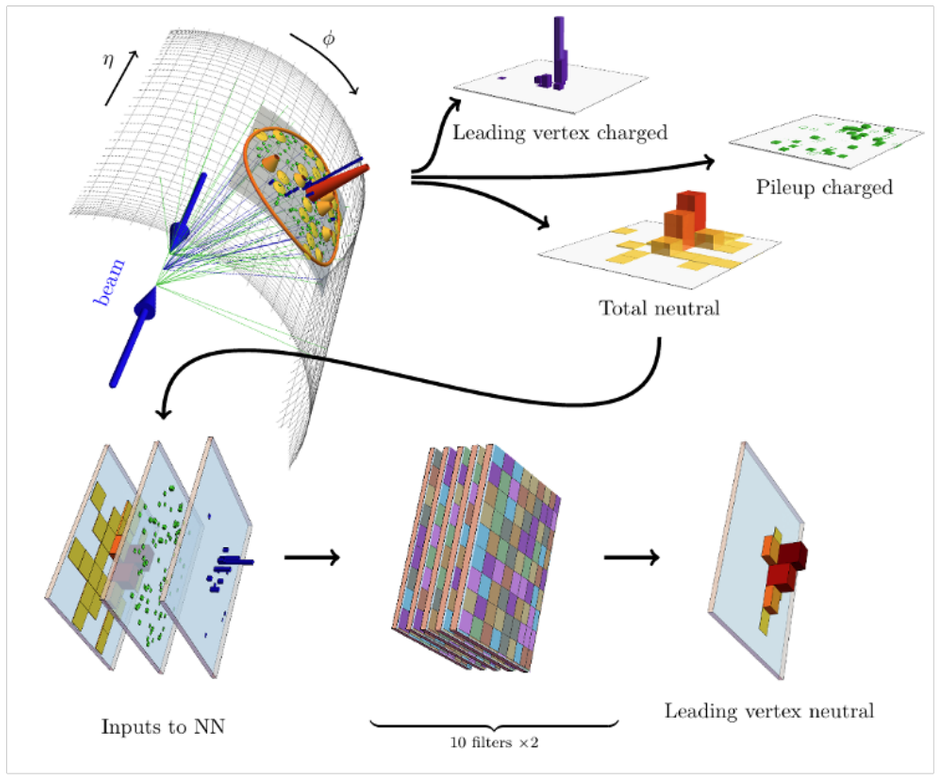


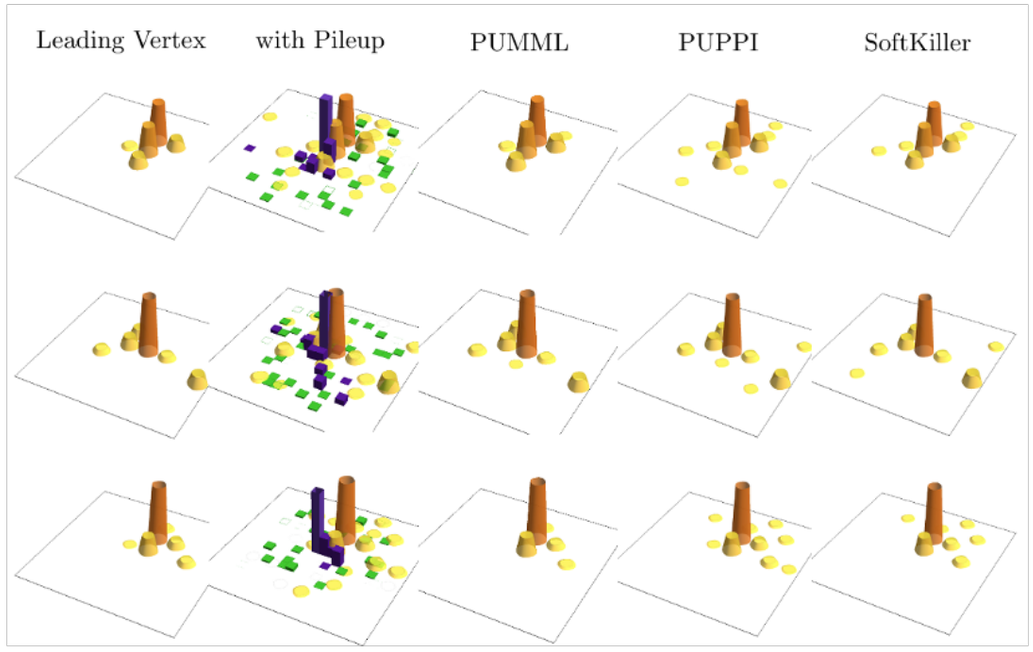


- 基于神经网络提高液体闪烁体探测器在事件位置和能量重建效率

Qian, Z., et al., Nucl. Instrum. Methods Phys. Res., Sect. A 1010, 165527.

# 机器学习在物理中的应用

- 量子多体系统

- 基于神经网络研究多体波函数

Carleo, Torcer, Science 355(2017)602-606

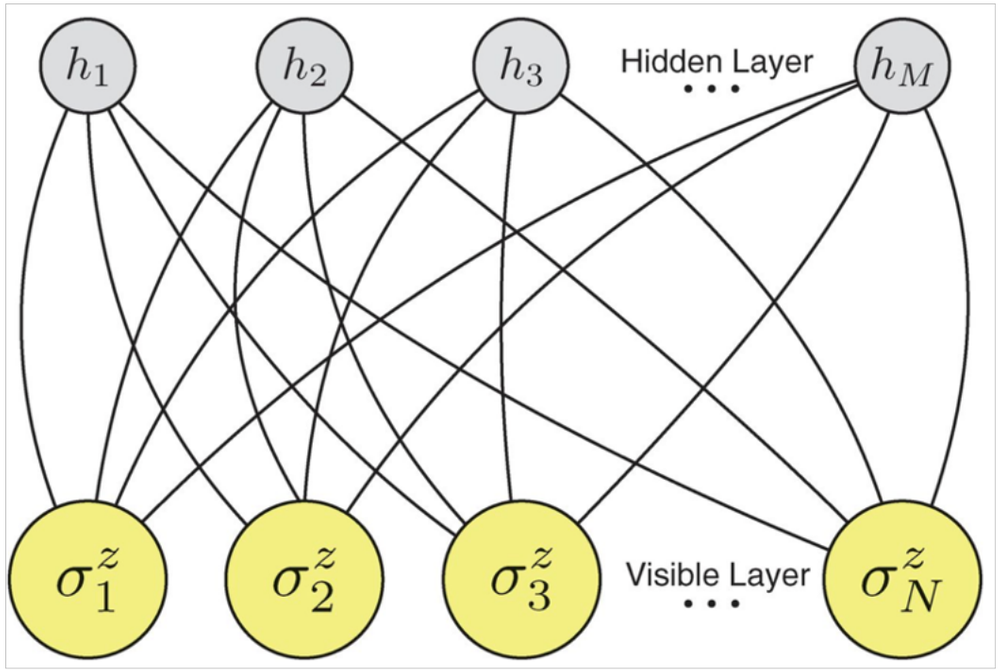


- 机器学习解决高维强关联问题

Orus, Annals Phys.349(2014)117-158

- 基于变分蒙特卡洛神经网络研究多体核子系统

Corey Adams, Phys.Rev.Lett. 127 (2021) 2, 022502

# 机器学习在物理中的应用

Corey Adams, Phys.Rev.Lett. 127 (2021) 2, 022502

- 基于变分蒙特卡洛神经网络研究多体核子系统

量子物理中多体问题主要的挑战源于难以描述多体波函数的复杂相关性。神经网络的复杂结构与高效计算效率在多体问题中可以发挥巨大优势。

系统哈密顿量及变分基态能量如下所示，

$$H_{\mathrm{LO}} = -\sum_i \frac{\vec{\nabla}_i^2}{2m_N} + \sum_{i<j}(C_1 + C_2\vec{\sigma}_i\cdot\vec{\sigma}_j)e^{-r_{ij}^2\Lambda^2/4} + D_0\sum_{i<j<k}\sum_{\mathrm{cyc}} e^{-(r_{ik}^2+r_{ij}^2)\Lambda^2/4},$$

$$\frac{\langle\Psi_V|H|\Psi_V\rangle}{\langle\Psi_V|\Psi_V\rangle} = E_V \geq E_0$$

神经网络表示多体波函数，

$$|\Psi_V^{\mathrm{ANN}}\rangle = e^{\mathcal{U}(\mathbf{r}_1,\ldots,\mathbf{r}_A)}\ \tanh[\mathcal{V}(\mathbf{s}_1,\mathbf{r}_1,\ldots,\mathbf{r}_A,\mathbf{s}_A)]|\Phi\rangle$$

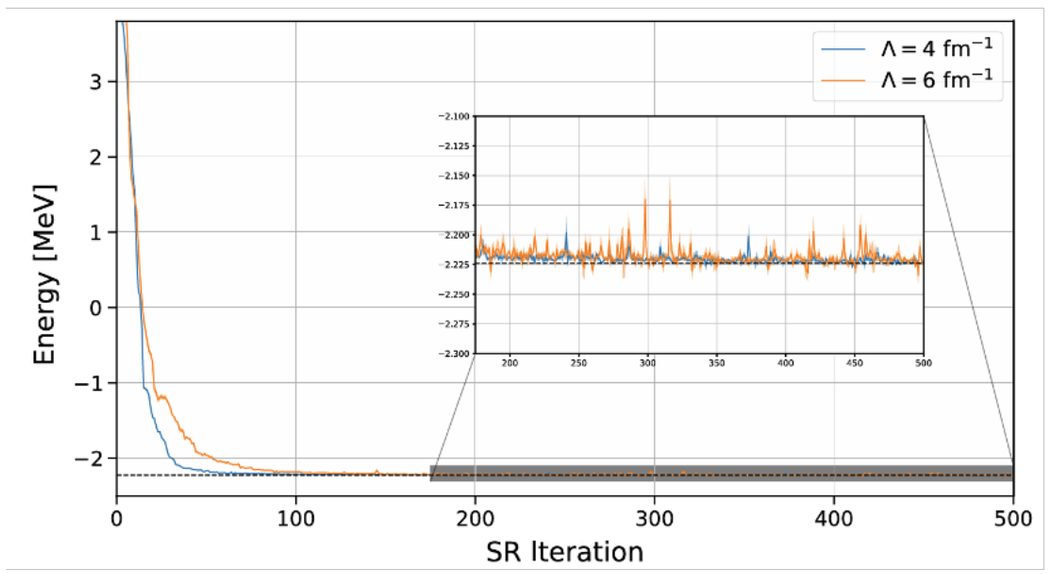


| | Λ | VMC-ANN | VMC-JS | GFMC |
|---|---|---|---|---|
| $^2$H | 4 fm$^{-1}$ | −2.224(1) | −2.223(1) | −2.224(1) |
| | 6 fm$^{-1}$ | −2.224(4) | −2.220(1) | −2.225(1) |
| $^3$H | 4 fm$^{-1}$ | −8.26(1) | −7.80(1) | −8.38(2) |
| | 6 fm$^{-1}$ | −8.27(1) | −7.74(1) | −8.38(2) |
| $^4$He | 4 fm$^{-1}$ | −23.30(2) | −22.54(1) | −23.62(3) |
| | 6 fm$^{-1}$ | −24.47(3) | −23.44(2) | −25.06(3) |

# 机器学习在物理中的应用

- 物理推导机器学习

发现物理规律（遗传算法）

Schmidt and Lipson, Science 324(2009)81-85

⇒ 基于遗传算法进行符号回归发现守恒律和对称性

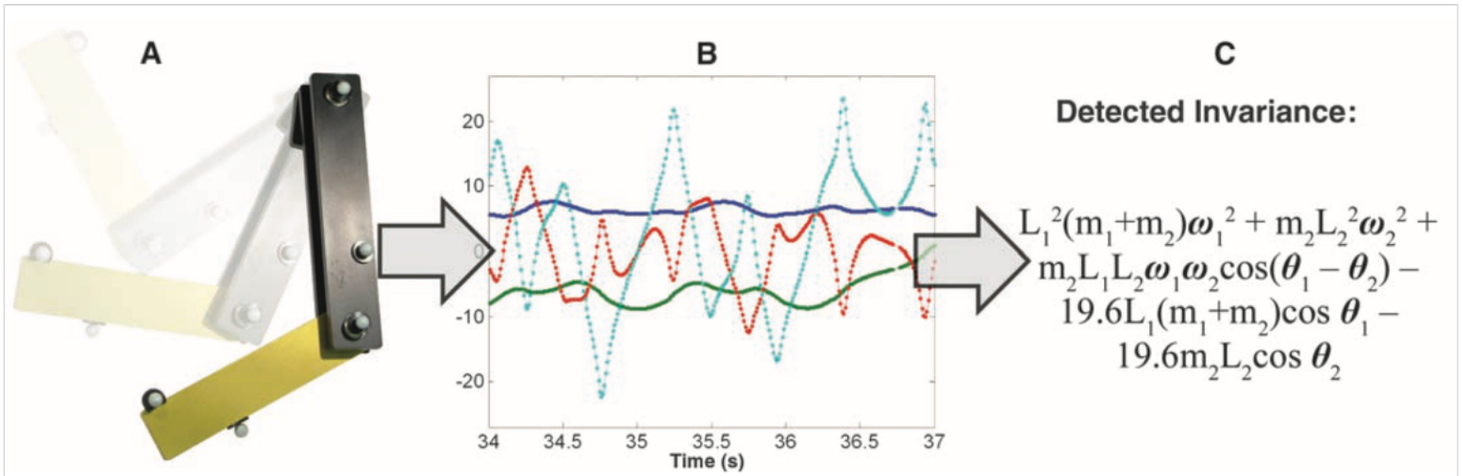


在没有任何物理学的先验知识的情况下，该算法发现了哈密顿量、拉格朗日量以及其他几何和动量守恒定律。

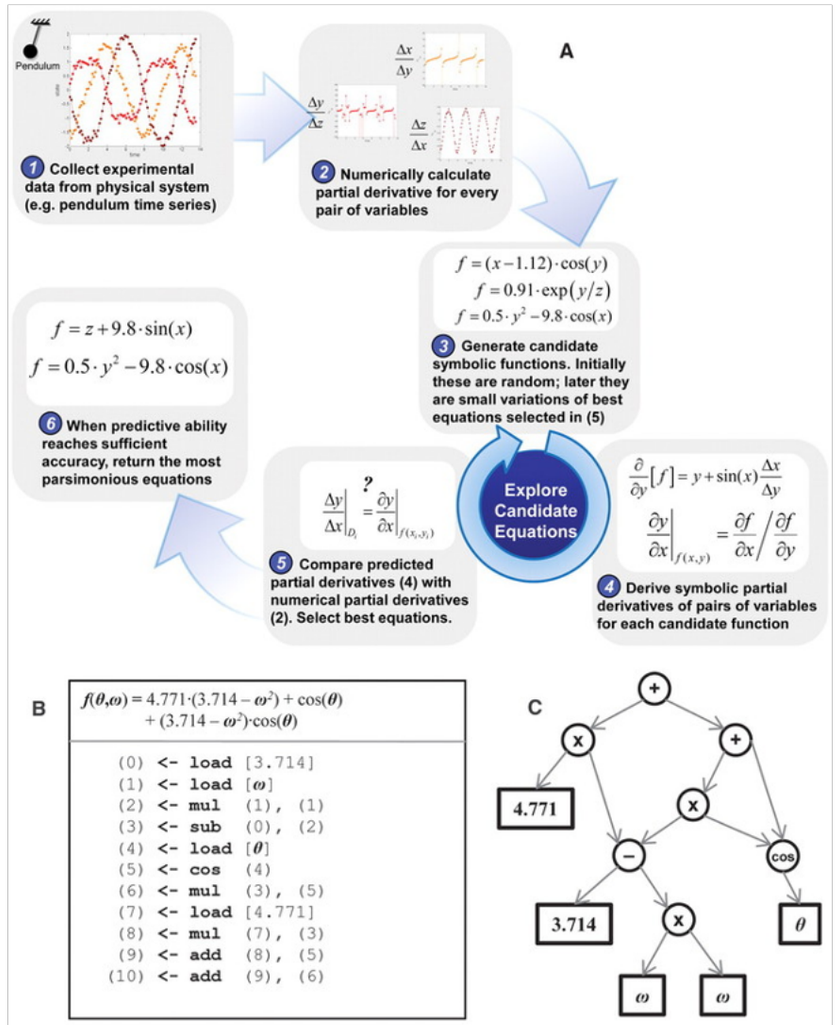

# 机器学习在物理中的应用

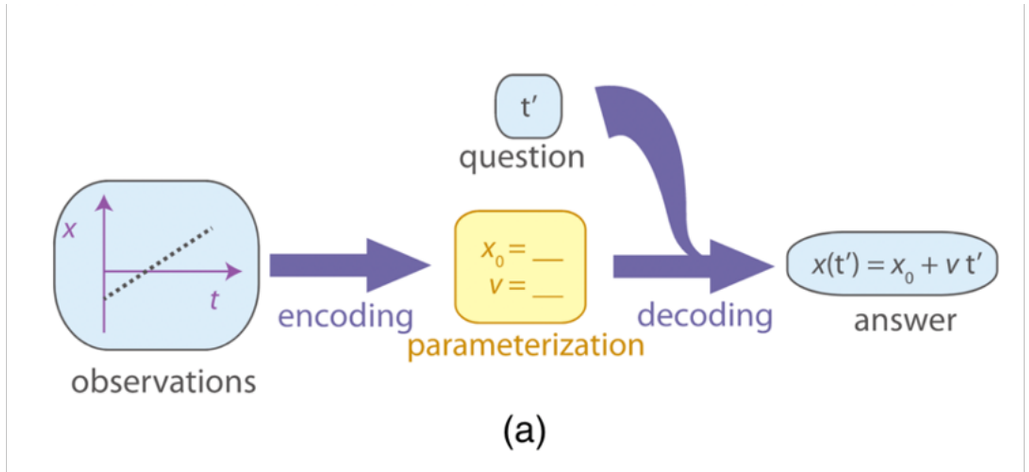

(a)

Iten R et al., Phys Rev Lett. 124(1):010508.

泛化思想可以发现新自由度

基于太阳与地球相互作用数据得到——$F = Constant1\ \frac{1}{r^2}$

基于月球与地球相互作用数据得到——$F = Constant2\ \frac{1}{r^2}$

如何统一两个相同类型数据得到的公式？——引入新自由度星球质量

基于太阳与地球相互作用数据得到——$F = Constant3\ \frac{M_{太阳}}{r^2}$

基于月球与地球相互作用数据得到——$F = Constant3\ \frac{M_{月球}}{r^2}$

如果引入太阳月球相互作用数据？

- 物理信息神经网络

Raissi et al, J. Compute. Phys. 378(2019)686-707

⇒ 求解偏微分方程问题

# 机器学习在物理中的应用

- 粒子物理与宇宙学

  - 数据分析

Baldi et al., Nat. Commun. 5 (2014) 4308

⇒ 粒子轨迹和喷注分类

  - 加速LQCD模拟

Alexandru et al., PRD96(2017)094505,

Kanwar et al., PRL125(2020)121601

⇒ 机器学习寻找匹配路径积分流形解决符号问题及加速组态采样

  - 解决逆问题

Shi et al., PRD105(2022)014017

⇒ 研究强子化过程中的物理状态，基于神经网络表示夸克反夸克之间相互作用势

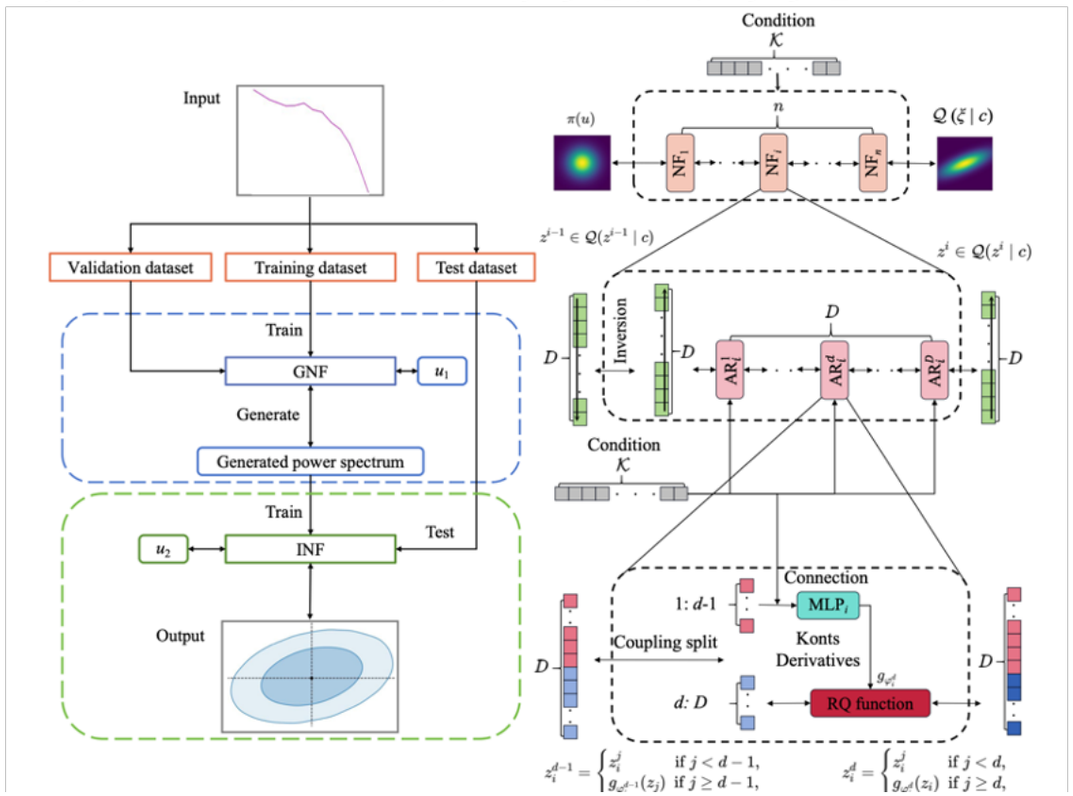


- 宇宙学

⇒ 探测早期宇宙中的小尺度结构（18厘米宇宙）

Sun et al., arXiv:2407.14298

# 机器学习在物理中的应用

- 重离子物理

- 通过可解释机器学习减除HIC 中射流背景

  Mengel et al., PRC108(2023)L021901

- 基于深度学习研究量子色动力学相变状态方程

  Pang et al., Nat. Commun. 9(2018)210

- 基于深度学习进行 HIC 喷注断层扫描

  Du et al., PRL128(2022)012301

- 基于机器学习的HIC上喷注动量重建

  Haake et al., PRC99(2019)064904

- 基于深度学习的淬火喷注分类

  Apolinario et al., JHEP11(2021)219

- 基于机器学习研究HIC夸克和胶子喷注子结构

  Chien, NPA982(2019)619-622

- ……

# 机器学习在物理中的应用

- 机器学习解决传统方法已经解决的问题（粒子分类等）

  ⇒ 证明机器学习的可行性

- 机器学习加速传统数值计算/提高数值计算精度（VMC、偏微分等）

  ⇒ 发挥机器学习的数值计算优势

- 机器学习发现新物理理论（对称性、守恒律、强子化等）

  ⇒ 发挥机器学习的表达能力优势

- 可解释/物理化机器学习（KAN、PINN等）

⇒ 基于物理规律进一步促进机器学习发展

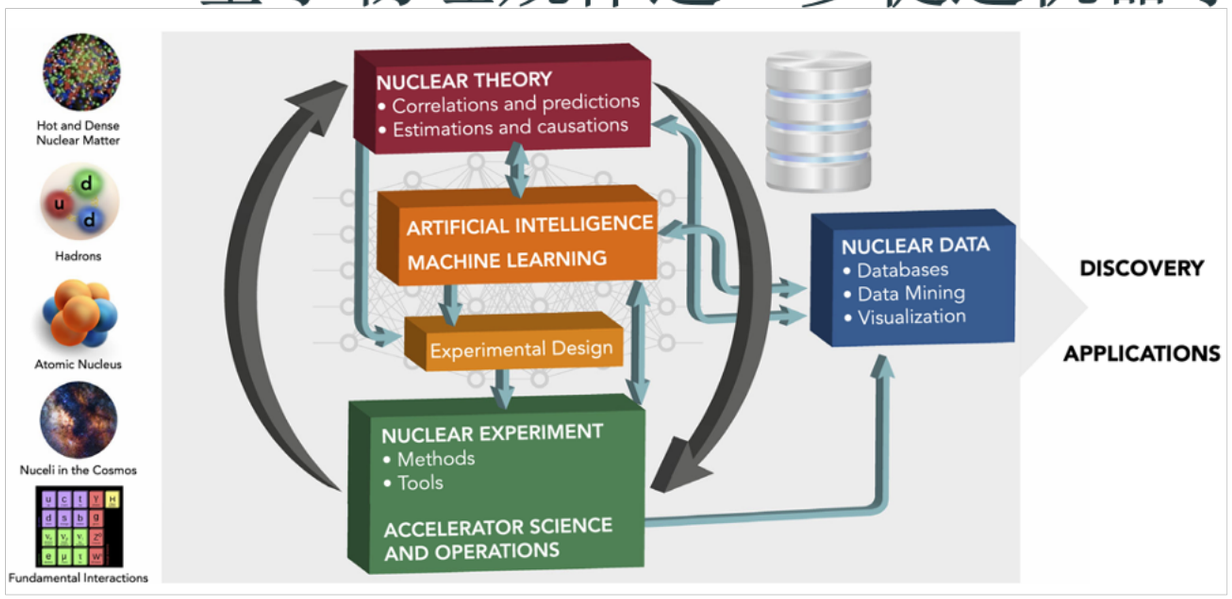


Boehnlein et al., Rev.Mod.Phys. 94 (2022) 3, 031003

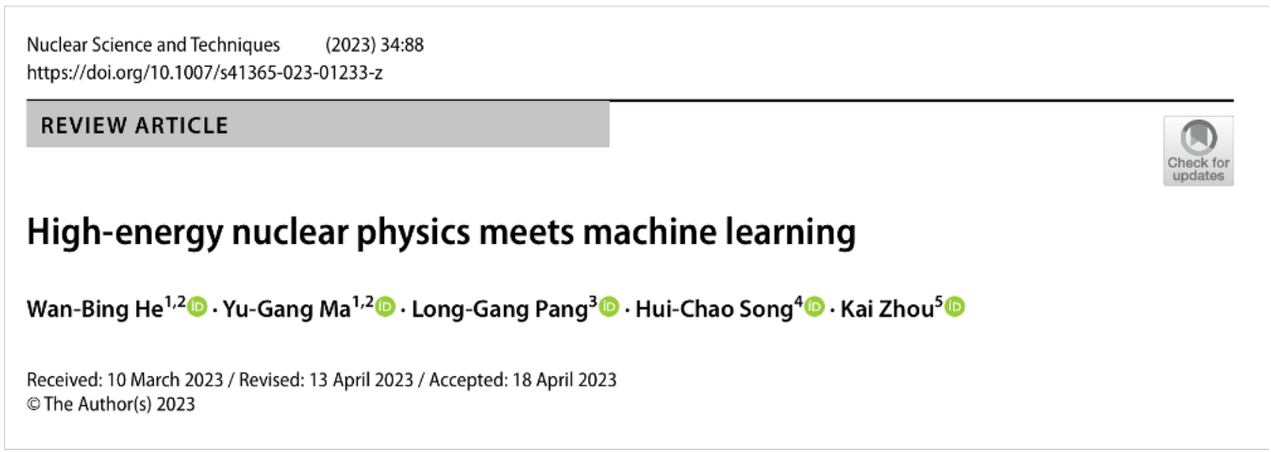
Nuclear Science and Techniques (2023) 34:88
https://doi.org/10.1007/s41365-023-01233-z
REVIEW ARTICLE
Check for updates

**High-energy nuclear physics meets machine learning**

Wan-Bing He[1,2] · Yu-Gang Ma[1,2] · Long-Gang Pang[3] · Hui-Chao Song[4] · Kai Zhou[5]

Received: 10 March 2023 / Revised: 13 April 2023 / Accepted: 18 April 2023
© The Author(s) 2023

He et al., Nucl.Sci.Tech. 34 (2023) 6, 88

# Machine learning in hadron physics

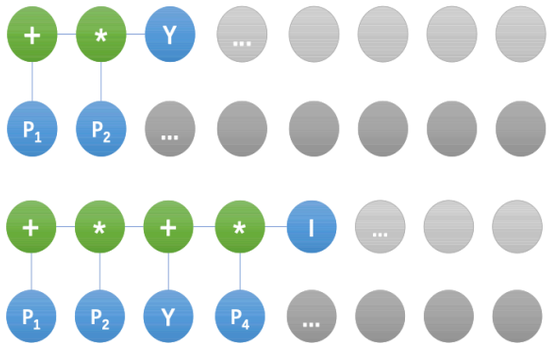


Regress Gell-Mann-Okubo formula

CPL39(2022)111201

2022

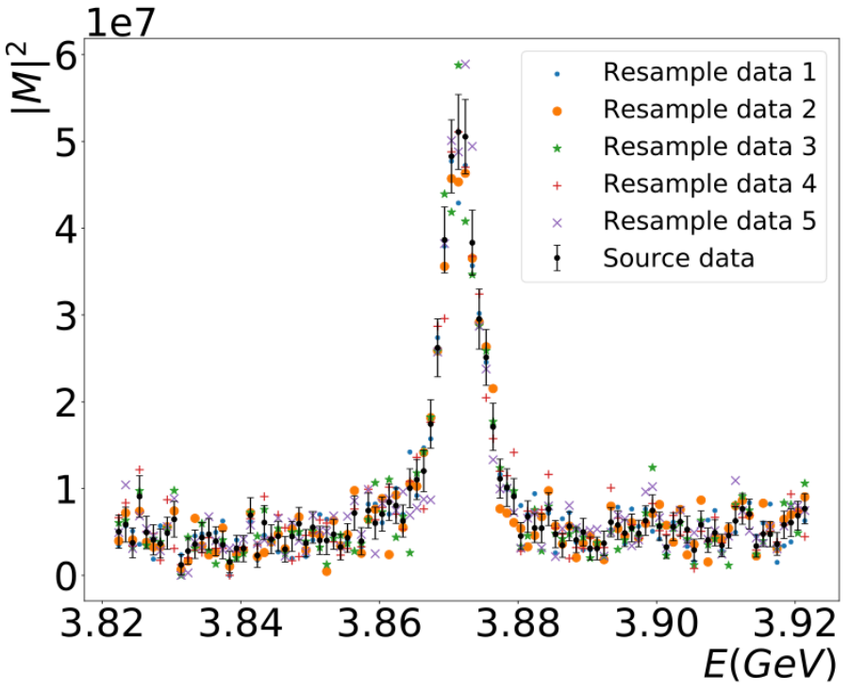


One-channel analysis

PRD105(2022)076013

# Machine learning in hadron physics

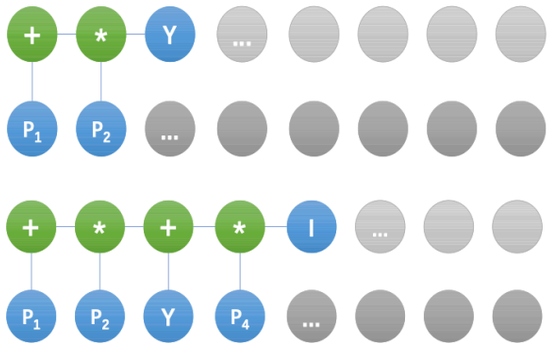


Regress Gell-Mann-Okubo formula

CPL39(2022)111201

2022 2023

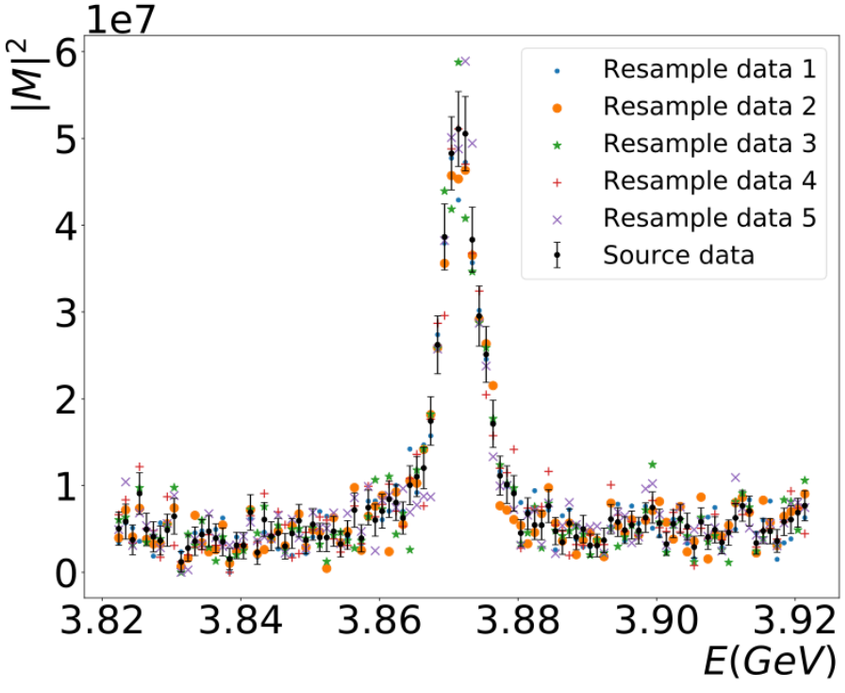


One-channel analysis

PRD105(2022)076013

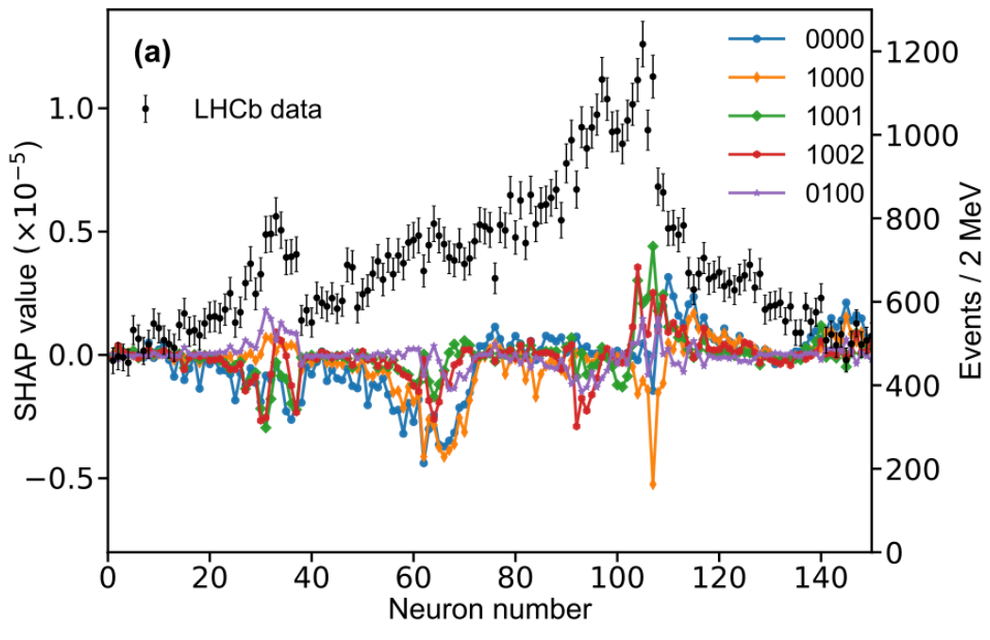


Coupled channel analysis

Sci.Bull.68(2023)981

# Machine learning in hadron physics

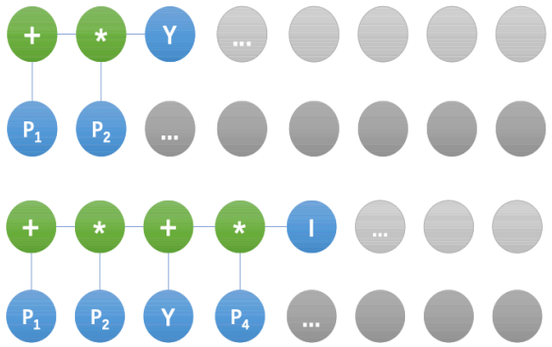


Regress Gell-Mann-Okubo formula

CPL39(2022)111201

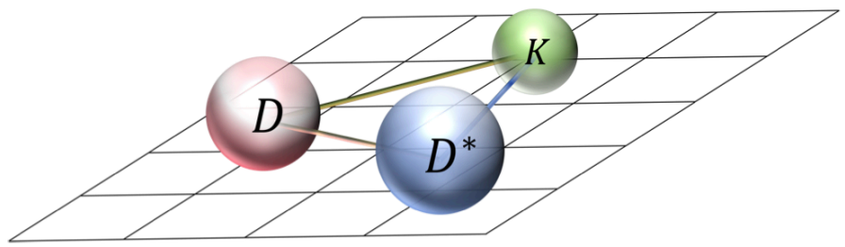


Three-body system on the lattice

PRD(2025)036002

2022 2023 2024

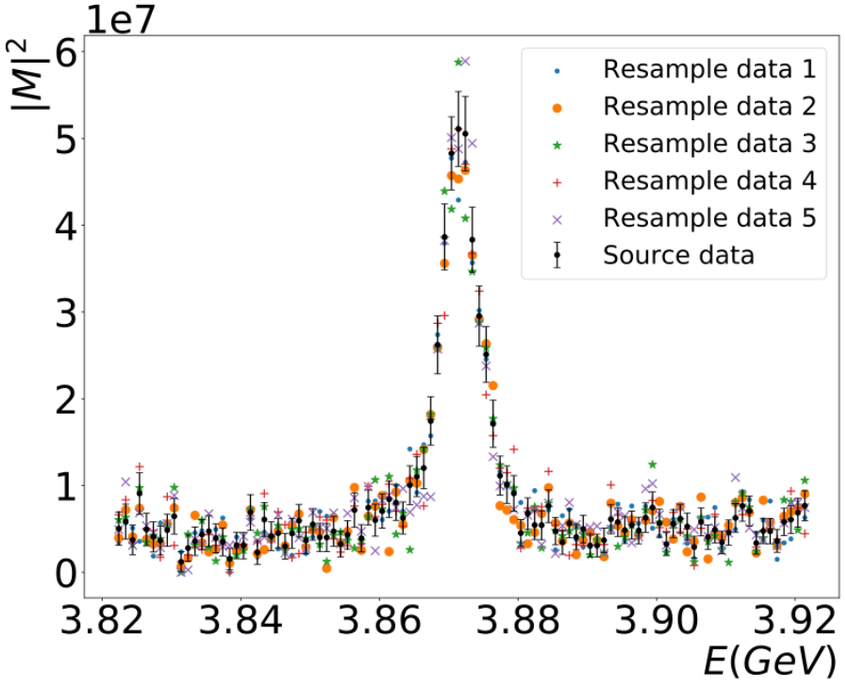


One-channel analysis

PRD105(2022)076013

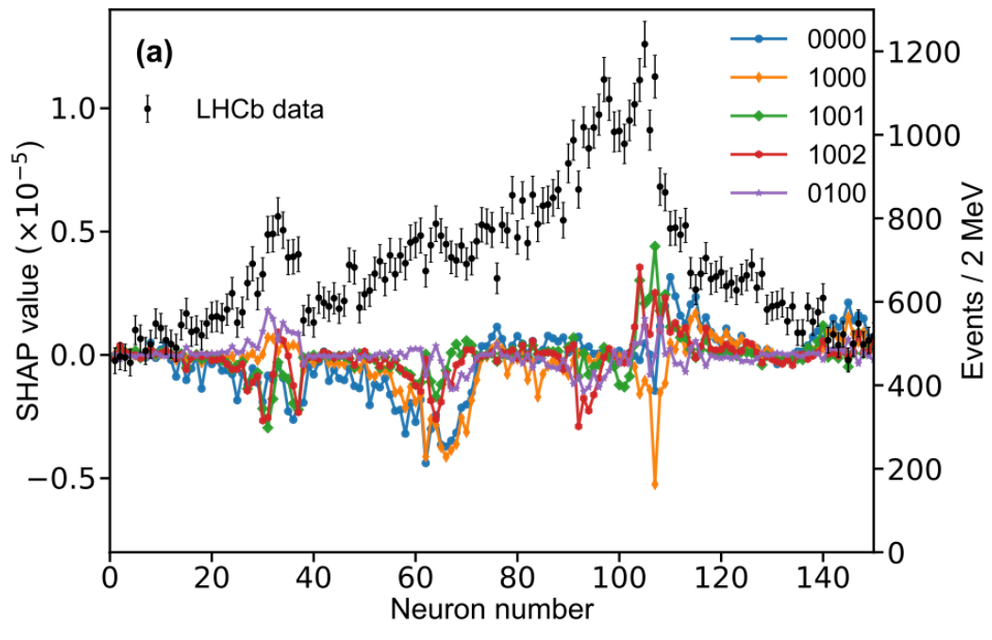


Coupled channel analysis

Sci.Bull.68(2023)981

# Machine learning in hadron physics

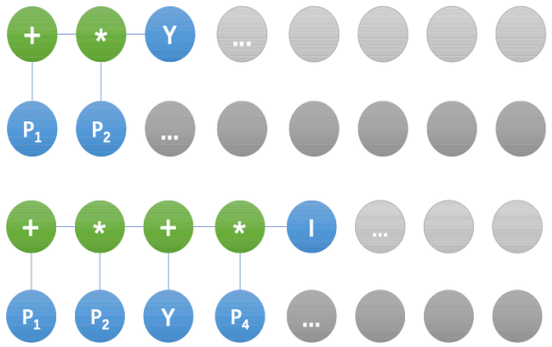


Regress Gell-Mann-Okubo formula

CPL39(2022)111201

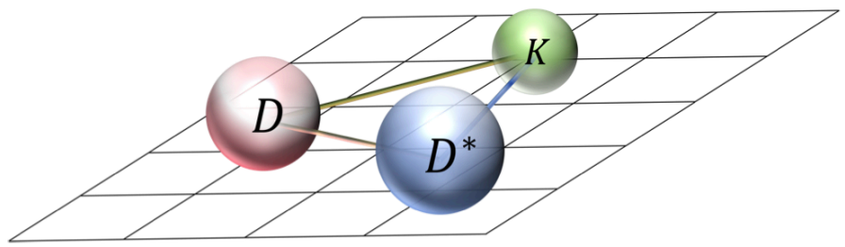


Three-body system on the lattice

PRD(2025)036002

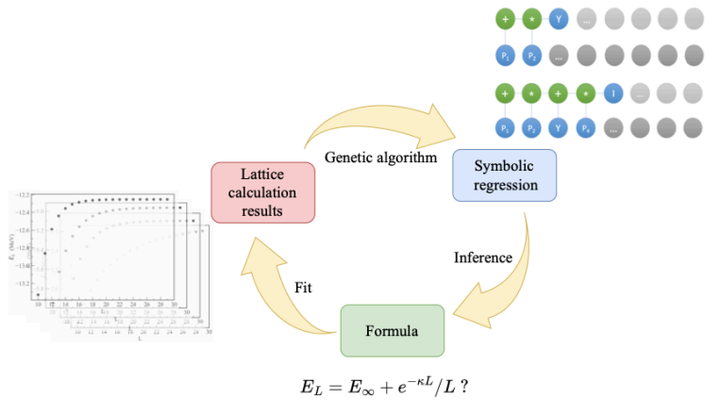


The power law of FV energy shift

arXiv:2503.06496

2022 2023 2024 2025

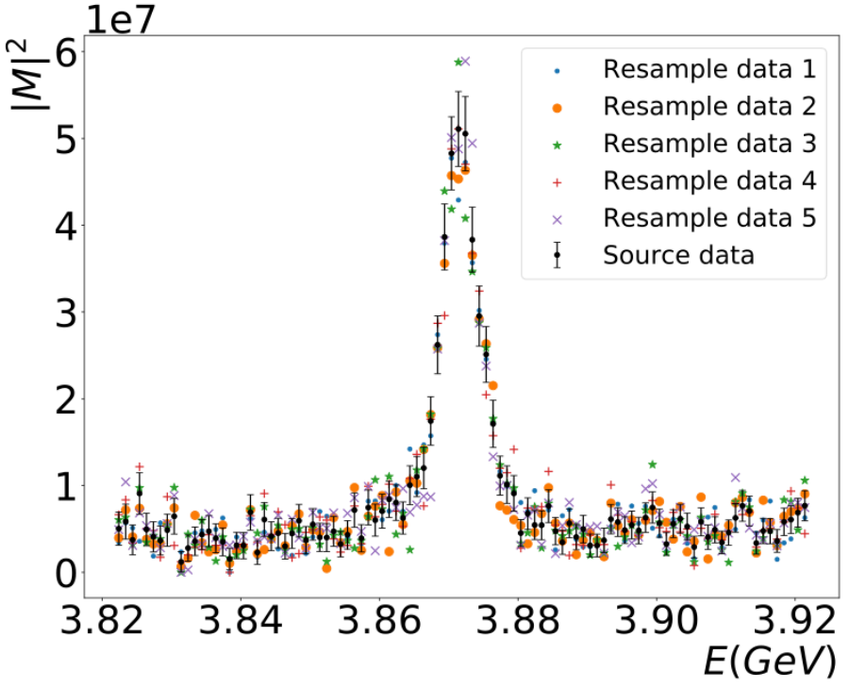


One-channel analysis

PRD105(2022)076013

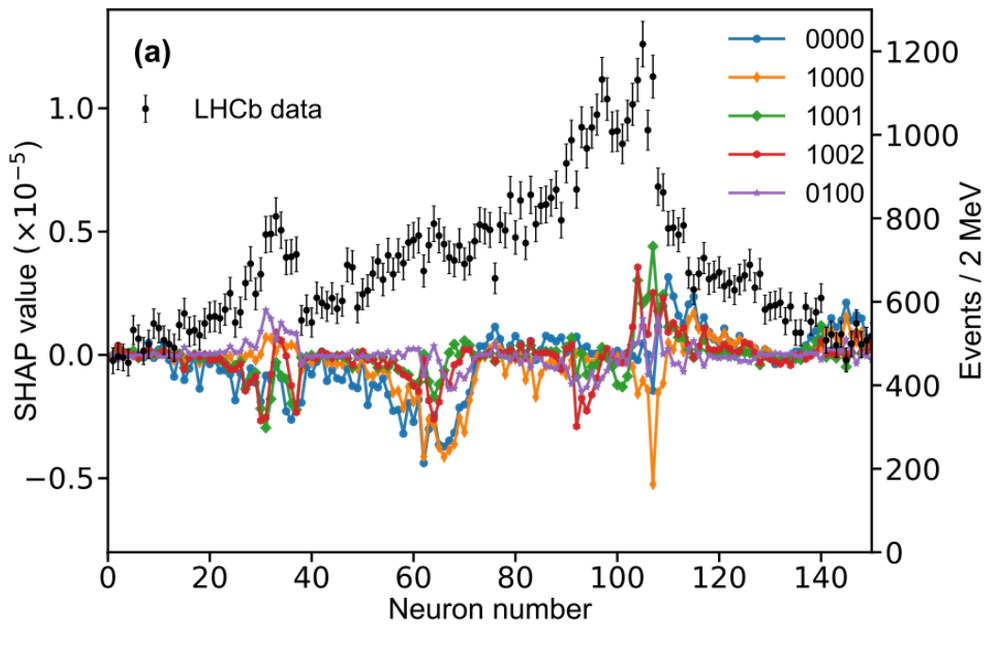


Coupled channel analysis

Sci.Bull.68(2023)981

# 符号回归重现盖尔曼大久保公式

- 非平衡二叉树模型

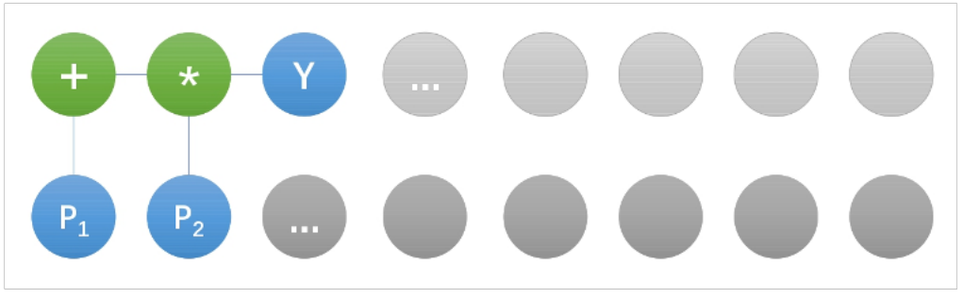


$$f(Y,I) = p_1 + p_2 Y$$

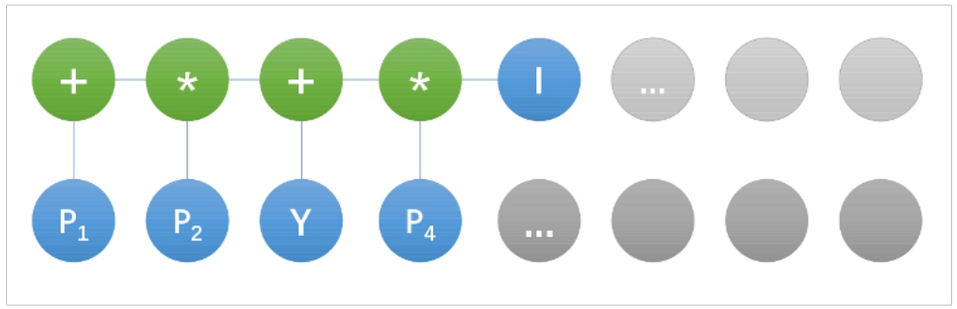


$$f(Y,I) = p_1 + p_2(Y + p_4 I)$$

- 演化流程

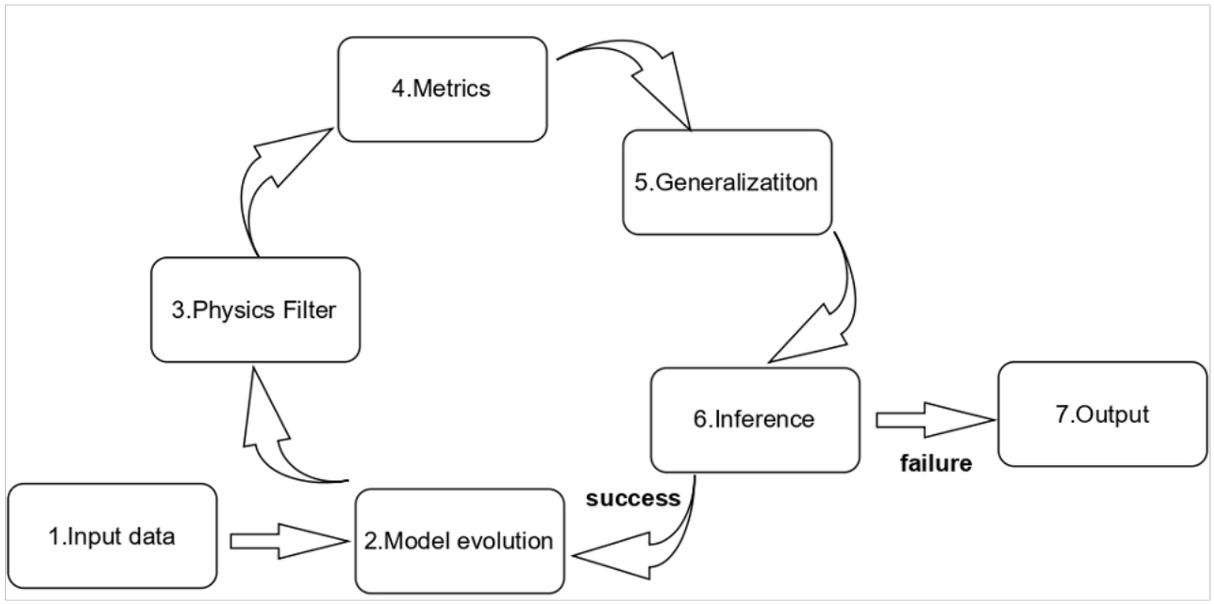


物理滤波限制：量纲（要求任何两个具有相同量纲的观测量才可以加减。具有不同维度的观测量仅允许乘法或除法）。
评估：符号表达式通过对均方差函数梯度下降得到待拟合参数，根据均方差函数的结果指导下一步进化方向。枚举每次进化的所有可能，选择评估最好的结果作为进化结果，进行下一次进化。

$$\chi^2 = \sum_k^N \frac{(f_C(Y,I) - M)_k^2}{\epsilon_k^2}$$

# 符号回归重现盖尔曼大久保公式

- 运算符和观测量

| operators | descriptions | observable | descriptions |
|---|---|---|---|
| + | addition | M | hadron mass |
| - | subtraction | Y | hypercharge |
| * | multiplication | I | isospin |
| / | division | **p** | free parameters |

- 重子八重态及十重态质量

| Y | I | $J^P = \frac{1}{2}^+$ | $J^P = \frac{3}{2}^+$ | Mass (MeV/c$^2$) |
|---|---|---|---|---|
| 1 | $\frac{1}{2}$ | $n, p$ | | 939±1 |
| 0 | 0 | $\Lambda$ | | 1116±1 |
| 0 | 1 | $\Sigma^-, \Sigma^0, \Sigma^+$ | | 1193±4 |
| -1 | $\frac{1}{2}$ | $\Xi^-, \Xi^0$ | | 1318±3 |
| 1 | $\frac{3}{2}$ | | $\Delta^-, \Delta^0, \Delta^+, \Delta^{++}$ | 1232±2 |
| 0 | 1 | | $\Sigma^{*-}, \Sigma^{*0}, \Sigma^{*+}$ | 1385±3 |
| -1 | $\frac{1}{2}$ | | $\Xi^{*-}, \Xi^{*0}$ | 1533±2 |
| -2 | 0 | | $\Omega^-$ | 1672±1 |

- 重子十重态演化过程

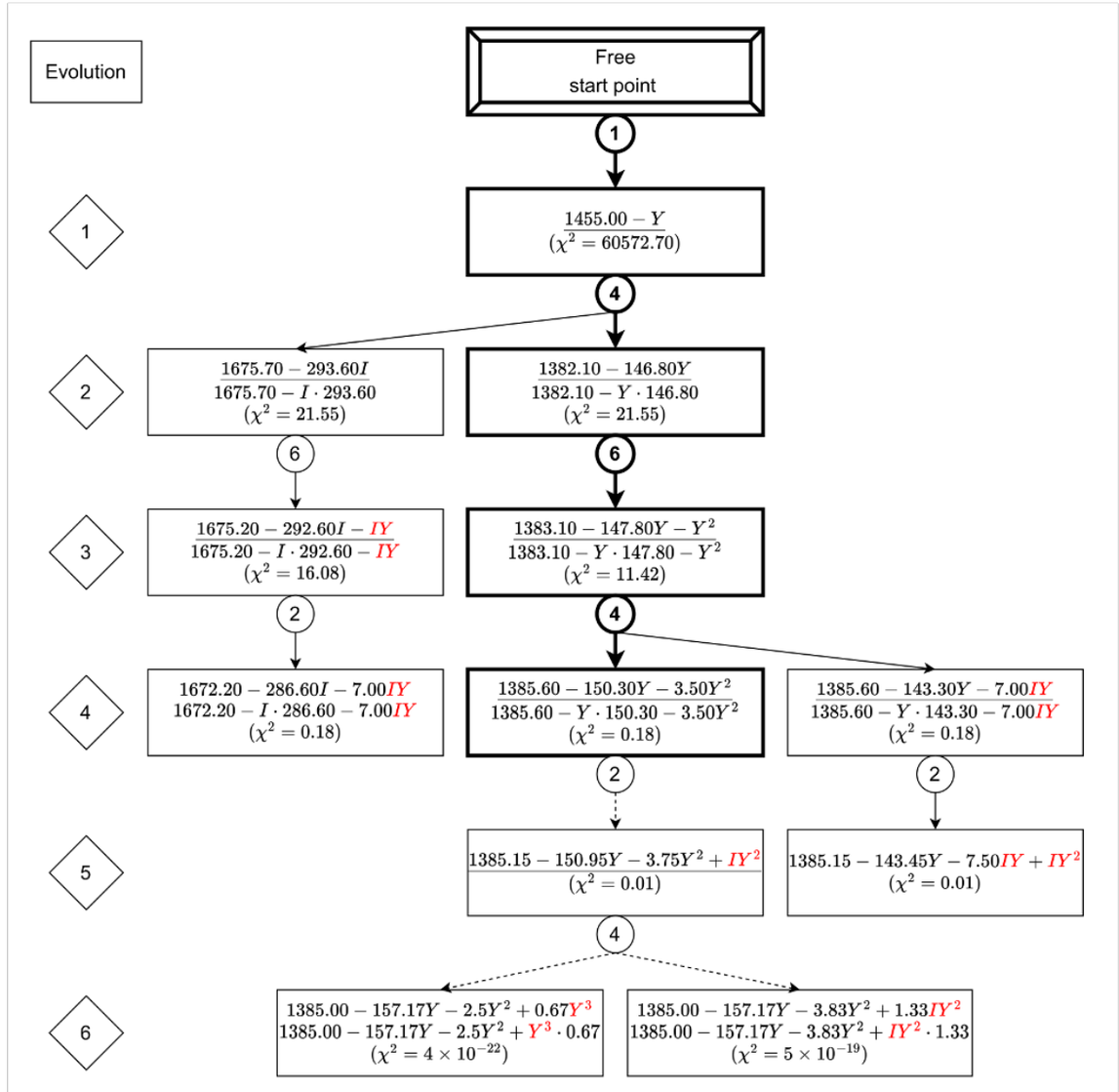


$$M_{\text{decuplet}} = C_1 - C_2 Y - C_3 Y^2.$$

# 符号回归重现盖尔曼大久保公式

- 重子八重态演化过程

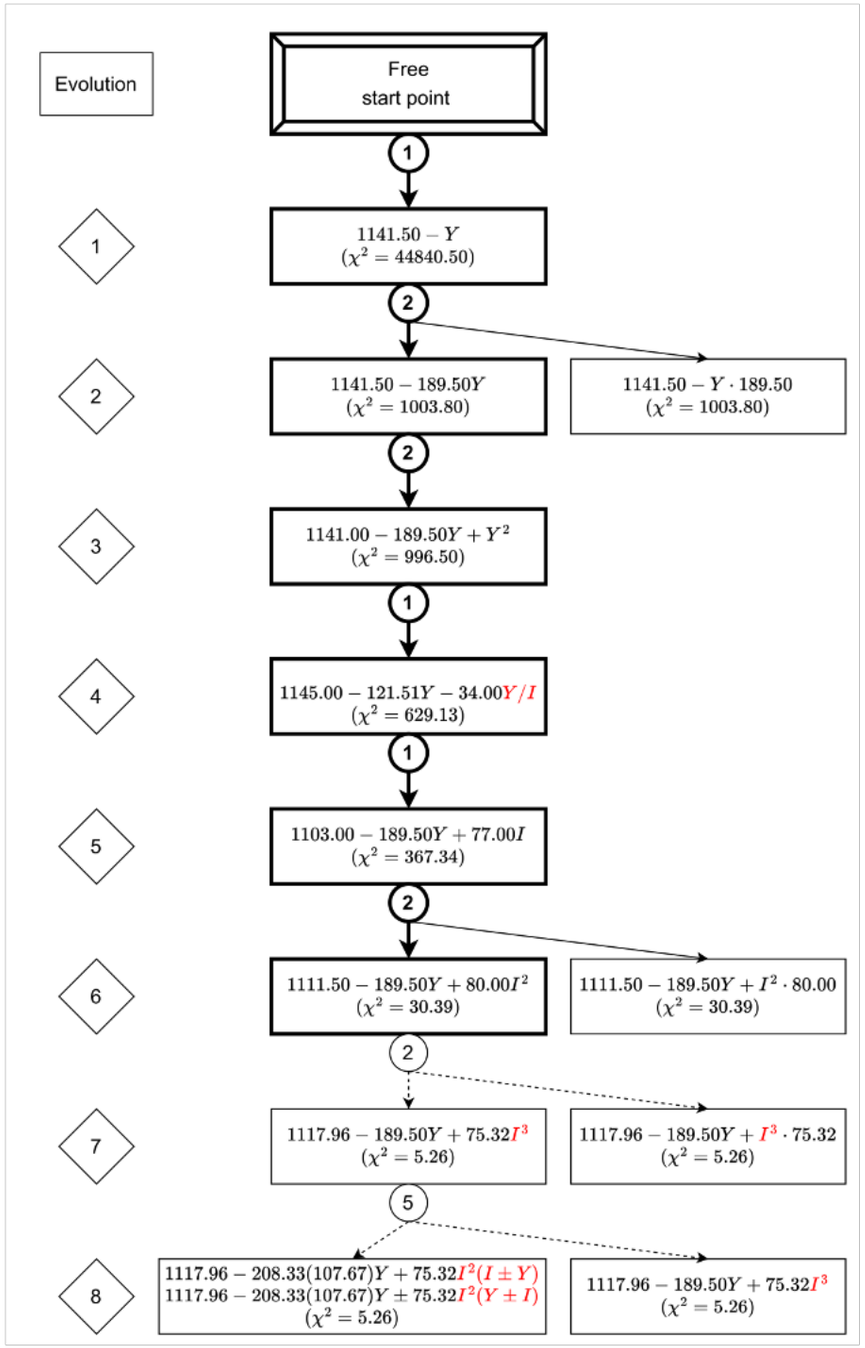


$$M_{\text{octet}} = C_a - C_b Y + C_c I^2.$$

- 重子八重态与十重态的统一

| Evolution | $\chi_8^2 + \chi_{10}^2$ | Decuplet |
|---|---|---|
| 1 | 0.2055520 | $803.16 - 441.52Y - 3.50Y^2 + 582.44I$ |
| 2 | 0.1800060 | $511.97 - 587.12Y - 3.50Y^2 + 873.63I$ |
| 3 | 0.1799985 | $\mathbf{689.54 - 672.34Y - 90.51Y^2 + 348.03I(I+1)}$ |
| 4 | 0.1208117 | $1381.94 - 153.19Y - 4.12Y^2 + 2.48(\underline{I(Y^2+1)})$ |
| 5 | $1 * 10^{-10}$ | $1384.33 - 151.50Y - 3.83Y^2 + 0.67\overline{I} + 1.33\underline{IY^2}$ |

| Evolution | $\chi_8^2 + \chi_{10}^2$ | Octet |
|---|---|---|
| 1 | 0.2055520 | $1115.84 - 189.50Y - 25.95Y^2 + 77.24I$ |
| 2 | 0.1800060 | $1116.00 - 189.50Y - 26.00Y^2 + 77.00I$ |
| 3 | 0.1799985 | $\mathbf{1116.00 - 189.50Y - 16.38Y^2 + 38.50I(I+1)}$ |
| 4 | 0.1208117 | $1116.00 - 189.50Y - 64.50Y^2 + 77.00(\underline{I(Y^2+1)})$ |
| 5 | $1 * 10^{-10}$ | $1116.00 - 189.50Y - 103.00Y^2 + 77.00\overline{I} + 154.00\underline{IY^2}$ |

- 盖尔曼大久保质量公式

$$M = a + bY + c[I(I+1) - \frac{1}{4}Y^2]$$

# Workflow

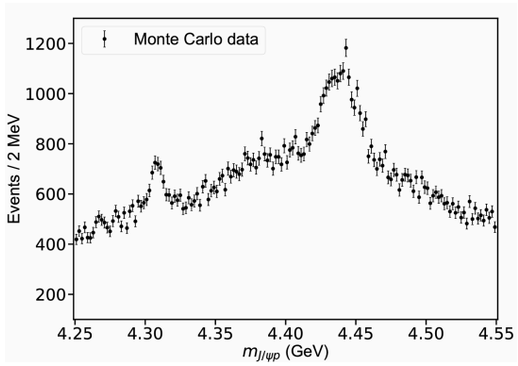


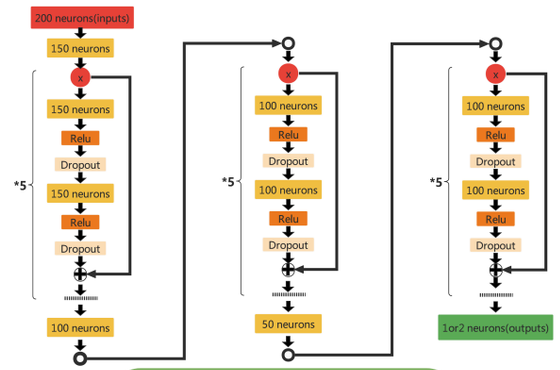


Samples generation

Monte Carlo method

ResNet

Neural network

Adam optimizer

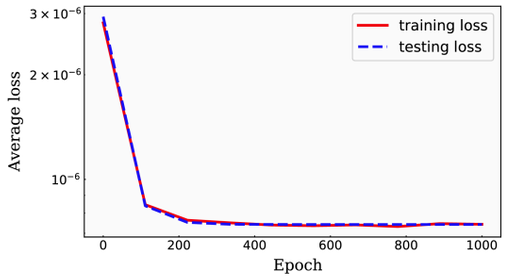


Model training

Comparison

Model evaluation

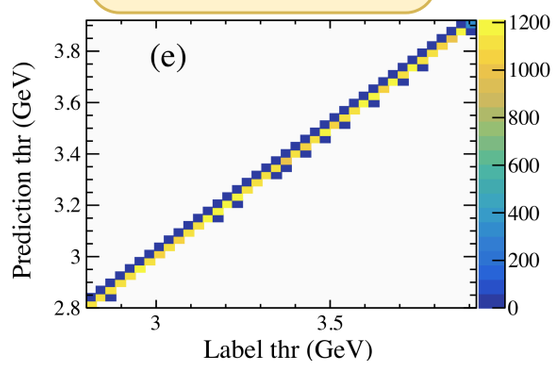


Input data

Experimental data analysis

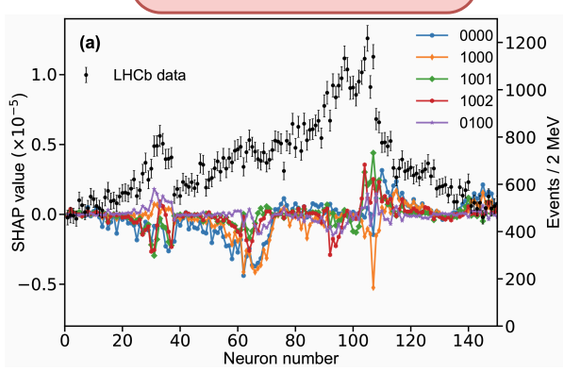


Proof theory

Theoretical model

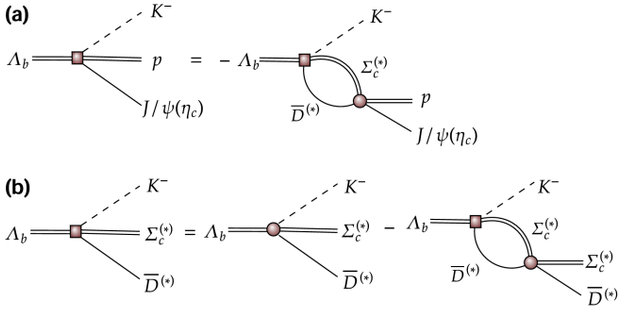


Extract dynamics

Distinguish models

# One-channel case in 2022

## 奇特强子态

传统夸克模型

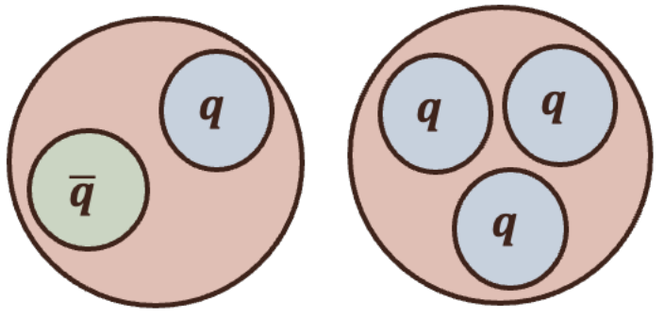


介子　　重子

量子色动力学(QCD)的色禁闭特性允许任何色中性的粒子存在。在过去二十年里，我们发现了数十种所谓的奇异强子候选者的出现，它们超越了传统介子和重子的构型。

紧致四夸克态

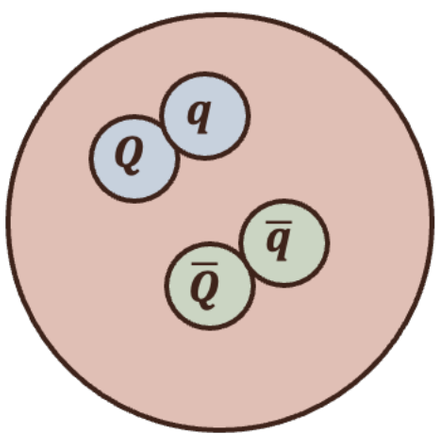


强子分子态

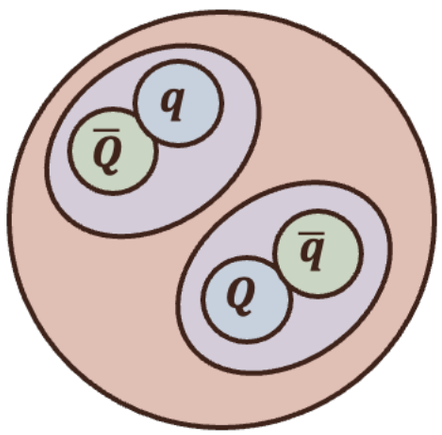


混杂态

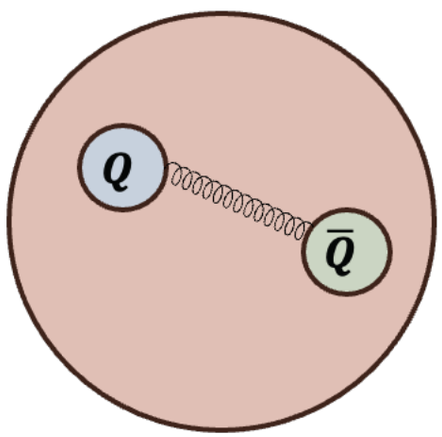


胶球

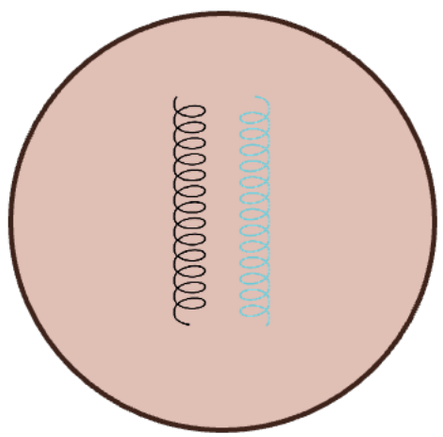

# One-channel case in 2022

神经网络

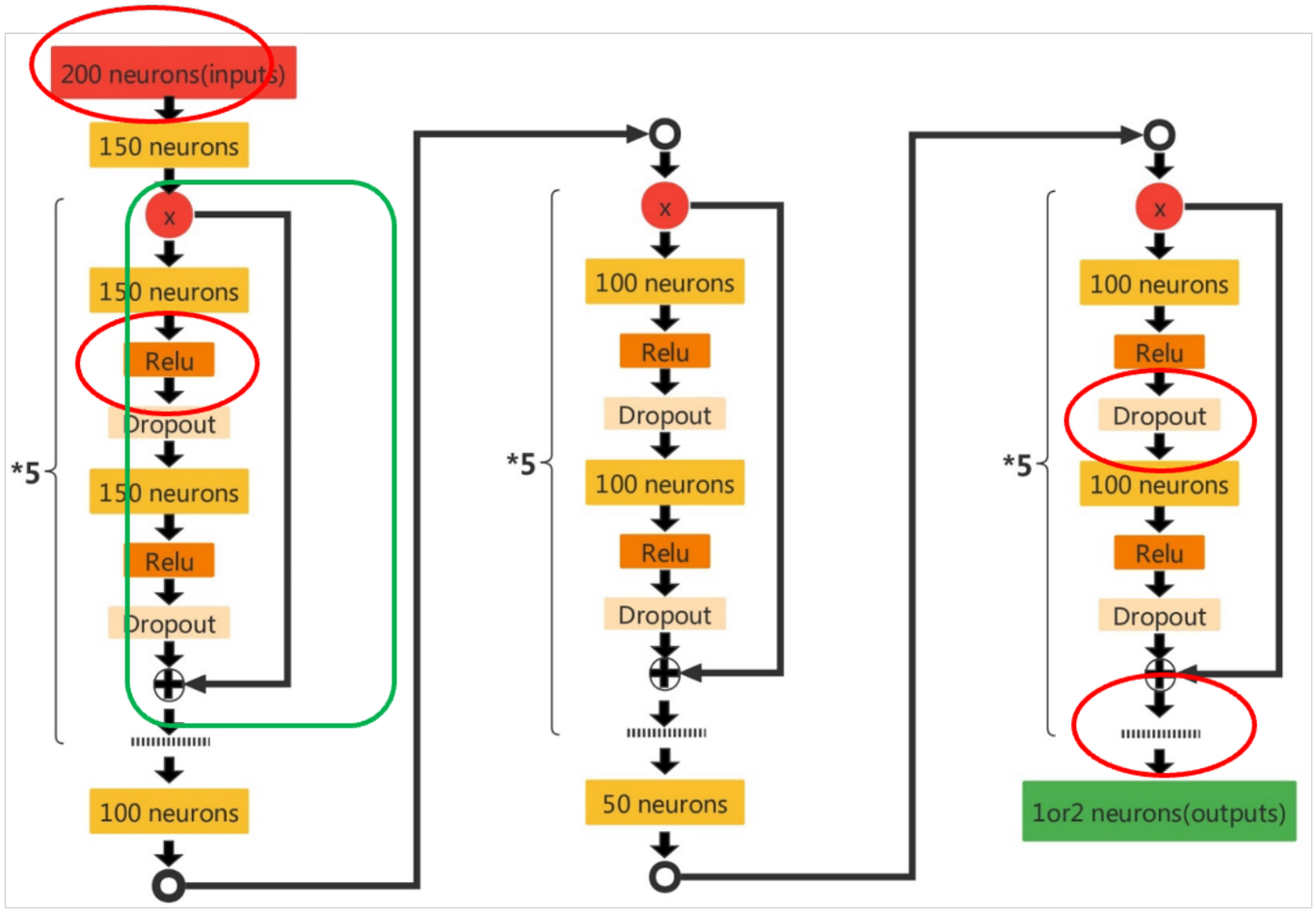


训练过程

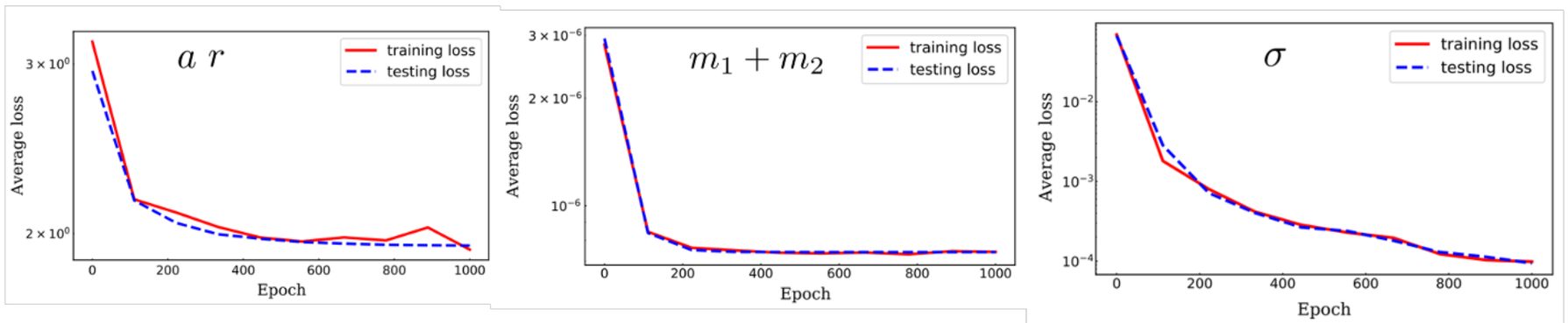


| | model for a,r | model for threshold | model for $\sigma$ |
|---|---|---|---|
| Loss function | MSELoss | MSELoss | MSELoss |
| Optimizer | Adam | Adam | Adam |
| Initial learning rate | 0.001 | 0.001 | 0.0001 |
| Learning rate dynamic adjustment (each 100 epochs) | 50% | 50% | 10% |
| Total epochs | 1000 | 1000 | 1000 |

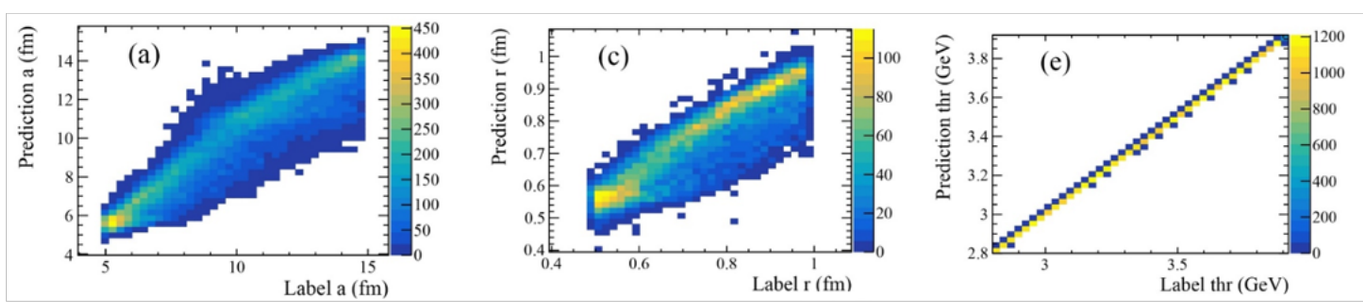

# One-channel case in 2022

The first step: One-channel line shape in HM picture

## Why one-channel case?

- The most simple case
- A given structure has one foremost channel
- In the isospin limit, sometimes the requirement can be satisfied

$X(3872)$ $D\bar{D}^* + c.c.$

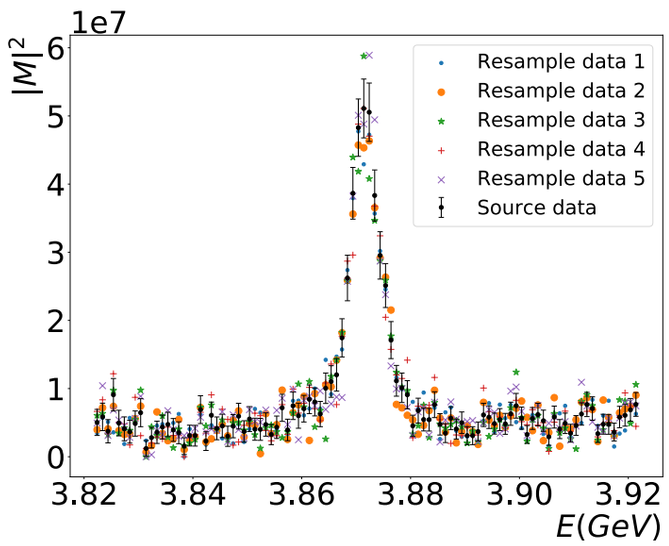


$T_{cc}^+$ $DD^*$

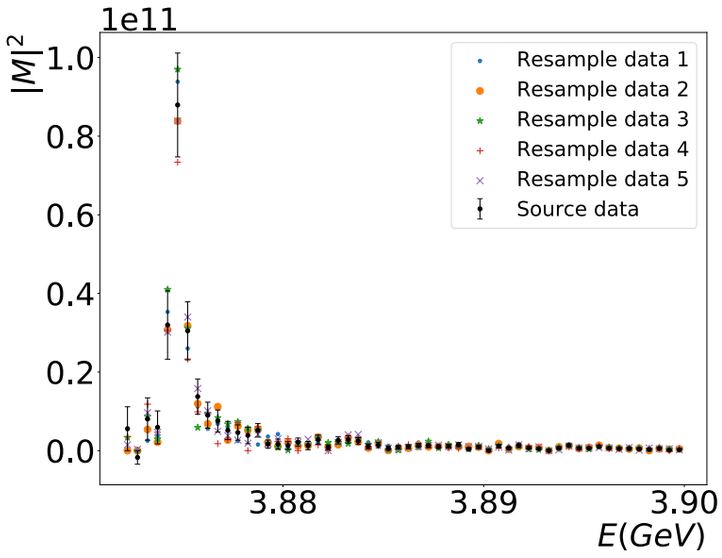


Liu, Zhang, Hu, **QW**, PRD105(2022)076013

# One-channel case in 2022

## Generate samples

Choose parameter region

$$a \in [4.93, 14.80] \text{ fm},$$
$$r \in [0.49, 0.99] \cup [-9.87, -0.49] \text{ fm},$$
$$m_1 + m_2 \in [2.8, 3.9] \text{ GeV},$$
$$\sigma \in [0.5, 10] \text{ MeV}.$$

- Allow for bound state, virtual state and resonances
- Cover charmonium(-like) region
- Resolution is set to cover usual experimental values
- Generate 150000 samples (100 data points)
- 45000 samples for testing

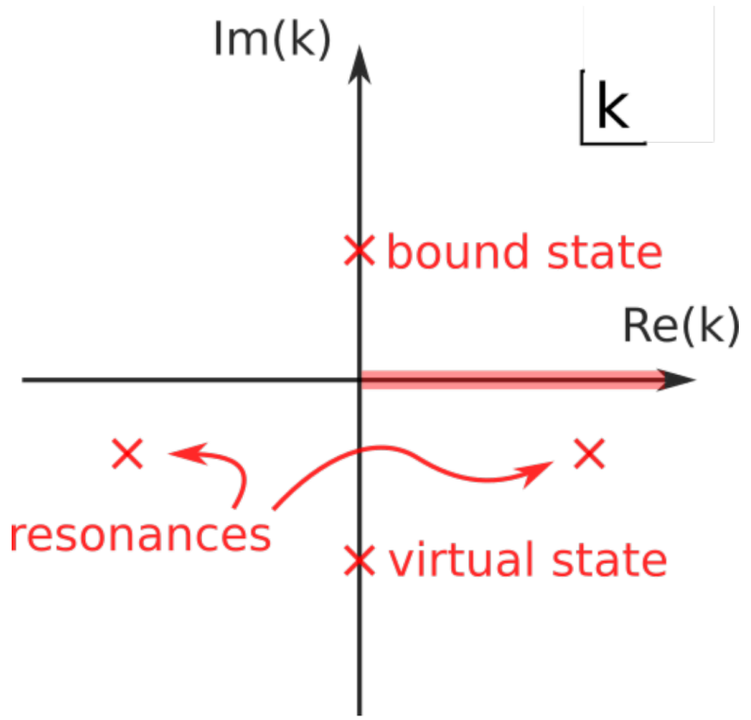


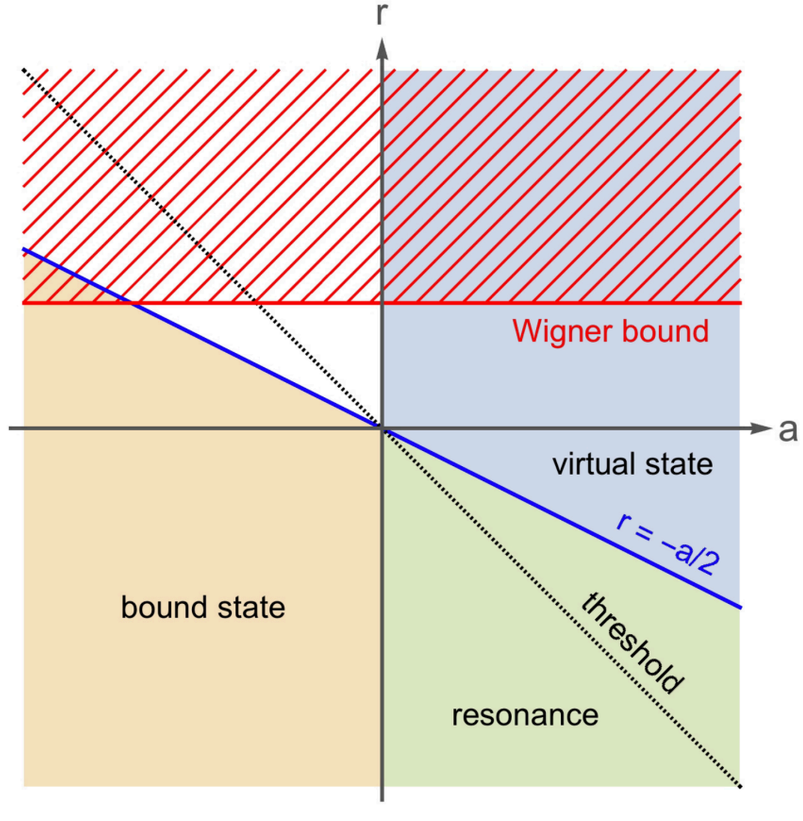


Matuschek, **Baru**, **Guo, Hanhart**, EPJA57(2021)101

# One-channel case in 2022

## Evaluation

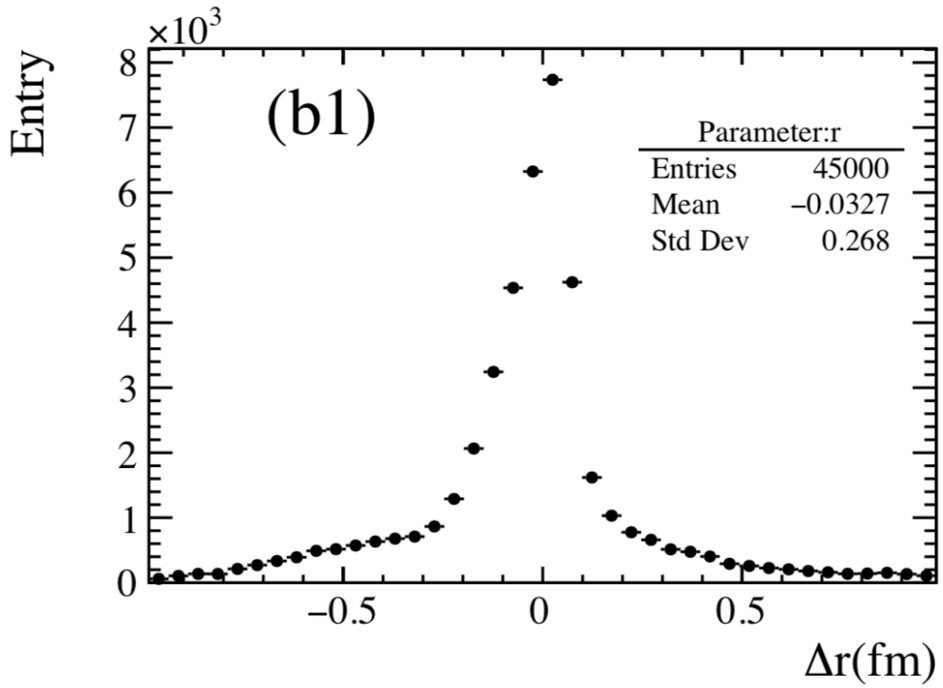


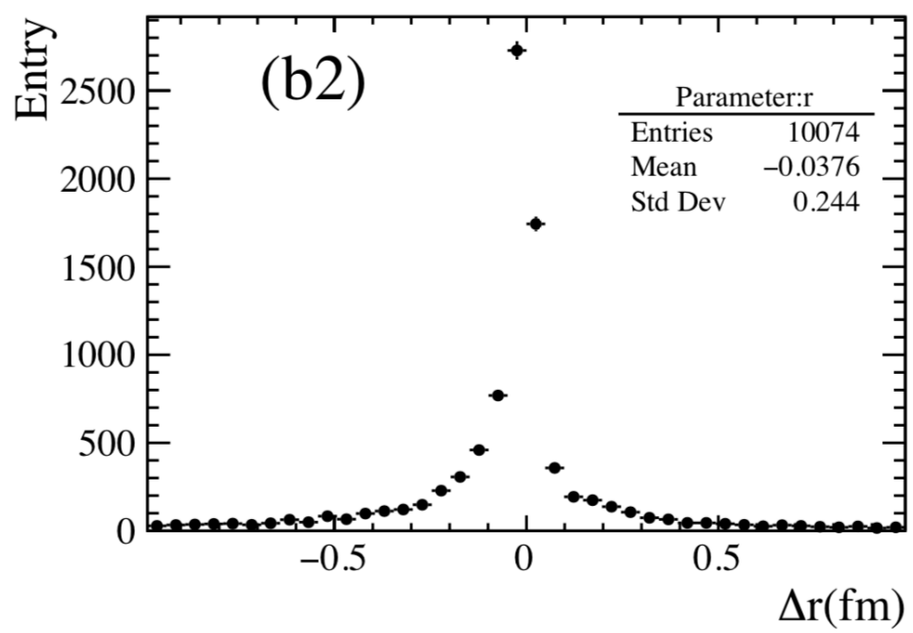


- The difference between the predicted values and the label values.
- The distributions are obtained by testing 45000 samples.
- The means measure the deviation of the predicted values from the label ones.
- The root-of-mean-square (RMS) measures the intrinsic uncertainties.
- Compare to the 10074/45000 fitting results.

Liu, Zhang, Hu, **QW**, PRD105(2022)076013

# One-channel case in 2022

## Evaluation

Liu, Zhang, Hu, **QW**, PRD105(2022)076013

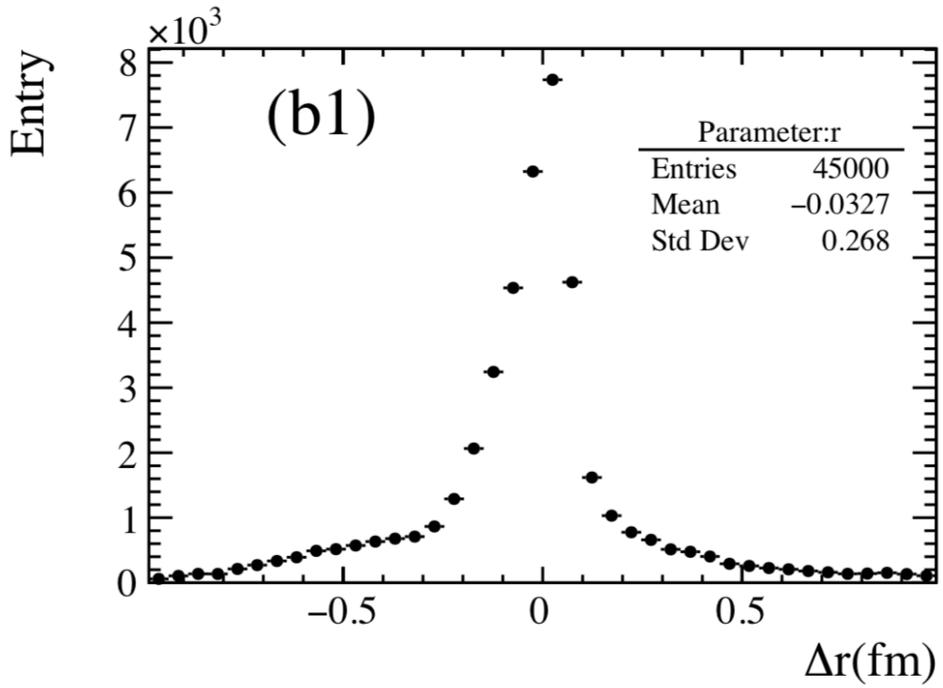


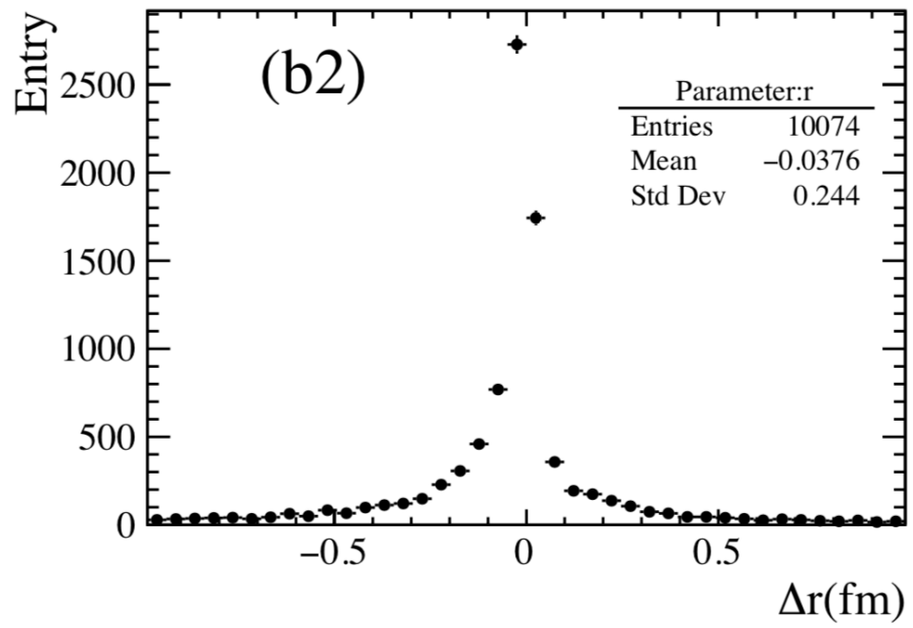


Table I. The biases and errors information of models

| methods→ | Deep learning | | Fitting | |
|---|---|---|---|---|
| parameters↓ | bias | uncertainty | bias | uncertainty |
| a (fm) | -0.010 | 1.040 | -1.67 | 2.740 |
| r (fm) | -0.033 | 0.268 | -0.038 | 0.244 |
| threshold (MeV) | 0.75 | 0.52 | -0.16 | 0.31 |
| $\sigma$ (MeV) | -0.0001 | 0.06 | -0.0098 | 0.10 |

# One-channel case in 2022

## Apply to the $X(3872)$

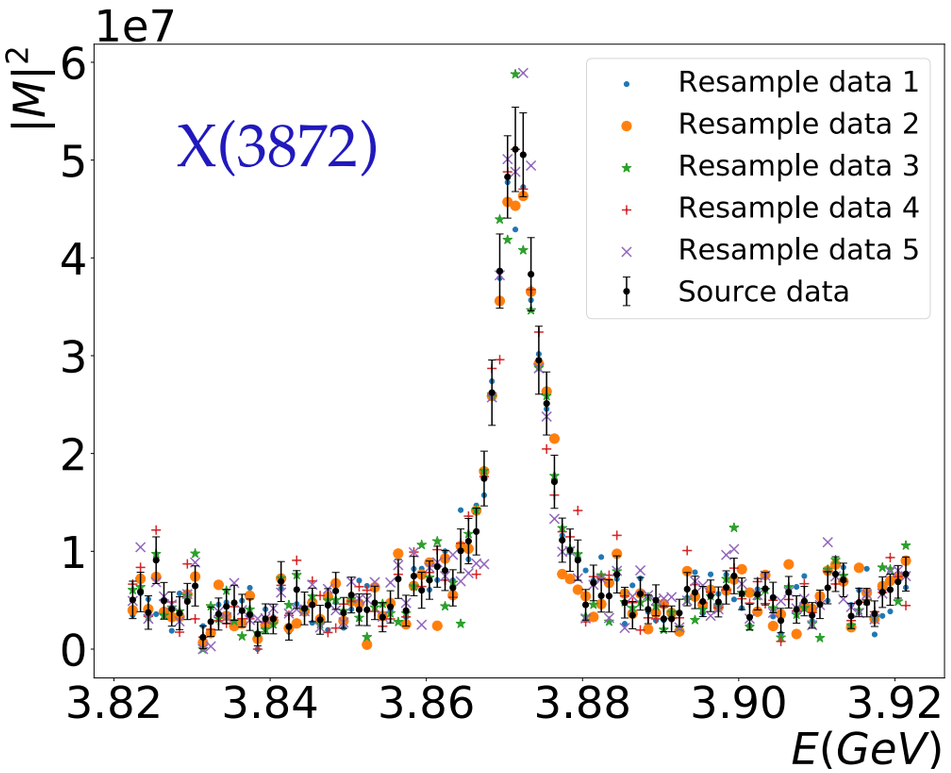


Liu, Zhang, Hu, **QW**, PRD105(2022)076013

- $D\bar{D}^* + c.c.$ channel
- a, r and threshold are consistent with those from fitting within $1\sigma$
- The errors are obtained in bootstrap (10000 data sets)

| $X(3872)$ **parameters** | Deep Learning | Fit |
|---|---|---|
| parameter a (fm) | $8.76 \pm 1.75$ | $9.95 \pm 0.34$ |
| parameter r (fm) | $0.56 \pm 0.55$ | $0.32 \pm 0.08$ |
| parameter threshold (MeV) | $3871.30 \pm 0.52$ | $3871.20 \pm 0.01$ |
| parameter $\sigma$ (MeV) | $1.20 \pm 0.15$ | $1.70 \pm 0.16$ |

# One-channel case in 2022

## Apply to the $T_{cc}^+$

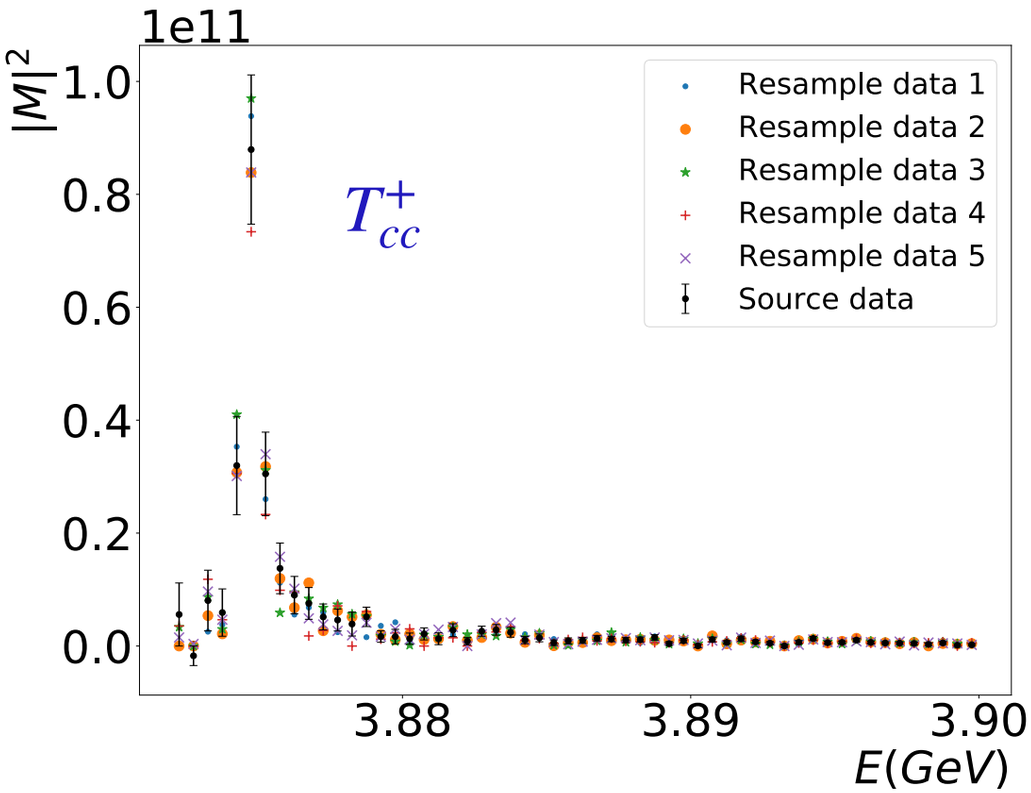


- $DD^*$ channel
- a, r and threshold are consistent with those from fitting within $1\sigma$
- The errors are obtained in bootstrap (10000 data sets)

| $T_{cc}^+$ **parameters** | Deep Learning | Fit |
|---|---|---|
| parameter a (fm) | $8.23 \pm 1.04$ | $13.74 \pm 4.77$ |
| parameter r (fm) | $-2.79 \pm 0.27$ | $-2.15 \pm 0.21$ |
| parameter threshold (MeV) | $3874.83 \pm 0.51$ | $3874.53 \pm 0.13$ |
| parameter $\sigma$ (MeV) | $1.10 \pm 0.06$ | $0.11 \pm 0.12$ |

Liu, Zhang, Hu, **QW**, PRD105(2022)076013

# One-channel case in 2022

Apply to the $T_{cc}^{+}$

**ML can do as good as normal fitting approach**

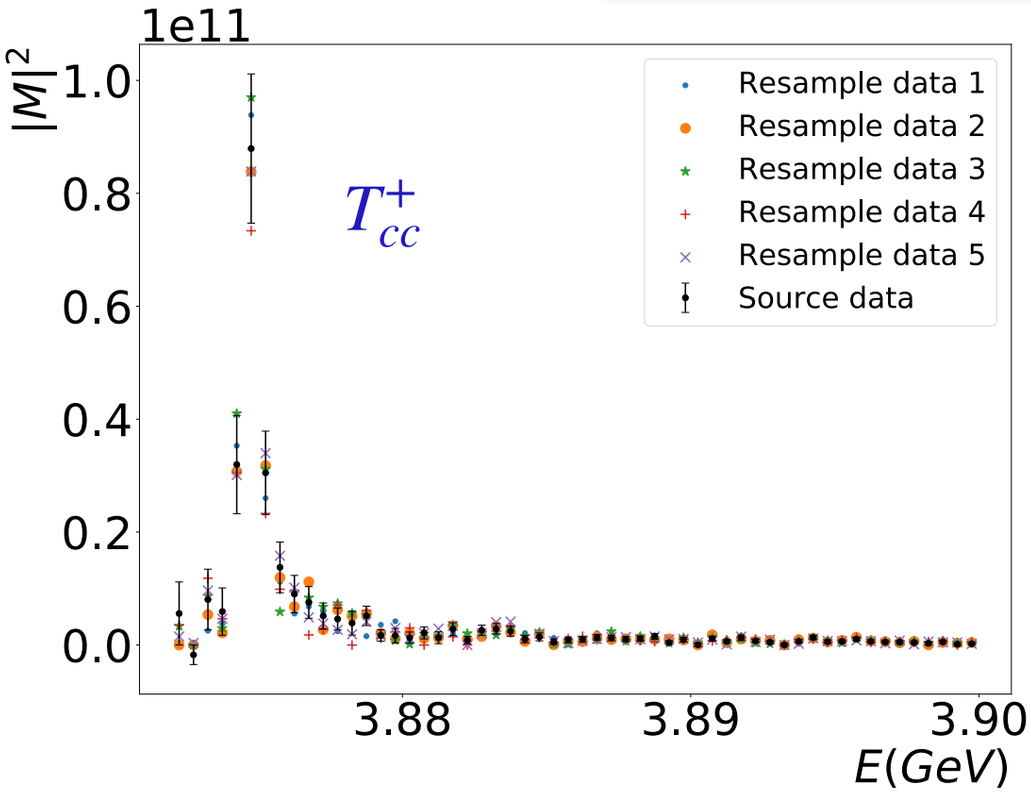


- $DD^*$ channel
- a, r and threshold are consistent with those from fitting within $1\sigma$
- The errors are obtained in bootstrap (10000 data sets)

| $T_{cc}^{+}$ **parameters** | Deep Learning | Fit |
|---|---|---|
| parameter a (fm) | $8.23 \pm 1.04$ | $13.74 \pm 4.77$ |
| parameter r (fm) | $-2.79 \pm 0.27$ | $-2.15 \pm 0.21$ |
| parameter threshold (MeV) | $3874.83 \pm 0.51$ | $3874.53 \pm 0.13$ |
| parameter $\sigma$ (MeV) | $1.10 \pm 0.06$ | $0.11 \pm 0.12$ |

Liu, Zhang, Hu, **QW**, PRD105(2022)076013

# Multi-channel case in 2023

The history of pentaquarks **Bing-Song Zou**, Sci.Bull.66(2021)1258

$\Lambda(1405)$ predicted by Dalitz and Tuan in 1959 Dalitz and Tuan, PRL2(1959)425

- An excited state of a three-quark ($uds$) system
- $\bar{K}N$ hadronic molecule with $uds q\bar{q}$

A similar situation for $N^\star(1535)$

- An excited state of a three-quark ($uds$) system
- $\bar{K}\Sigma - \bar{K}\Lambda$ dynamical generated state with $qqqs\bar{s}$ **Kaiser**, Siegel, **Weise**, NPA594(1995)325

Liu, **Zou**, PRL96(2006)042002

Pentaquark in hidden charm sector

**Wu**, Molina, Oset, **Zou**, PRL105(2010)232001

| $(I,S)$ | $z_R$ (MeV) | $g_a$ | | |
|---|---|---|---|---|
| $(1/2,0)$ | | $\bar{D}\Sigma_c$ | $\bar{D}\Lambda_c^+$ | |
| | 4269 | 2.85 | 0 | |
| $(0,-1)$ | | $\bar{D}_s\Lambda_c^+$ | $\bar{D}\Xi_c$ | $\bar{D}\Xi_c'$ |
| | 4213 | 1.37 | 3.25 | 0 |
| | 4403 | 0 | 0 | 2.64 |

| $(I,S)$ | $z_R$ (MeV) | $g_a$ | | |
|---|---|---|---|---|
| $(1/2,0)$ | | $\bar{D}^*\Sigma_c$ | $\bar{D}^*\Lambda_c^+$ | |
| | 4418 | 2.75 | 0 | |
| $(0,-1)$ | | $\bar{D}_s^*\Lambda_c^+$ | $\bar{D}^*\Xi_c$ | $\bar{D}^*\Xi_c'$ |
| | 4370 | 1.23 | 3.14 | 0 |
| | 4550 | 0 | 0 | 2.53 |

# Multi-channel case in 2023

R. Aaij et al., Phys.Rev.L 115, 072001(2015)

R. Aaij et al., Phys.Rev.L 122, 222001 (2019)

首个实验发现的隐粲五夸克态

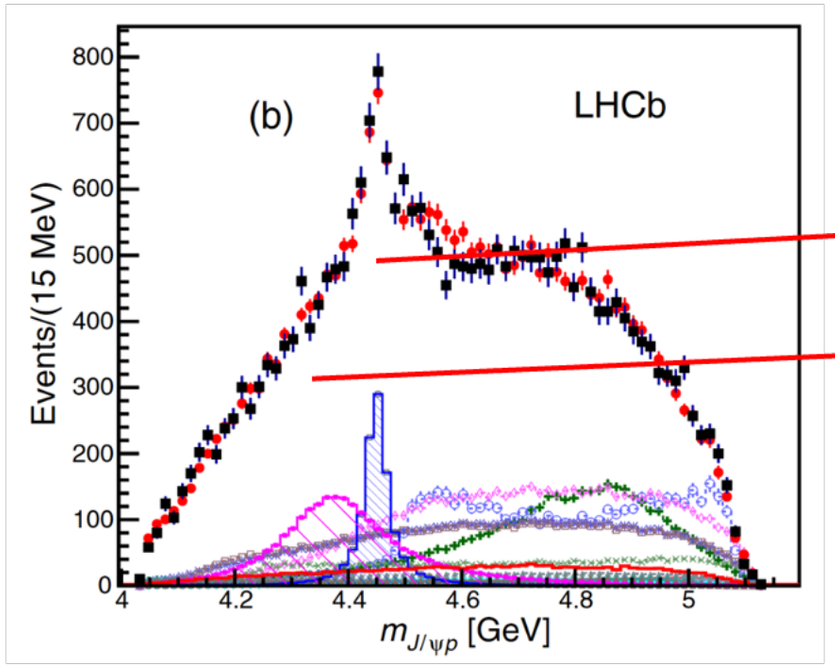


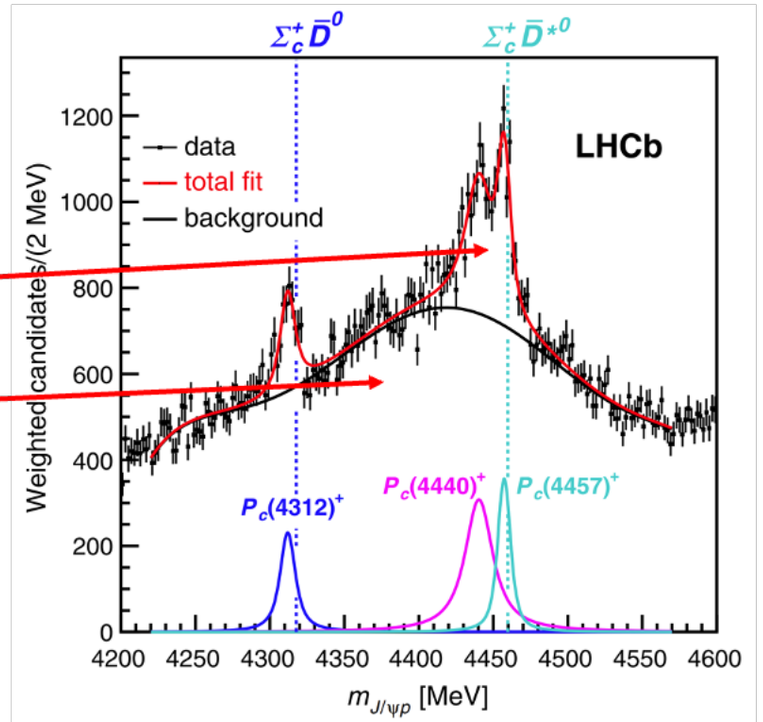


2015年LHCb合作组在$\Lambda_b \to K^- J/\Psi p$过程中发现了$P_c(4380)$和$P_c(4450)$。

2019年LHCb合作组在相同过程中增大统计量发现了$P_c(4312)$，$P_c(4440)$和$P_c(4457)$。

S波情况下, $(\Sigma_c^+, \Sigma_c^{+*}) = (1/2,3/2)$，$(\bar{D}, \bar{D}^*) = (0,1)$

| Hadronic molecular | $J^P$ |
|---|---|
| $\Sigma_c^+\bar{D}$ | $\frac{1}{2}^-$ |
| $\Sigma_c^{+*}\bar{D}$ | $\frac{3}{2}^-$ |
| $\Sigma_c^+\bar{D}^*$ | $\frac{1}{2}^-, \frac{3}{2}^-$ |
| $\Sigma_c^{+*}\bar{D}^*$ | $\frac{1}{2}^-, \frac{3}{2}^-, \frac{5}{2}^-$ |

由于$P_c(4312)$十分接近$\Sigma_c^+\bar{D}$的阈值，而且$P_c(4440)$和$P_c(4457)$十分接近$\Sigma_c^+\bar{D}^*$的阈值，可以考虑强子分子态图像解释实验数据。

# Multi-channel case

The $\Sigma_c^{(*)}\bar{D}^{(*)}$ molecular picture

Du, Baru, Guo, Hanhart, Meißner, Oller, **QW,** PRL124(2020)072001

$m_Q \to \infty$ the strong interaction independent of the spin of heavy quark

Heavy Quark Spin Symmetry

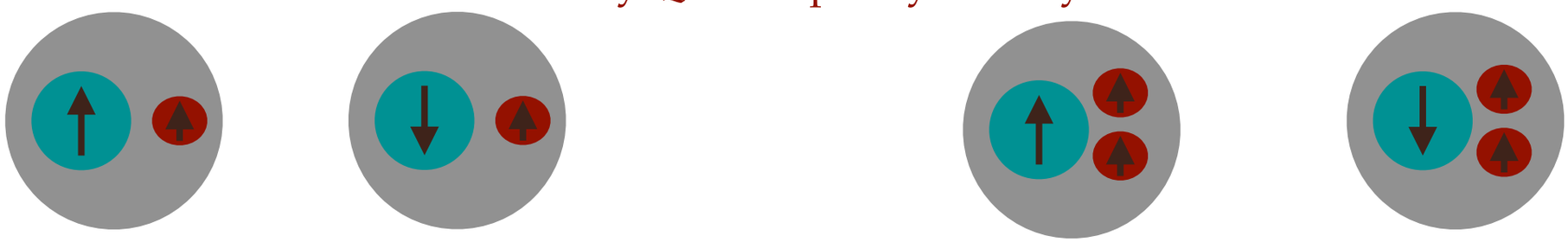

$$J = s_l + \frac{1}{2} \qquad J = s_l - \frac{1}{2} \qquad J = s_l + \frac{1}{2} \qquad J = s_l - \frac{1}{2}$$

$$m_{D^*} - m_D = 142 \text{ MeV} \qquad m_{\Sigma_c^*} - m_{\Sigma_c} = 64 \text{ MeV}$$

$s_l = \frac{1}{2}^-$ doublet $\qquad$ $s_l = 1^+$ doublet

Spin rearrangement

$$\left([\bar{Q}q_{J_{l_1}}]_{j_1}[Q(qq)_{J_{l_2}}]_{j_2}\right)_J \sim \sum_{HL} \mathscr{C}^{j_1 j_2 J}_{j_{l_1} j_{l_2} HL} \left((\bar{Q}Q)_H (qqq)_L\right)_J$$

$\bar{D}^{(*)}$ $\qquad$ $\Sigma_c^{(*)}$

Two LECs to LO

$$C_{\frac{1}{2}} \equiv \langle H \otimes \frac{1}{2} | \hat{H} | H \otimes \frac{1}{2} \rangle$$

$$C_{\frac{3}{2}} \equiv \langle H \otimes \frac{3}{2} | \hat{H} | H \otimes \frac{3}{2} \rangle$$

# Multi-channel case in 2023

## The $\Sigma_c^{(*)}\bar{D}^{(*)}$ molecular picture

Liu et.al., PRL122(2019)242001

| Scenario | Molecule | $J^P$ | B (MeV) | M (MeV) |
|---|---|---|---|---|
| $A$ | $\bar{D}\Sigma_c$ | $\frac{1}{2}^-$ | 7.8 – 9.0 | 4311.8 – 4313.0 |
| $A$ | $\bar{D}\Sigma_c^*$ | $\frac{3}{2}^-$ | 8.3 – 9.2 | 4376.1 – 4377.0 |
| $A$ | $\bar{D}^*\Sigma_c$ | $\frac{1}{2}^-$ | Input | 4440.3 |
| $A$ | $\bar{D}^*\Sigma_c$ | $\frac{3}{2}^-$ | Input | 4457.3 |
| $A$ | $\bar{D}^*\Sigma_c^*$ | $\frac{1}{2}^-$ | 25.7 – 26.5 | 4500.2 – 4501.0 |
| $A$ | $\bar{D}^*\Sigma_c^*$ | $\frac{3}{2}^-$ | 15.9 – 16.1 | 4510.6 – 4510.8 |
| $A$ | $\bar{D}^*\Sigma_c^*$ | $\frac{5}{2}^-$ | 3.2 – 3.5 | 4523.3 – 4523.6 |
| $B$ | $\bar{D}\Sigma_c$ | $\frac{1}{2}^-$ | 13.1 – 14.5 | 4306.3 – 4307.7 |
| $B$ | $\bar{D}\Sigma_c^*$ | $\frac{3}{2}^-$ | 13.6 – 14.8 | 4370.5 – 4371.7 |
| $B$ | $\bar{D}^*\Sigma_c$ | $\frac{1}{2}^-$ | Input | 4457.3 |
| $B$ | $\bar{D}^*\Sigma_c$ | $\frac{3}{2}^-$ | Input | 4440.3 |
| $B$ | $\bar{D}^*\Sigma_c^*$ | $\frac{1}{2}^-$ | 3.1 – 3.5 | 4523.2 – 4523.6 |
| $B$ | $\bar{D}^*\Sigma_c^*$ | $\frac{3}{2}^-$ | 10.1 – 10.2 | 4516.5 – 4516.6 |
| $B$ | $\bar{D}^*\Sigma_c^*$ | $\frac{5}{2}^-$ | 25.7 – 26.5 | 4500.2 – 4501.0 |

- Two parameters determined by $P_c(4440)$, $P_c(4457)$
- Two solutions

Solution A ( $\chi^2$/d.o.f. = 1.01)

Solution B ( $\chi^2$/d.o.f. = 1.03)

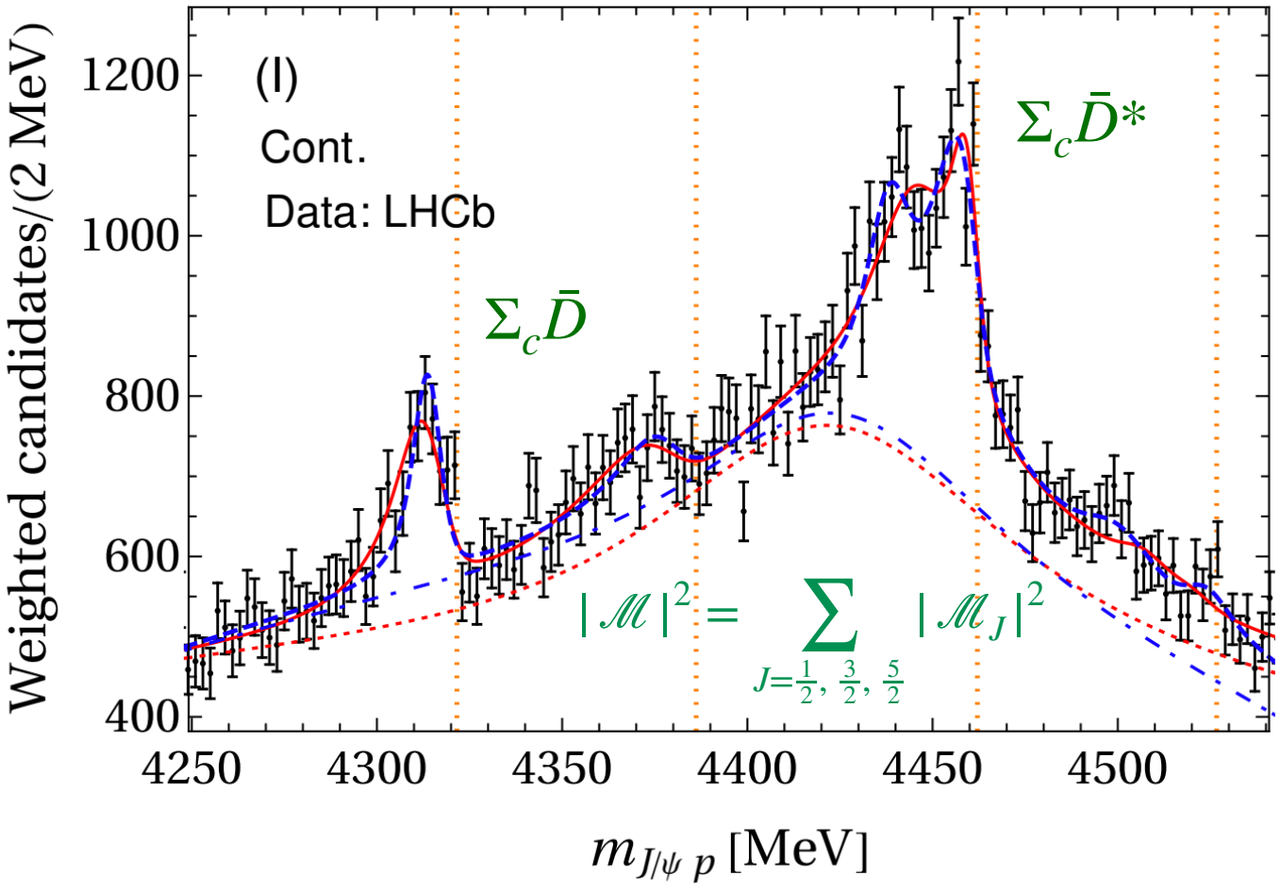


- Two parameters $g_S$, $g_D$ for $J/\psi p$, $\eta_c p$
- Predict pole positions accurately
- $\chi^2_A < \chi^2_B$
- The effect of each data point is different

**Du, Baru, Guo, Hanhart, Meißner**, Oller, **QW,** PRL124(2020)072001

# Multi-channel case in 2023

## The $\Sigma_c^{(*)}\bar{D}^{(*)}$ molecular picture

Liu et.al., PRL122(2019)242001

| Scenario | Molecule | $J^P$ | B (MeV) | M (MeV) |
|---|---|---|---|---|
| $A$ | $\bar{D}\Sigma_c$ | $\frac{1}{2}^-$ | 7.8 – 9.0 | 4311.8 – 4313.0 |
| $A$ | $\bar{D}\Sigma_c^*$ | $\frac{3}{2}^-$ | 8.3 – 9.2 | 4376.1 – 4377.0 |
| $A$ | $\bar{D}^*\Sigma_c$ | $\frac{1}{2}^-$ | Input | 4440.3 |
| $A$ | $\bar{D}^*\Sigma_c$ | $\frac{3}{2}^-$ | Input | 4457.3 |
| $A$ | $\bar{D}^*\Sigma_c^*$ | $\frac{1}{2}^-$ | 25.7 – 26.5 | 4500.2 – 4501.0 |
| $A$ | $\bar{D}^*\Sigma_c^*$ | $\frac{3}{2}^-$ | 15.9 – 16.1 | 4510.6 – 4510.8 |
| $A$ | $\bar{D}^*\Sigma_c^*$ | $\frac{5}{2}^-$ | 3.2 – 3.5 | 4523.3 – 4523.6 |
| $B$ | $\bar{D}\Sigma_c$ | $\frac{1}{2}^-$ | 13.1 – 14.5 | 4306.3 – 4307.7 |
| $B$ | $\bar{D}\Sigma_c^*$ | $\frac{3}{2}^-$ | 13.6 – 14.8 | 4370.5 – 4371.7 |
| $B$ | $\bar{D}^*\Sigma_c$ | $\frac{1}{2}^-$ | Input | 4457.3 |
| $B$ | $\bar{D}^*\Sigma_c$ | $\frac{3}{2}^-$ | Input | 4440.3 |
| $B$ | $\bar{D}^*\Sigma_c^*$ | $\frac{1}{2}^-$ | 3.1 – 3.5 | 4523.2 – 4523.6 |
| $B$ | $\bar{D}^*\Sigma_c^*$ | $\frac{3}{2}^-$ | 10.1 – 10.2 | 4516.5 – 4516.6 |
| $B$ | $\bar{D}^*\Sigma_c^*$ | $\frac{5}{2}^-$ | 25.7 – 26.5 | 4500.2 – 4501.0 |

- Two parameters determined by $P_c(4440),\ P_c(4457)$
- Two solutions

Solution A ( $\chi^2$/d.o.f. = 1.01)

Solution B ( $\chi^2$/d.o.f. = 1.03)

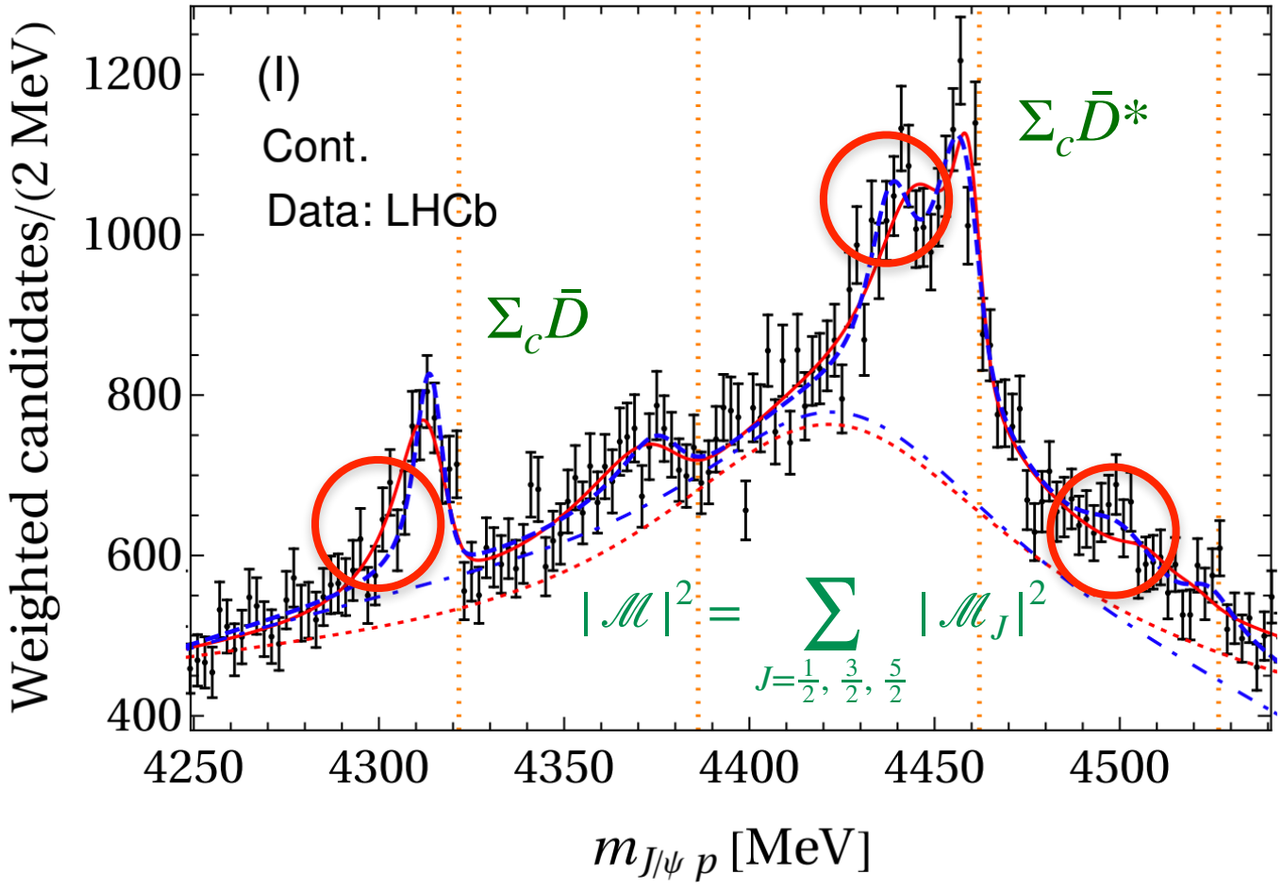


- Two parameters $g_S,\ g_D$ for $J/\psi p,\ \eta_c p$
- Predict pole positions accurately
- $\chi^2_A < \chi^2_B$
- The effect of each data point is different

**Du, Baru, Guo, Hanhart, Meißner**, Oller, **QW,** PRL124(2020)072001

# Multi-channel case in 2023

LHCb, PRL122(2019)222001

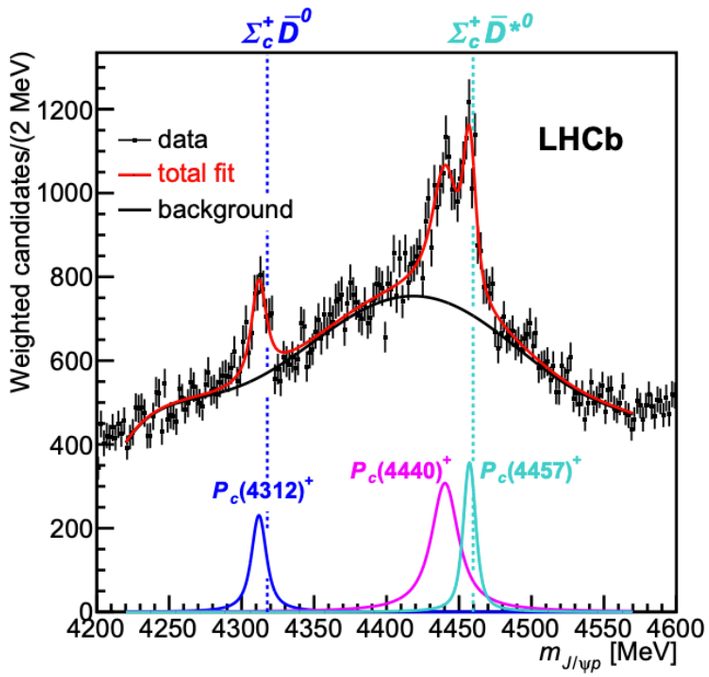


## The $\Sigma_c^{(*)}\bar{D}^{(*)}$ molecular picture

- $P_c(4312)$ bound state or virtual state?
- Spin assignment of $P_c(4440)$ and $P_c(4457)$?
- The pole situations for all the $P_c$ states?
- Whether NN approach obtains more than the normal fitting approach?

LO HQEFT, **Du, Baru, Guo, Hanhart, Meißner**, Oller, **QW,** PRL124(2020)072001

## The decay amplitude for $\Lambda_b \to J/\psi p K^-$ process

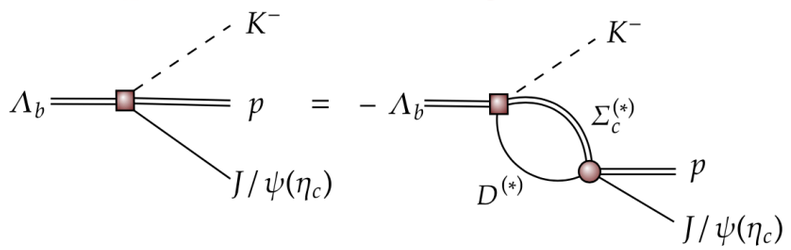


Zhang, Liu, Hu, **QW, Meißner**, Sci.Bull.68(2023)981-989

## The decay amplitude for $\Lambda_b \to \Sigma_c^{(*)}\bar{D}^{(*)}K^-$ process

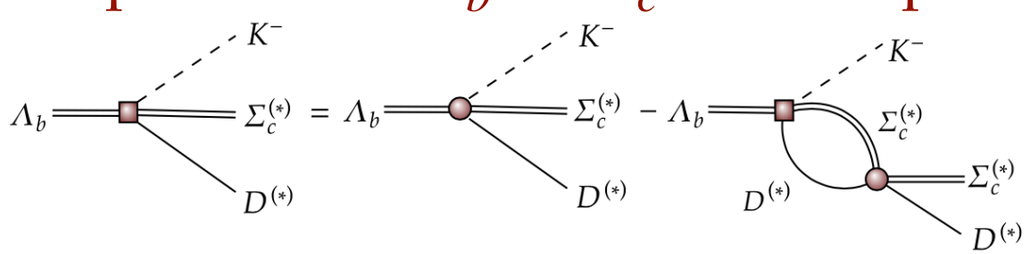

# Multi-channel case in 2023

## States and labels

- "+" and "-" for phy. and unphy. sheets
- $\frac{1}{2}^-$ dyn. Channels: $\Sigma_c\bar{D}$, $\Sigma_c\bar{D}^*$, $\Sigma_c^*\bar{D}^*$
- $\frac{3}{2}^-$ dyn. Channels: $\Sigma_c^*\bar{D}$, $\Sigma_c\bar{D}^*$, $\Sigma_c^*\bar{D}^*$
- $\frac{5}{2}^-$ dyn. Channel: $\Sigma_c^*\bar{D}^*$

LHCb, PRL122(2019)222001

Bound state for $J = \frac{1}{2}, \frac{3}{2}, \frac{5}{2}$ channels

Solution B 0000

States for 3-channel case

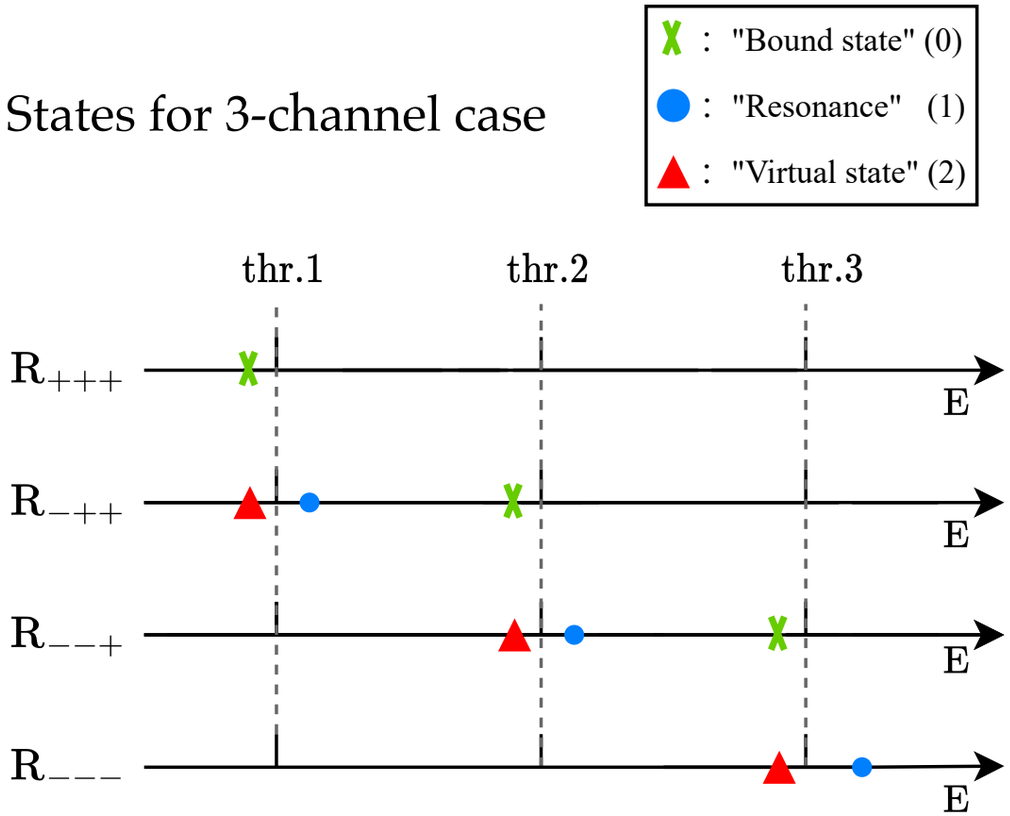


States for 1-channel case

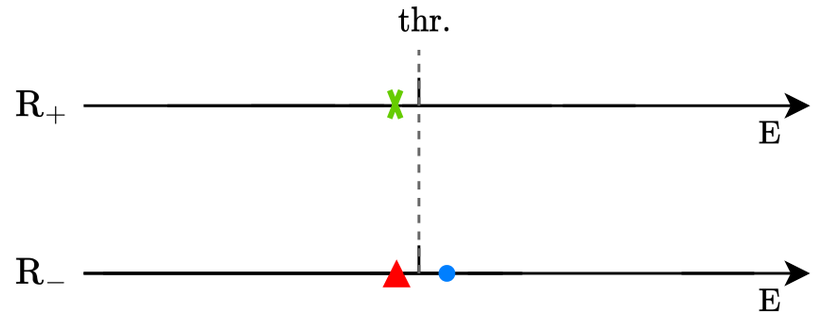


Zhang, Liu, Hu, **QW, Meißner**, Sci.Bull.68(2023)981-989

- Mass label 1 and 0 for $J_{P_c(4440)} = \frac{1}{2}$, $J_{P_c(4457)} = \frac{3}{2}$ and $J_{P_c(4440)} = \frac{3}{2}$, $J_{P_c(4457)} = \frac{1}{2}$,

i.e. solution A and B in PRL122(2019)242001, PRL124(2020)072001, JHEP08(2021)157

# Multi-channel case in 2023

## Training and verification

240184 samples

| Mass Relation Label | State Label | Number of Samples |
|---|---|---|
| 0 | 000 | 46951 |
| 1 | 000 | 4283 |
| 1 | 001 | 1260 |
| 1 | 002 | 4360 |
| 0 | 100 | 3740 |
| 0 | 110 | 4320 |
| 0 | 111 | 7520 |
| 1 | 111 | 360 |
| 0 | 200 | 9590 |
| 1 | 200 | 280 |
| 1 | 210 | 3980 |
| 1 | 211 | 2690 |
| 1 | 220 | 50240 |
| 1 | 221 | 50512 |
| 1 | 222 | 50098 |

Predicted probability

| Output(%) / Label / NN | 0000 | 1000 | 1001 | 1002 | 100X | others |
|---|---|---|---|---|---|---|
| prediction of NN trained with $\{S^{90}\}$ samples. | | | | | | |
| NN 1 | 0.69 | 89.13 | 1.42 | 8.75 | 99.30 | 0.01 |
| NN 2 | 0.03 | 5.83 | 38.47 | 55.30 | 99.60 | 0.37 |
| NN 3 | 0.03 | 5.39 | 15.79 | 78.41 | 99.59 | 0.11 |
| NN 4 | 0.01 | 1.9 | 27.01 | 70.95 | 99.86 | 0.13 |
| NN 5 | 2.40 | 94.45 | 0.15 | 2.99 | 97.59 | 0.01 |
| 5 NNs Average | 0.63(1.03) | 39.34 | 16.57 | 43.28 | 99.19(0.91) | 0.13(0.15) |
| 10 NNs Average | 0.36(0.74) | 21.16 | 20.69 | 57.62 | 99.47(0.68) | 0.12(0.13) |
| prediction of NN trained with $\{S^{92}\}$ samples. | | | | | | |
| NN 1 | 0.00 | 0.15 | 5.37 | 94.47 | 99.99 | 0.00 |
| NN 2 | 0.00 | 0.07 | 4.11 | 95.81 | 99.99 | 0.00 |
| NN 3 | 0.00 | 0.78 | 13.57 | 85.61 | 99.96 | 0.03 |
| NN 4 | 0.00 | 0.81 | 19.02 | 80.16 | 99.99 | 0.00 |
| NN 5 | 0.14 | 15.13 | 16.91 | 67.80 | 99.84 | 0.00 |
| 5 NNs Average | 0.03(0.06) | 3.39 | 11.80 | 84.77 | 99.95(0.06) | 0.01(0.01) |
| 10 NNs Average | 0.01(0.04) | 1.78 | 9.50 | 88.70 | 99.97(0.04) | 0.00(0.01) |

- 5 and 10 NN models with an identical structure under different initialization
- The uncertainties decrease with the increasing number of NNs
- Top 3 probabilities, 1000,1001,1002 favor solution A
- Bound states in $J^P = \frac{1}{2}^-, \frac{3}{2}^-$ channels, Undetermined for $J^P = \frac{5}{2}^-$ channel
- The NNs successfully retrieve the state label with an accuracy (standard deviation) of

$75.91(1.18)\%$, $73.14(1.05)\%$, $65.25(1.80)\%$, $54.35(2.32)\%$ for the samples $\{\mathcal{S}^{90}\}, \{\mathcal{S}^{92}\}, \{\mathcal{S}^{94}\}, \{\mathcal{S}^{96}\}$

Zhang, Liu, Hu, **QW, Meißner**, Sci.Bull.68(2023)981-989

# Multi-channel case in 2023

## Why NN favors Solution A?

Generate 100 1xxx samples and 100 0xxx samples

Reduced chisq from the normal fitting

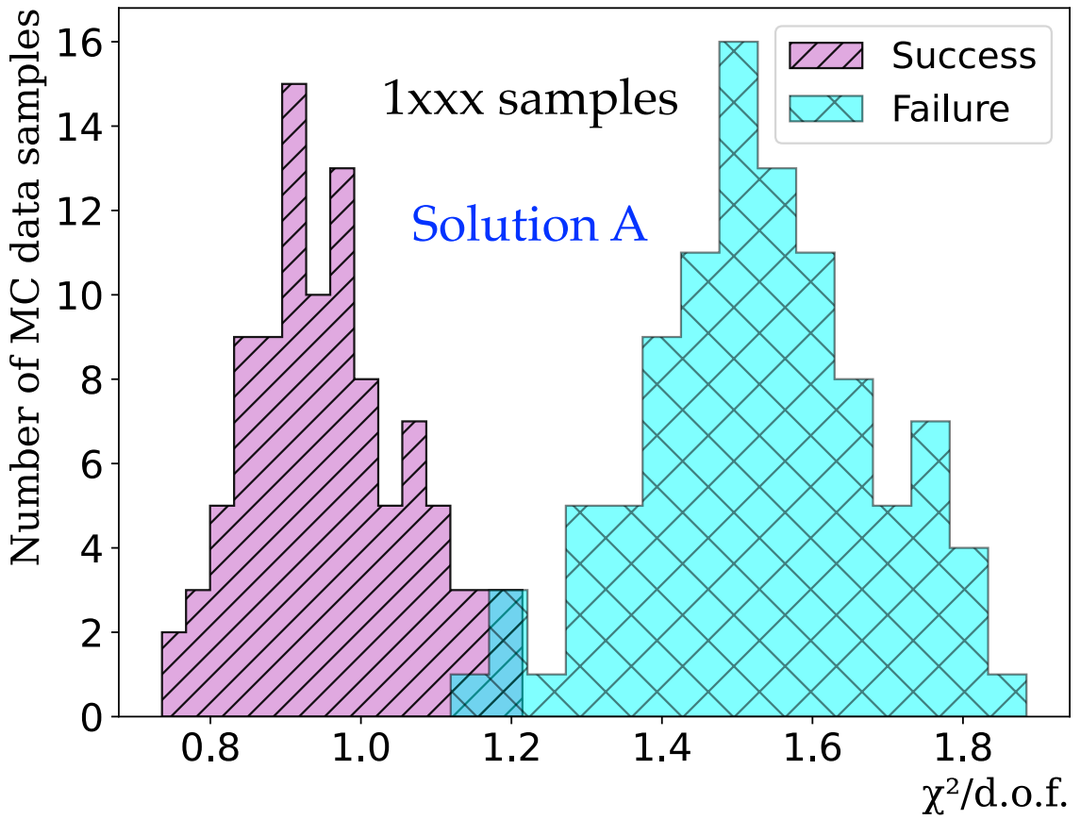


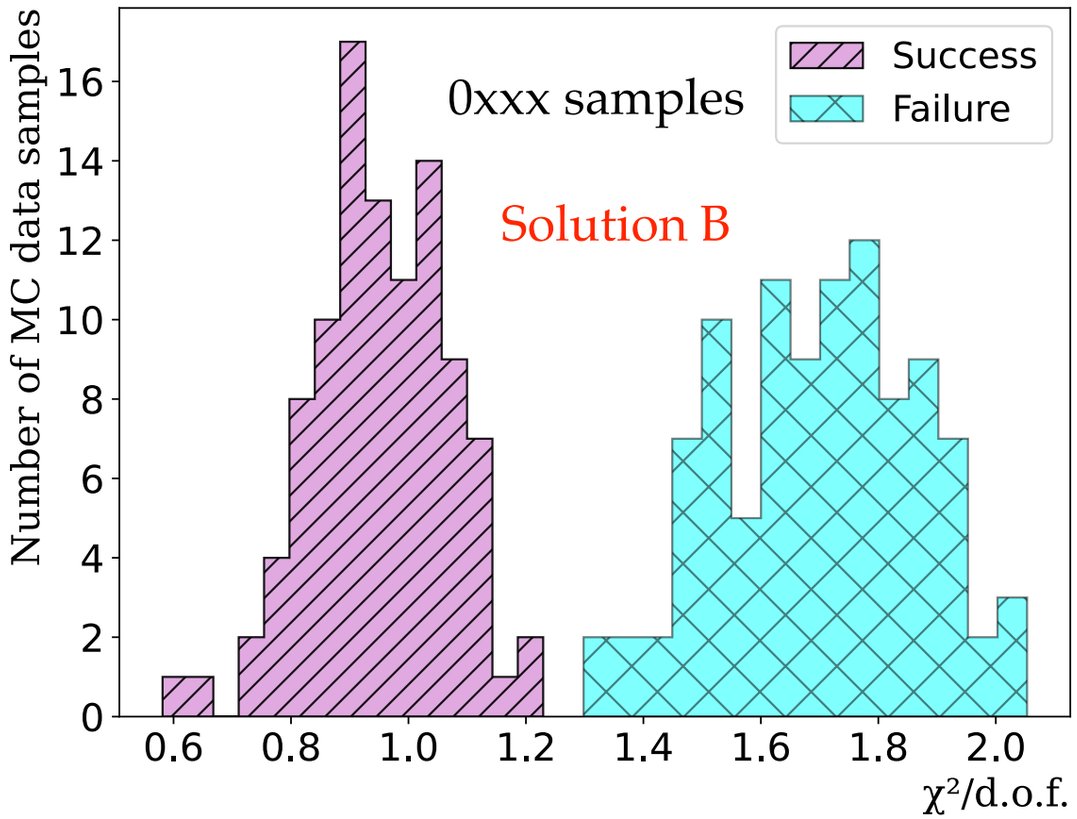


- A 3% misidentification for 1xxx samples

Zhang, Liu, Hu, **QW, Meißner**, Sci.Bull.68(2023)981-989

# Multi-channel case in 2023

## Why NN favors Solution A?

Generate 100 1xxx samples and 100 0xxx samples

Probabilities from NN

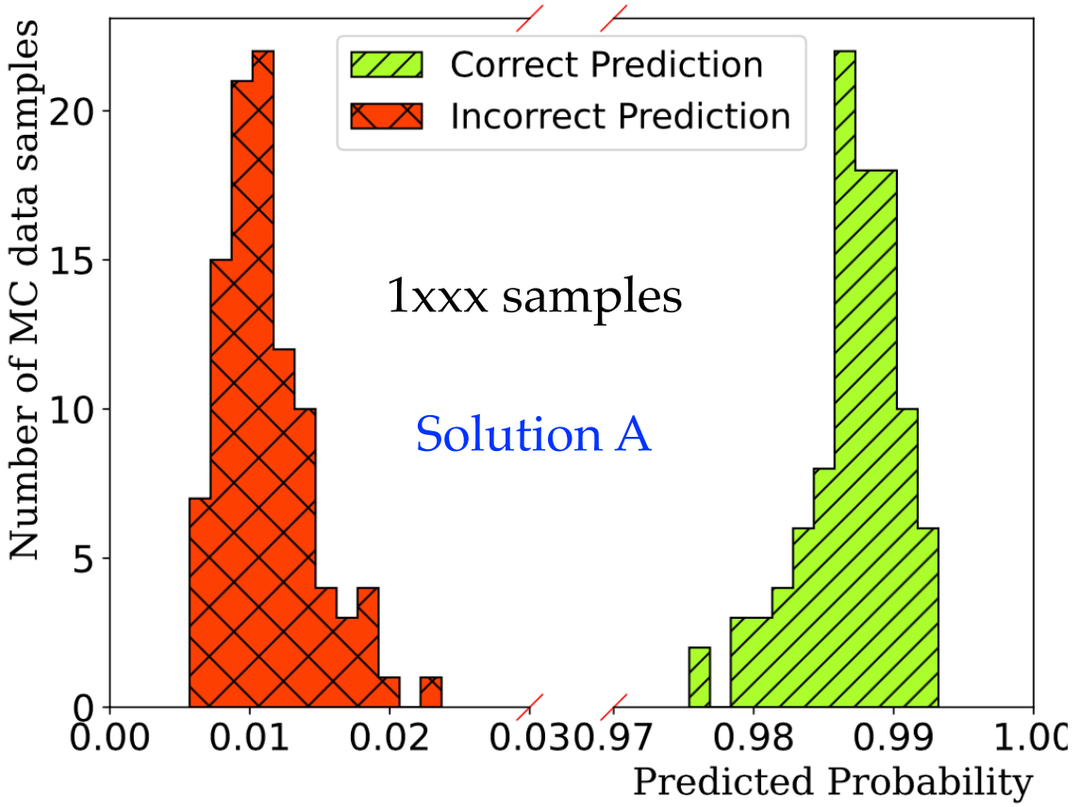


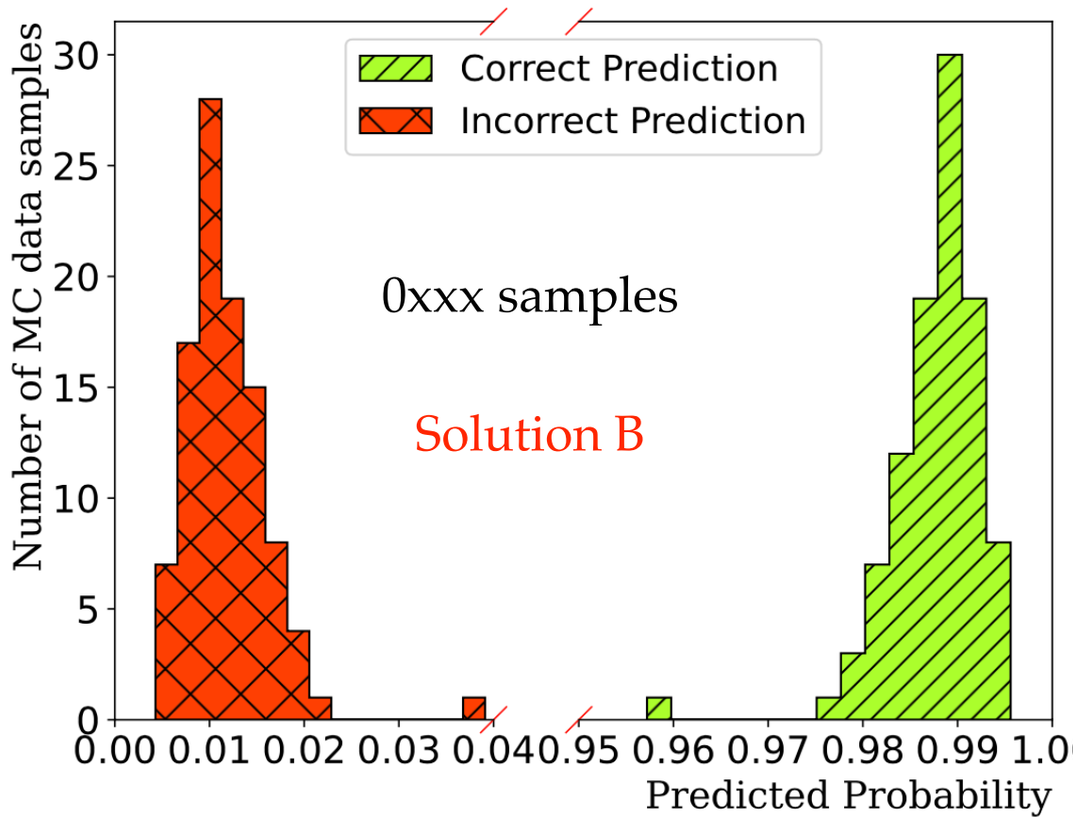


- The NN can make a good prediction
- The two solutions are well distinguished for both samples

Zhang, Liu, Hu, **QW, Meißner**, Sci.Bull.68(2023)981-989

# Multi-channel case in 2023

## The impact of each experimental data point in NN

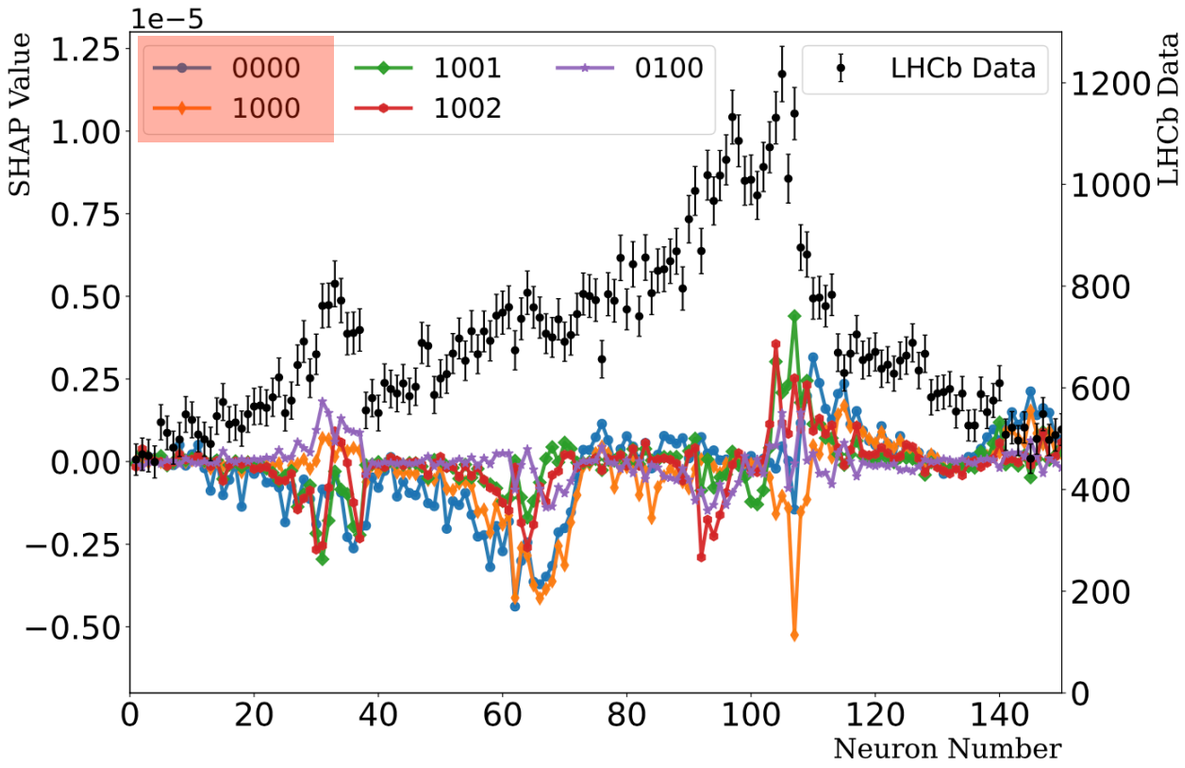


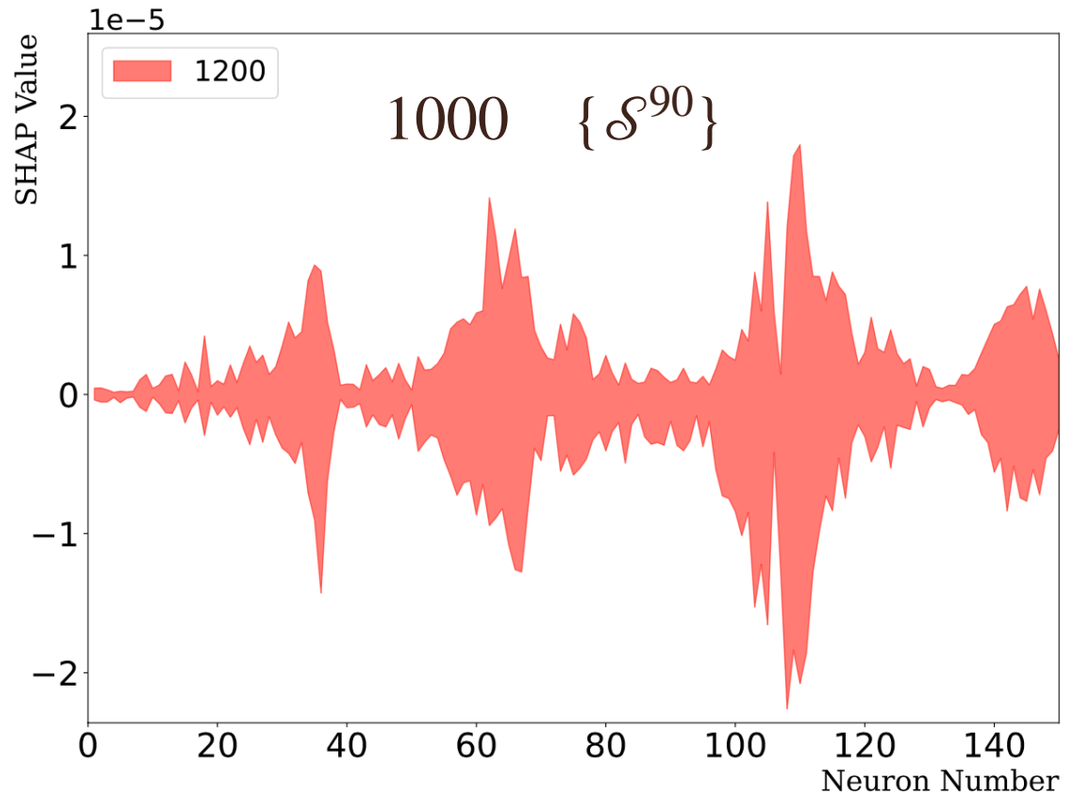


- The Shapley Additive exPlanation (SHAP) is investigated.
- A positive (negative) SHAP value indicates that a given data point is pushing the NN classification in favor of (against) a given class.
- The data points around the peaks in the mass spectrum have a greater impact.

Zhang, Liu, Hu, **QW, Meißner,** Sci.Bull.68(2023)981-989

# Multi-channel case in 2023

## The impact of each experimental data point in NN

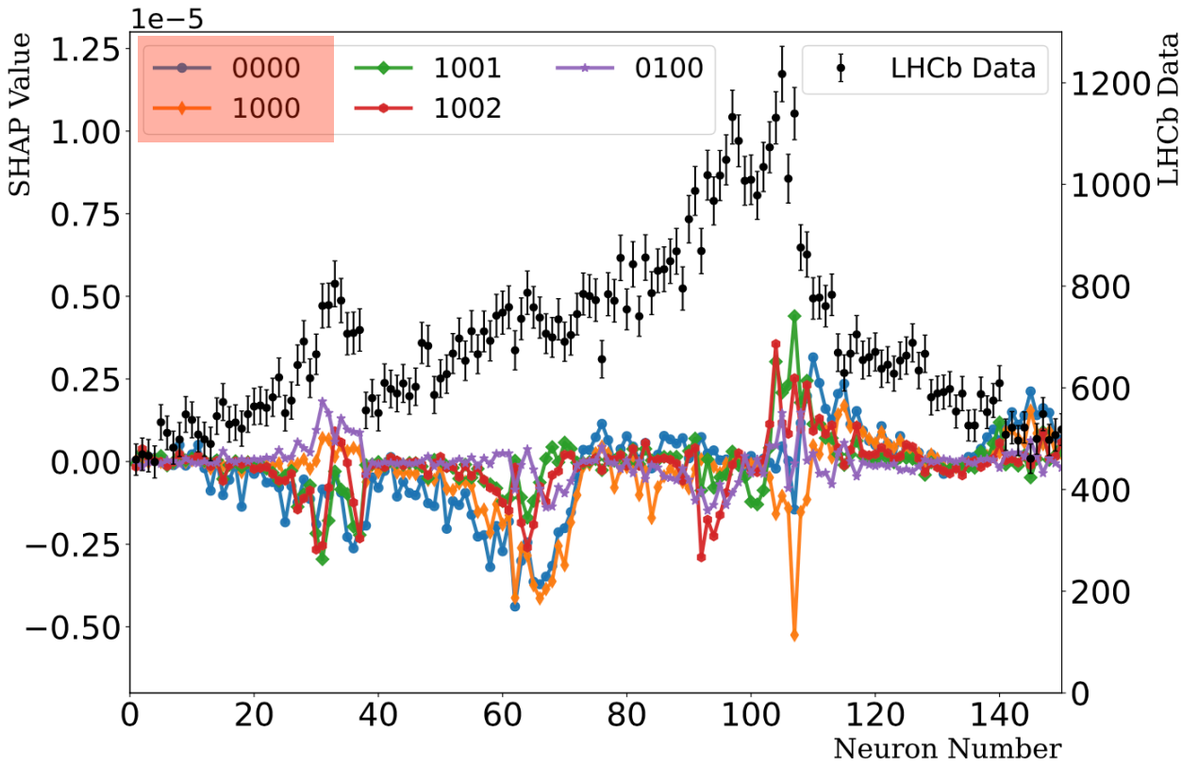


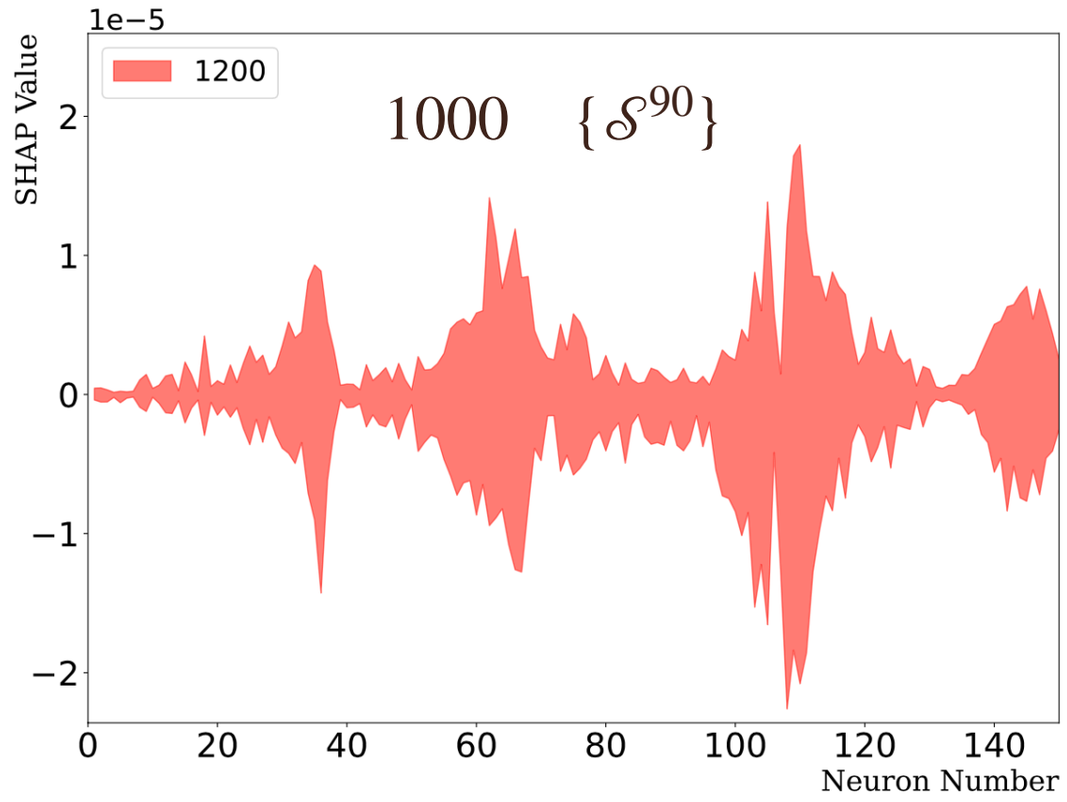


- The Shapley Additive exPlanation (SHAP) is investigated.
- A positive (negative) SHAP value indicates that a given data point is pushing the NN classification in favor of (against) a given class.

**ML can extract more information than normal fitting approach**

Zhang, Liu, Hu, **QW, Meißner,** Sci.Bull.68(2023)981-989

# Multi-channel case

The impact of each experimental data point in normal fitting

A analogous quantity

$$\Delta U_i \equiv \left| \frac{\mathscr{P}_i(\text{on}) - \mathscr{P}_i(\text{off})}{\mathscr{P}_i(\text{on})} \right| \text{for the ith para.}$$

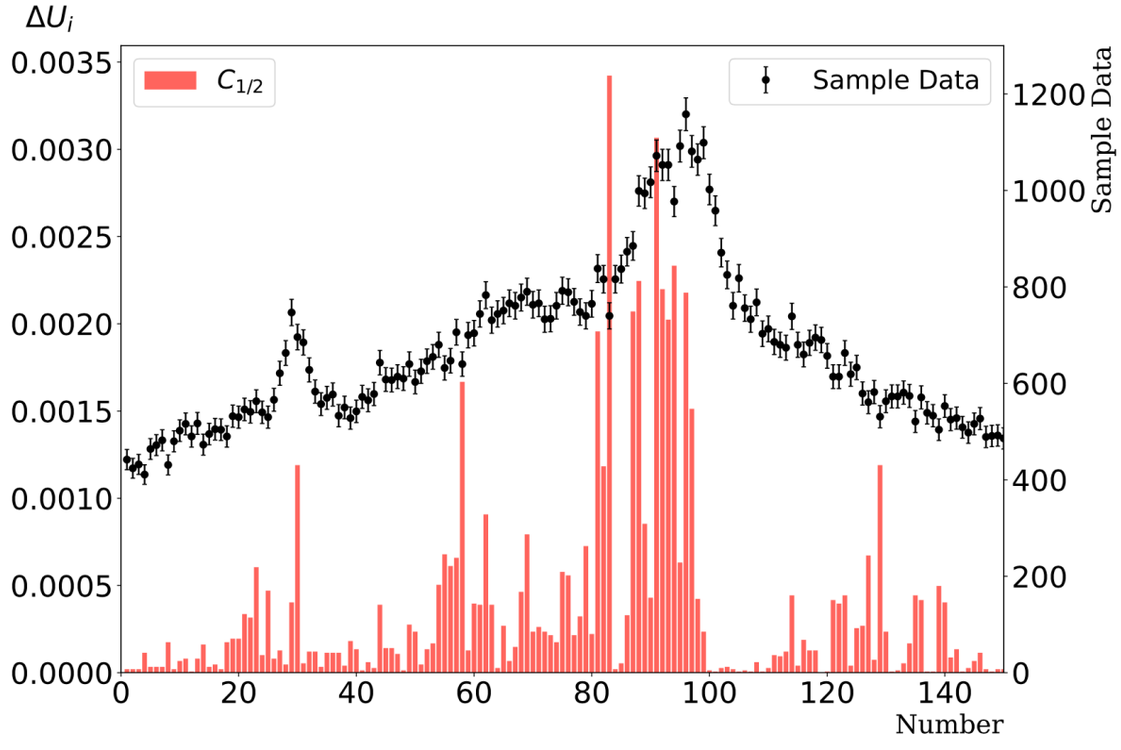


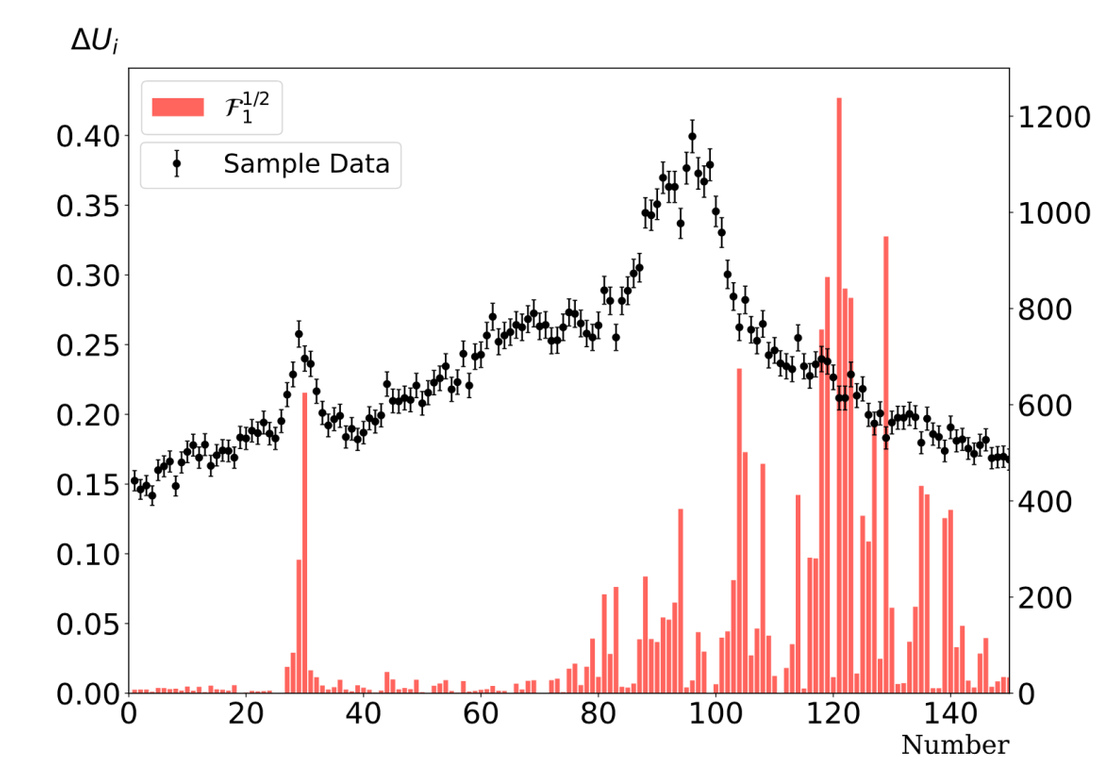


- The bins near threshold do not show strong constraints on parameters due to the large correlation among the parameters
- Data at higher energy have large constraints on the production parameters

Zhang, Liu, Hu, **QW,** Meißner, Sci.Bull.68(2023)981-989

# Multi-channel case

Zhang, Liu, Hu, **QW,** Meißner, Sci.Bull.68(2023)981-989

## The impact of each experimental data point in normal fitting

Another analogous quantity $\Delta U_i^{J^P} \equiv \left| \frac{\mathrm{Re[Pole}_i\mathrm{](on)} - \mathrm{Re[Pole}_i\mathrm{](off)}}{\mathrm{Re[Pole}_i\mathrm{](on)}} \right|$ for the ith pole

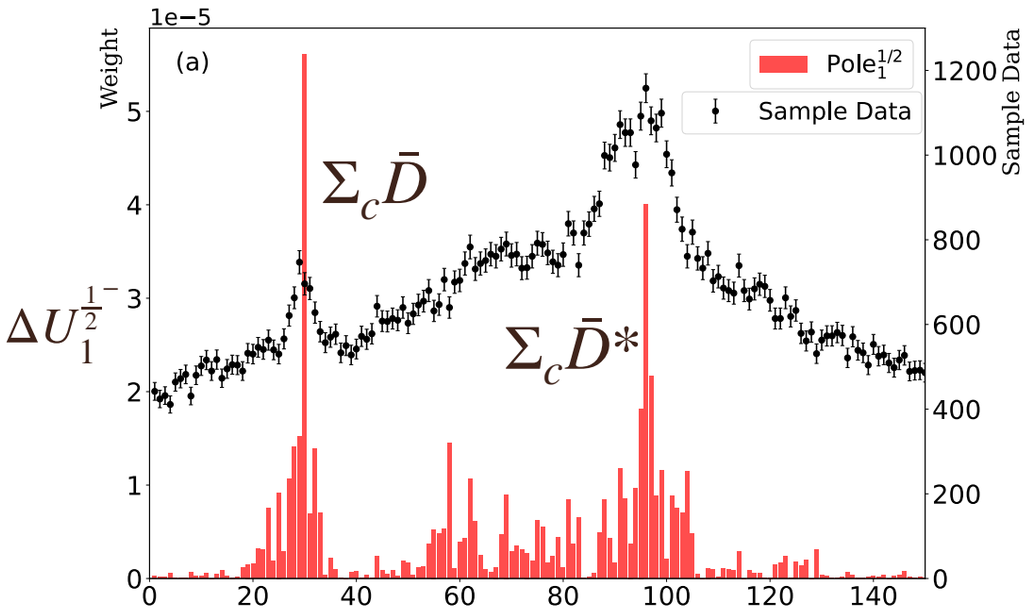


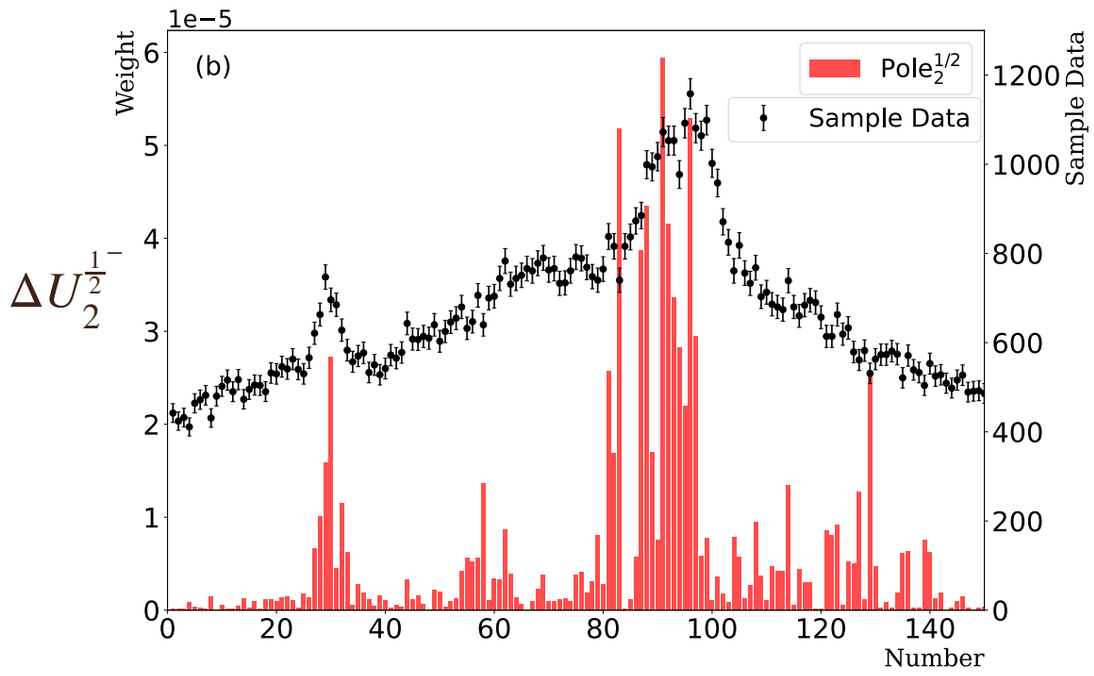


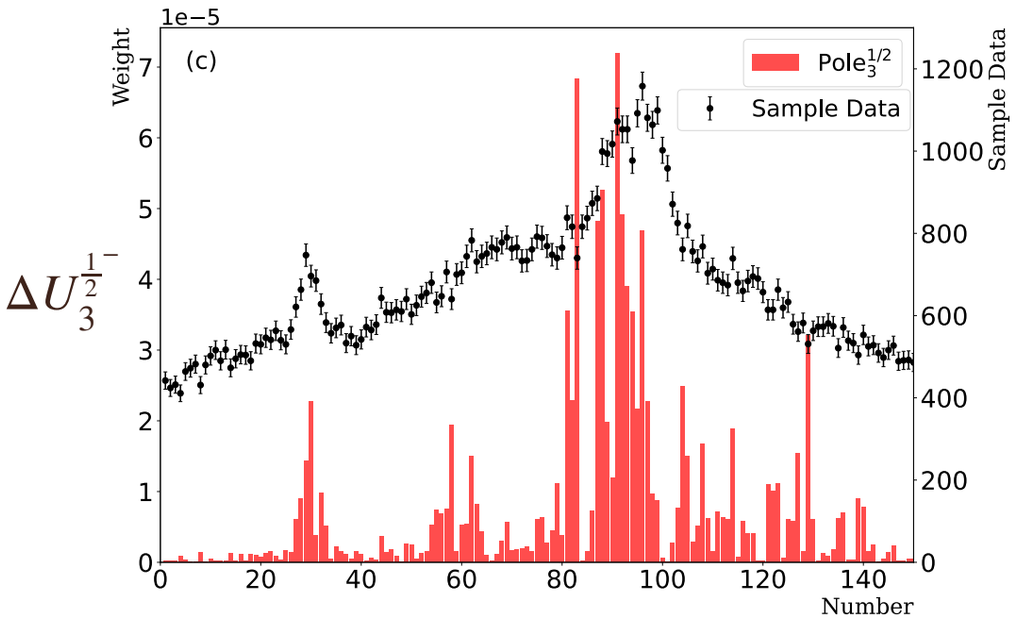


- The data around the $\Sigma_c\bar{D}$, $\Sigma_c\bar{D}*$ thresholds are more important
- The data around the $\Sigma_c^*\bar{D}*$ threshold are not important, due to its small production rate

# Multi-channel case

Zhang, Liu, Hu, **QW,** Meißner, Sci.Bull.68(2023)981-989

## The impact of each experimental data point in normal fitting

Another analogous quantity $\Delta U_i^{J^P} \equiv \left| \frac{\mathrm{Re[Pole}_i\mathrm{](on)} - \mathrm{Re[Pole}_i\mathrm{](off)}}{\mathrm{Re[Pole}_i\mathrm{](on)}} \right|$ for the ith pole

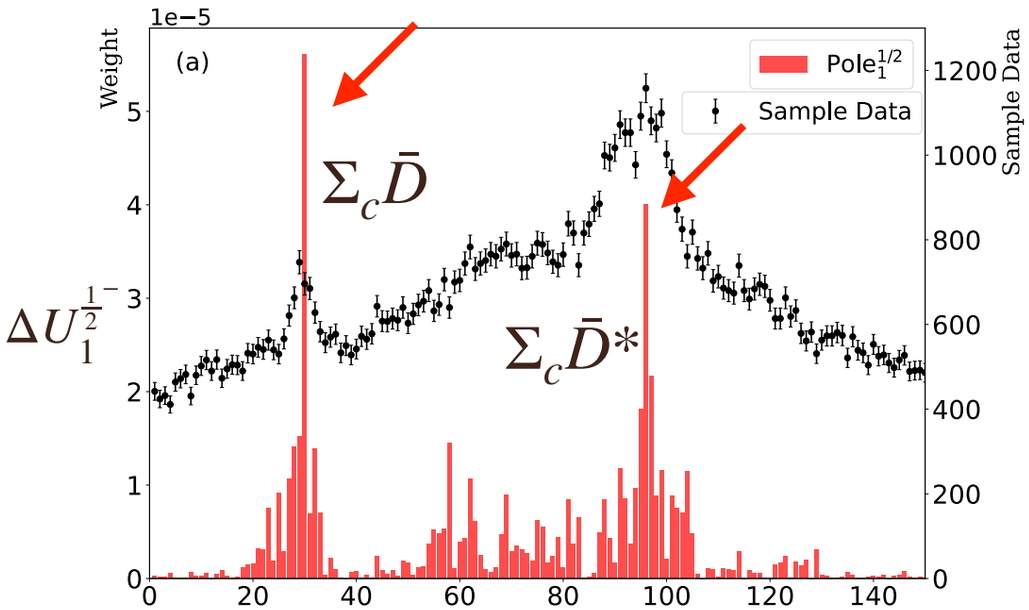


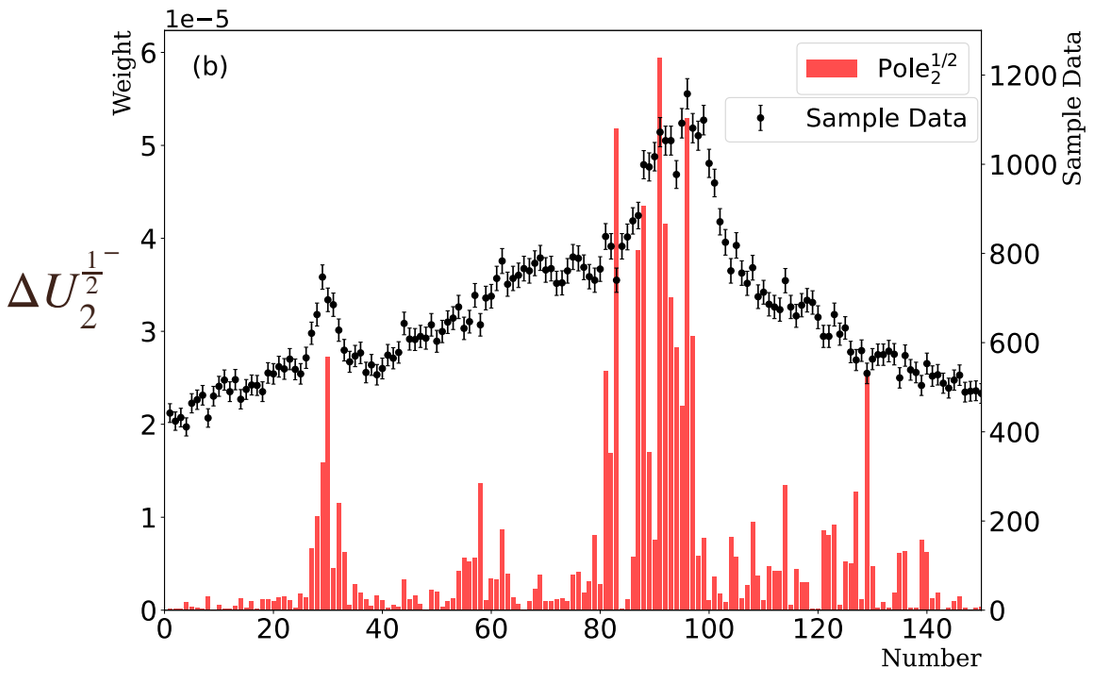


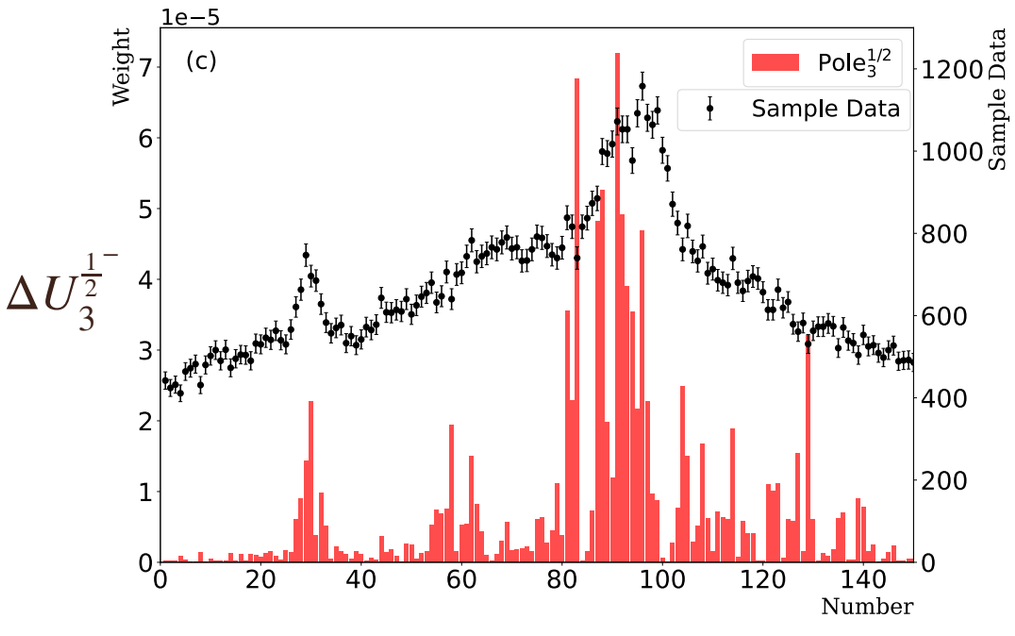


- The experimental data around the coupled-channels still have strong constraints on the physics

# Multi-channel case

Zhang, Liu, Hu, **QW,** Meißner, Sci.Bull.68(2023)981-989

## The impact of each experimental data point in normal fitting

Another analogous quantity $\Delta U_i^{J^P} \equiv \left| \frac{\mathrm{Re[Pole}_i\mathrm{](on)} - \mathrm{Re[Pole}_i\mathrm{](off)}}{\mathrm{Re[Pole}_i\mathrm{](on)}} \right|$ for the ith pole

The 2nd pole in $J^P = \frac{1}{2}^-$

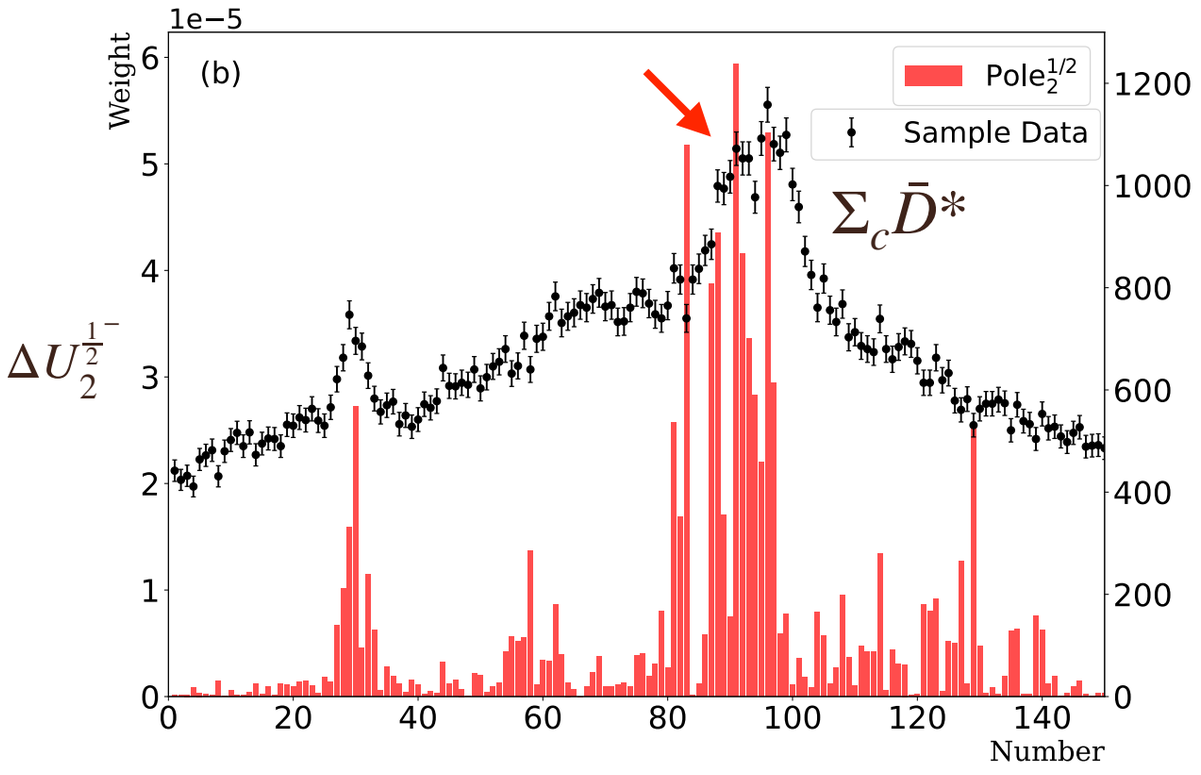


data around Pc(4440) have large constraints

The 2nd pole in $J^P = \frac{3}{2}^-$

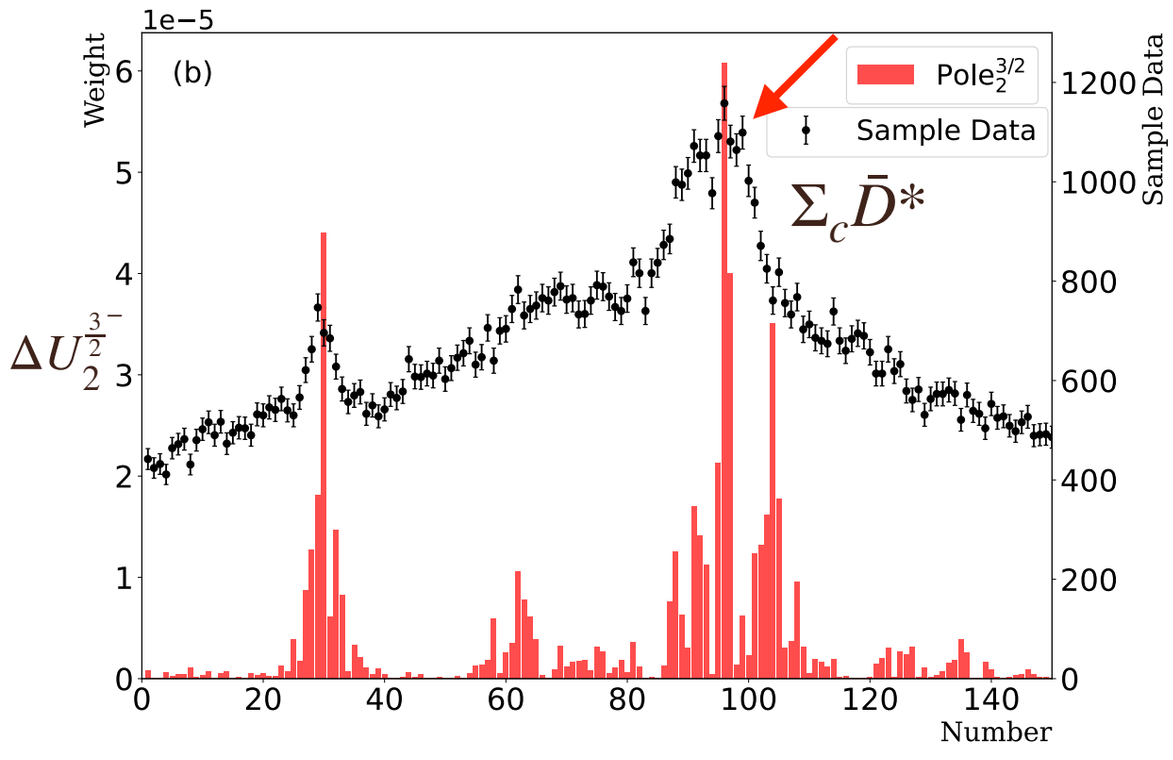


data around Pc(4457) have large constraints

- The sample corresponds to Solution A

# Three-body system on the lattice in 2024

## Many-body system

Science

Current Issue First release papers Archive About Submit manuscript

HOME > SCIENCE > VOL. 177, NO. 4047 > MORE IS DIFFERENT

ARTICLE

**More Is Different:** Broken symmetry and

P. W. ANDERSON Authors Info & Affiliations

*SCIENCE* • 4 Aug 1972 • Vol 177, Issue 4047 • pp. 393-396 • DOI: 10.1126/science.177.404

**Three ways to decipher the nature of exotic hadrons: Multiplets, three-body hadronic molecules, and correlation functions** #52

Ming-Zhu Liu (Lanzhou U. (main)), Ya-Wen Pan (Beihang U.), Zhi-Wei Liu (Beihang U.), Tian-Wei Wu (SYSU, Guangzhou), Jun-Xu Lu (Beihang U.) et al. (Apr 9, 2024)

Published in: *Phys.Rept.* 1108 (2025) 1-108 • e-Print: 2404.06399 [hep-ph]

pdf DOI cite claim reference search 71 citations

E. Oset, T. Hyodo, K.P. Khemchandani, A. Martinez Torres, L.S. Geng, C.W. Xiao, M.P. Valderramma, A. Hosaka, F.K. Guo……

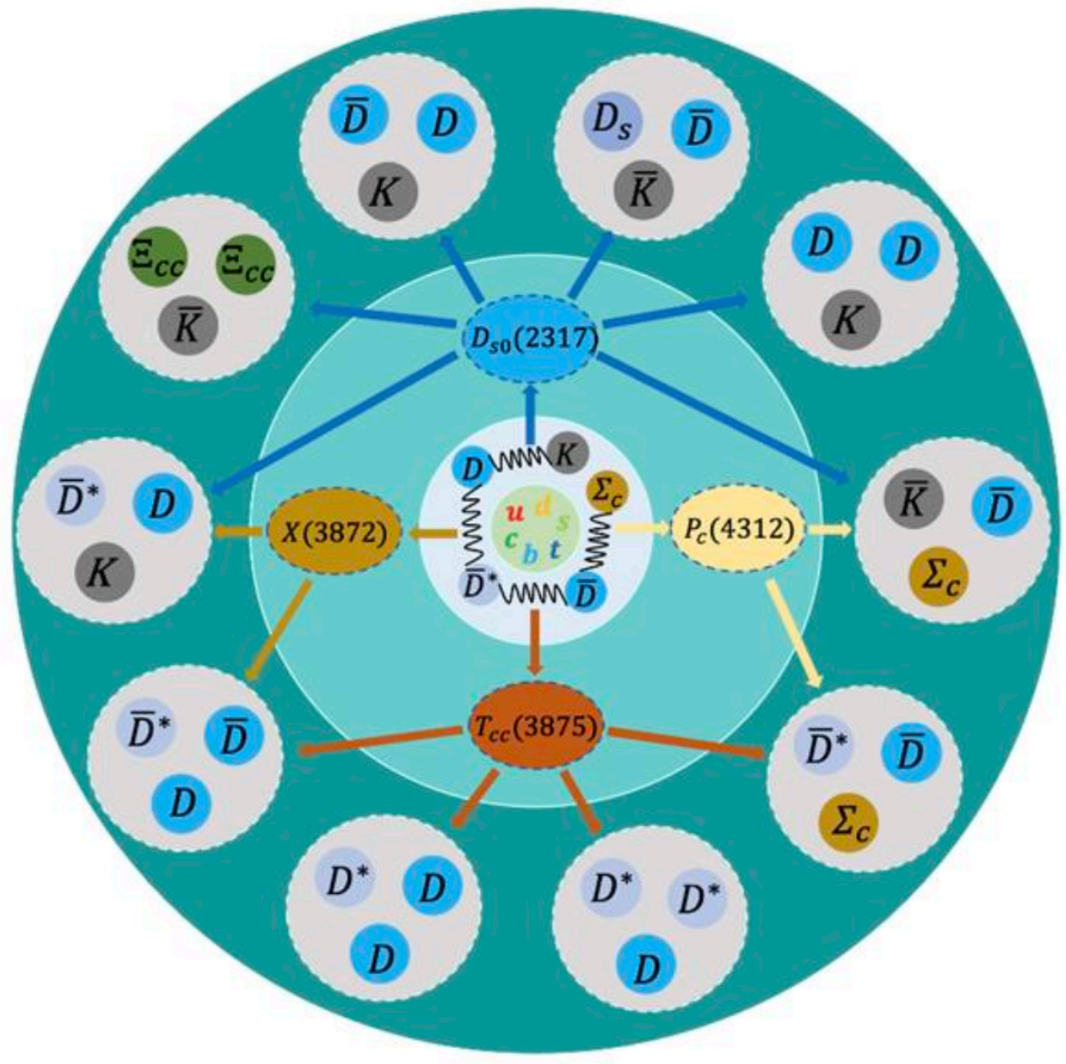


Liu et al., Phys.Rept.1108(2025)1

Wu et al., Sci.Bull.67(2022)1735-1738

# Three-body system on the lattice in 2024

## Applications in Hadron Physics

TABLE XXXIX. Summary for heavy-flavor three-body states. Energies are in units of MeV.

| Components | $I(J^P)$ | Results (Method) | Decay modes |
|---|---|---|---|
| $DNN$ | $\frac{1}{2}(0^-)$ | BS $\sim 3500-15i$ (FCA, V) [836] | $\Lambda_c\pi^- p, \Lambda_c p$ [836] |
| $NDK, NDar{K}, NDar{D}$ | $\frac{1}{2}(\frac{1}{2}^+)$ | BS $\sim 3050, 3150, 4400$ (FCA) [837] | † |
| $DD^*N$ | $\frac{1}{2}(\frac{1}{2}^+, \frac{3}{2}^+)$ | BS $\sim 4773.2, 4790.7$ (GEM) [838] | $T_{cc}p, DDp+\pi(\gamma), \Xi_{cc}+\pi(\gamma)$, charmed baryon + charmed meson [838] |
| $DD^*N$ | $\frac{3}{2}(-)$ | difficult to form bound states (GEM) [838] | † |
| $DKar{K}$ | $\frac{1}{2}(0^-)$ | $D$-like state $\sim 2845.5$ (FCA) [821], $D$-like state $\sim 2900$ (QCDSR, $\chi$F) [839] | $\pi\pi D$ [821] |
| $DKK$ | $\frac{1}{2}(0^-)$ | no bound state (FCA) [821] | † |
| $Dar{K}\Sigma_c$ | $1(\frac{1}{2}^+)$ | BS $\sim 4738.6$ (GEM) [840] | $D\Xi', D_s\Sigma_c$ [840] |
| $D^{(*)}$ multi $\rho$ | ... | several $D_J^{(*)}$ states (FCA) [841, 842] | † |
| $\rho Dar{D}$ | $0(?), 1(?)$ | BS $\sim 4241-10i, [4320-13i, 4256-14i]$ (FCA) [843] | † |
| $DDK$ | $\frac{1}{2}(0^-)$ | BS $\sim 4162$ (GEM) [273], 4140 ($\chi$F) [819], 4160 (FV) [820] | $DD_s^*, D^*D_s$ [826] |
| $Dar{D}K$ | $\frac{1}{2}(0^-)$ | BS $\sim 4181.2$ (GEM) [822], 4191 (FCA) [825] | $D_sar{D}^*, J/\psi K$ [822] |
| $DD^*K$ | $\frac{1}{2}(1^-)$ | BS $\sim 4317.9$ (BO) [823] | † |
| $Dar{D}^*K$ | $\frac{1}{2}(1^-)$ | BS $\sim 4294.1$ (GEM) [822], 4317.9 (BO) [823], 4307 (FCA) [824] | $D_s^{(*)}ar{D}^{(*)}, J/\psi K^*$ [823, 844] |
| $D^*D^*ar{K}^*$ | $\frac{1}{2}(0^-, 1^-, 2^-)$ | $4845-40i$, BS $\sim [4850-46i, 4754-50i]$, (FCA) [845] $[4840-43i, 4755-50i]$ | $D^*D^*ar{K}^*$, $D^*D^{(*)}ar{K}^*$, $[D^*D^*ar{K}^*, D^*D^{(*)}ar{K}^*]$ [845] |
| $Dar{D}^*\Sigma_c$ | $1(\frac{1}{2}^+, \frac{3}{2}^+)$ | BS $\sim 6292.3, 6301.5$ (GEM) [829] | $J/\psi par{D}^{(*)}, ar{T}_{cc}\Lambda_c\pi$ [829] |
| $J/\psi Kar{K}$ | $0(1^-)$ | $Y(4260) \sim 4150-45i$ ($\chi$F) [481] | † |
| $DDD^*$ | $\frac{1}{2}(1^-)$ | BS $\sim 5742.2$ (GEM) [833] | $DDD\pi(\gamma)$[833] |
| $DD^*D^*$ | $\frac{1}{2}(0^-, 1^-, 2^-)$ | several loosely bound states (GEM) [834] | charmed mesons + ... [834] |
| $D^*D^*D^*$ | $\frac{1}{2}(0^-, 1^-, 2^-, 3^-)$ | several loosely bound states (GEM)[834] | charmed mesons + ... [834] |
| | $\frac{1}{2}(0^-, 1^-, 2^-)$ | BS $\sim 5790.9-49.8i, 5990.2, 5989.4$ (FCA) [835] | |
| $D^*D^*D^{(*)}$ | $\frac{3}{2}(-)$ | difficult to form bound states (GEM) [834] | † |
| $D^*D^*ar{D}$ | $\frac{1}{2}(2^-)$ | BS $\sim 5879$ (F) [846] | † |
| $D^*D^*ar{D}^*$ | $\frac{1}{2}(3^-)$ | BS $\sim 6019$ (F) [846] | † |
| $\Omega_{ccc}\Omega_{ccc}\Omega_{ccc}$ | $?(\frac{3}{2}^+)$ | no bound state (GEM) [847] | † |
| $\Xi_{cc}\Xi_{cc}ar{K}$ | $\frac{1}{2}(0^-)$ | BS $\sim 7641.8$ (GEM) [848] | † |

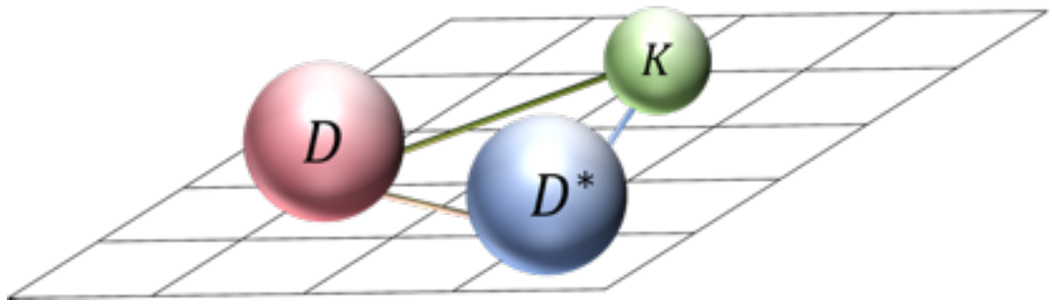


- Gaussian expansion method (GEM)
- QCD sum rule (QCDSR)
- Born-Oppenheimer approximation
- Fixed center approximation (FCA)
- Faddeev equation (F)

Without 3-body force!

Liu et al., Phys.Rept.1108(2025)1

# Three-body system on the lattice in 2024

**格点有效场论=有效场论+格点+蒙特卡洛**

(1) 有效场论描述强子相互作用(接触项+$\pi$交换势)

(2) 格点上强子作为基本自由度

(3) 格距a ≈ 1fm (手征对称性破缺极限)

(4) 非相对论下非连续极限计算

**解决低能多体问题!**

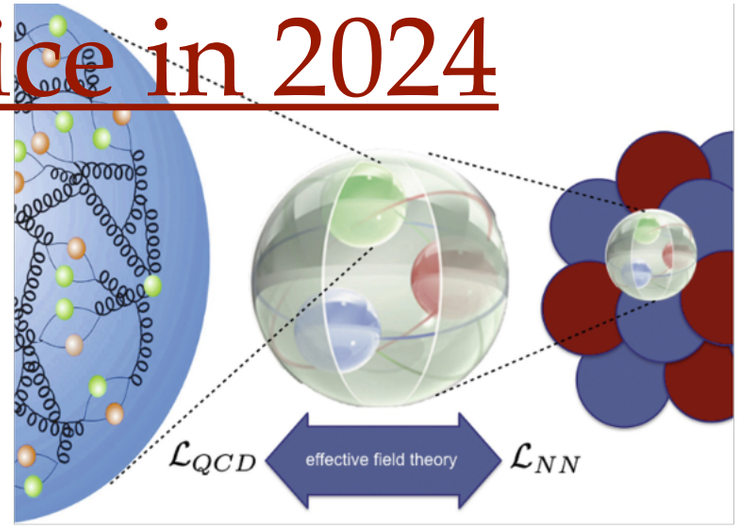


| | LQCD | LEFT |
|---|---|---|
| 自由度 | 夸克、胶子 | 强子 |
| 晶格间距 | ~0.1fm | ~1fm |
| 色散关系 | 相对论 | 非相对论 |
| 连续极限 | ✓ | ✖ |
| 出发点 | 拉格朗日量 | 薛定谔方程 |
| 求解方案 | 路径积分 | 矩阵计算 |

格点有效场论优势

(1)三体相互作用

格点有效场论可以自然引入三体相互作用。

(2)多体系统研究

在铅铅、金铅对撞下形成多核环境中奇特强子态的性质。

| $\Lambda$ (MeV) | 250 | 275 | 300 | 325 | 350 | 375 | 400 | Exp. |
|---|---|---|---|---|---|---|---|---|
| $c_E$ | 5.170 | 2.763 | 1.538 | 0.890 | 0.561 | 0.412 | 0.380 | |
| $E_{2NF}(^3H)$ | -6.17(4) | -6.63(4) | -7.05(2) | -7.39(2) | -7.64(1) | -7.77(1) | -7.78(1) | -8.482 |
| $E_{2NF+3NF}(^3H)$ | -8.482 | -8.482 | -8.489 | -8.485 | -8.483 | -8.483 | -8.483 | -8.482 |
| $E_{2NF}(^4He)$ | -30.6(7) | -30.3(6) | -30.7(4) | -30.0(4) | -29.8(4) | -29.4(4) | -29.2(4) | -28.34 |
| $E_{2NF+3NF}(^4He)$ | -29.8(7) | -29.5(6) | -29.9(4) | -29.2(4) | -29.0(4) | -28.6(4) | -28.4(4) | -28.34 |
| $E_{2NF}(^{16}O)$ | -144.0(21) | -135.1(14) | -136.3(11) | -139.1(9) | -140.6(8) | -141.7(8) | -141.8(9) | -127.6 |
| $E_{2NF+3NF}(^{16}O)$ | -135.8(20) | -124.8(14) | -124.5(11) | -126.3(9) | -127.3(8) | -128.1(8) | -128.1(8) | -127.6 |

多核子系统下基态能量

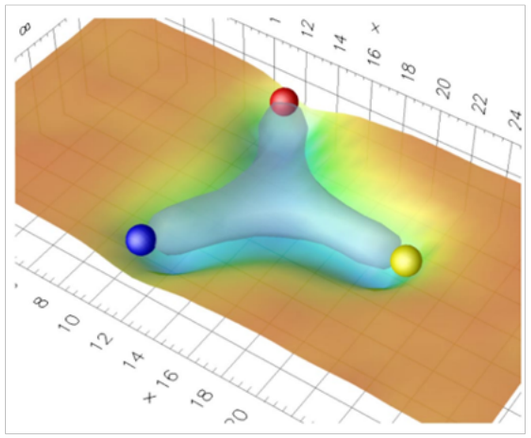

三夸克系统下色通量管结构

# Three-body system on the lattice in 2024

为什么选择$DD^*K$系统研究?

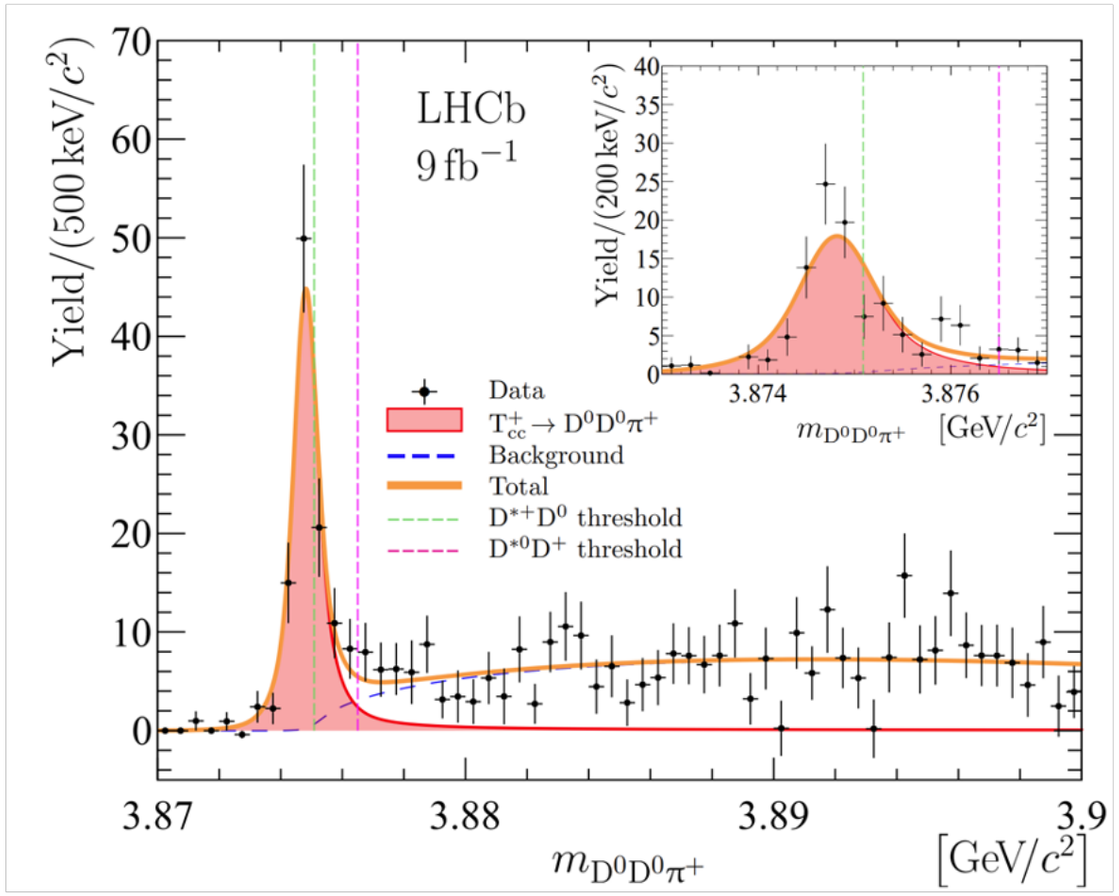


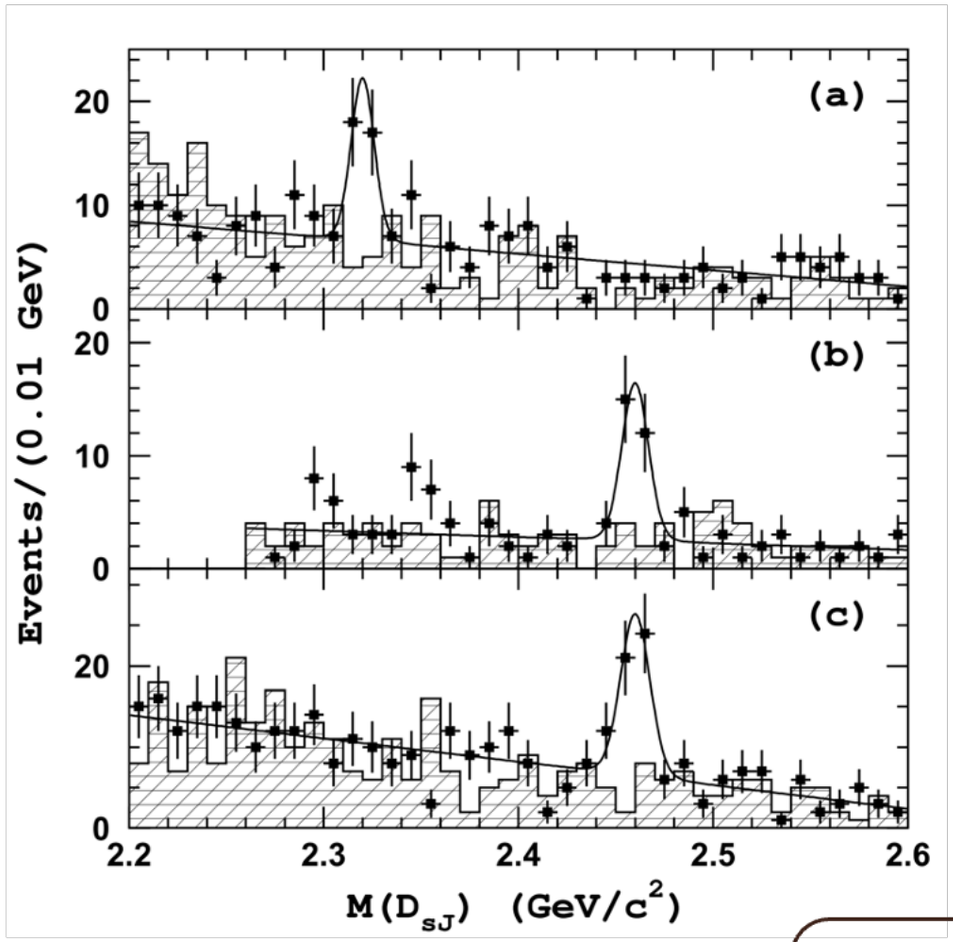


$DD^*K$系统两两之间形成束缚态(共振态)的实验证明。

2022年，LHCb上发现$T_{cc}^+$[1]，其阈值十分接近$DD^*$，作为$DD^*$强子分子态理论分析已经取得一系列成果。

2003年，Belle上发现$D_{s0}^*(2317), D_{s1}(2460)$.[2]其质量差十分接近$D, D^*$质量差，基于$DK, D^*K$强子分子态分析得到LQCD计算结果[3]的支持。


[1]R. Aaij et al.(LHCb), Nature Phys. 18, 751(2022). [2]P. Krokovny et al.(Belle), Phys. Rev. Lett. 91, 262002 (2003).
[3]L. Liu et al., Phys. Rev. D 87, 014508 (2013).

# Three-body system on the lattice in 2024

- The observation of $T_{cc}^{+}, D_{s0}^{*}(2317), D_{s1}(2460)$ in experiment

  - $DD^*$ interaction: LO+OPE

Du et al, PRD105(2022)014024


  - $DK$ interaction: LO+NLO

Guo et al, EPJA40(2009)171


  - $D^*K$ interaction: LO+NLO


  - Single particle regulator is used to obtain a better ren. Group invariant

Lu et al, arXiv:2308.14559

# Three-body system on the lattice in 2024

## Two-body parameters

$T_{cc}^{+} \Rightarrow v_0$

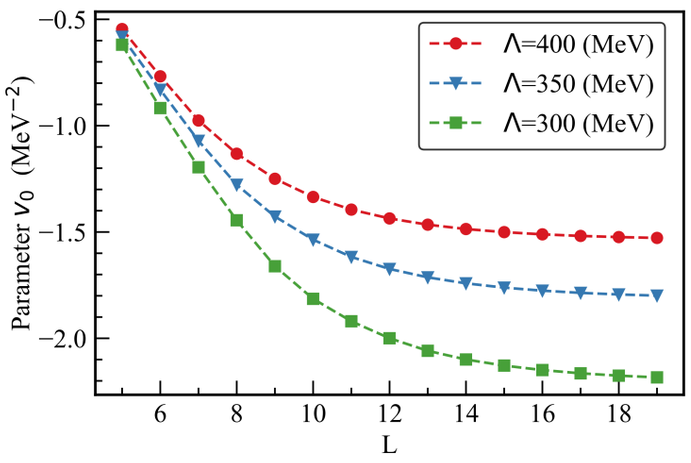


$D_{s0}^{*}(2317) \Rightarrow h_3$

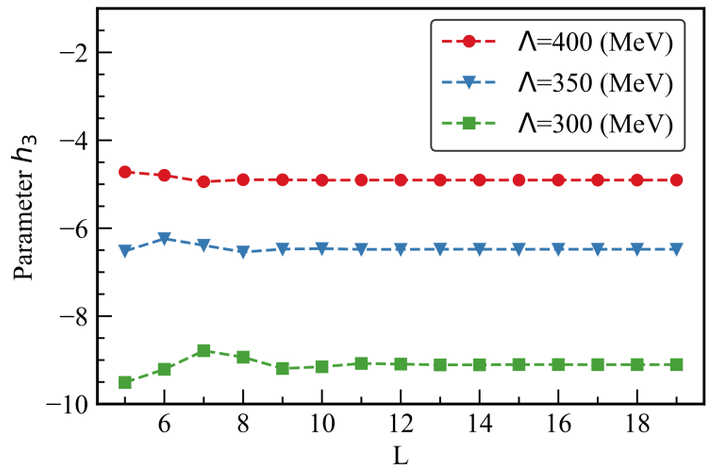


$D_{s1}(2460) \Rightarrow h_3^{*}$

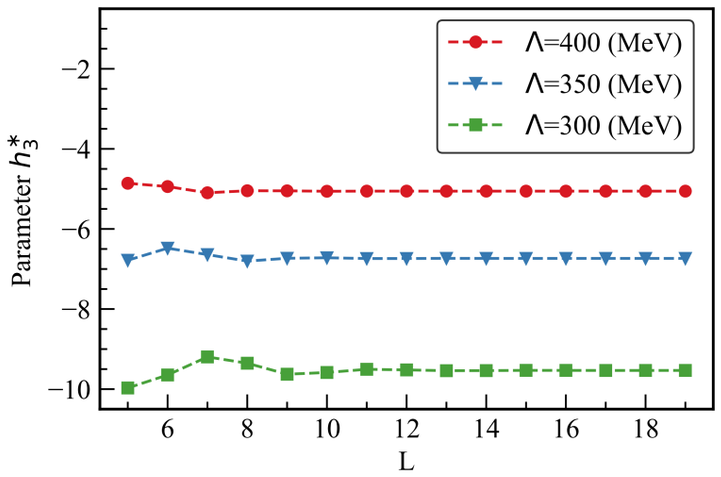


- Cubic lattice $L^3 = 5^3 \cdots 19^3$
- Cutoff $\Lambda = 300,\ 350,\ 400$ MeV in the regulator
- Lattice spacing $a = 1/200$ MeV $\sim 0.99$ fm
- $v_0$ converges slow $\Leftarrow$ long-ranged force+shallow bound state
- $\Lambda = 400$ MeV converges quickly

Zhang et al., Phys.Rev.D111(2025)036002

# Three-body system on the lattice in 2024

Three-body interaction

- $DD^*K$ Lag. $\mathscr{L} = c_3 \left\langle H\mathscr{D}_\mu H^\dagger H\mathscr{D}^\mu H^\dagger \right\rangle + c_3' \left\langle H\mathscr{A}_\mu H^\dagger H\mathscr{A}^\mu H^\dagger \right\rangle$

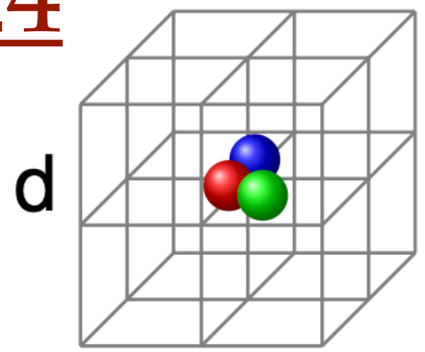


From Serdar's talk

- $DD^*K$ three-body force

$$V_{DD^*K}(p_i) = \frac{c_3}{4f_\pi^2}\left(p_1\cdot p_3 + p_1\cdot p_3' + p_2\cdot p_3 + p_2\cdot p_3' + p_1'\cdot p_3 + p_1'\cdot p_3' + p_2'\cdot p_3 + p_2'\cdot p_3'\right)\boldsymbol{\epsilon}\cdot\boldsymbol{\epsilon}^*$$

- $DD^*K$ binding energy

Zhang et al., Phys.Rev.D111(2025)036002

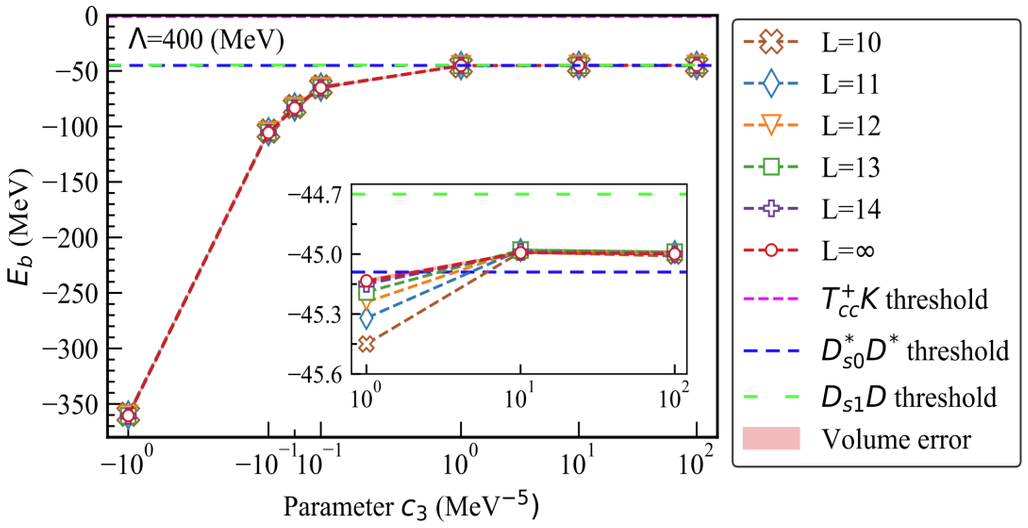


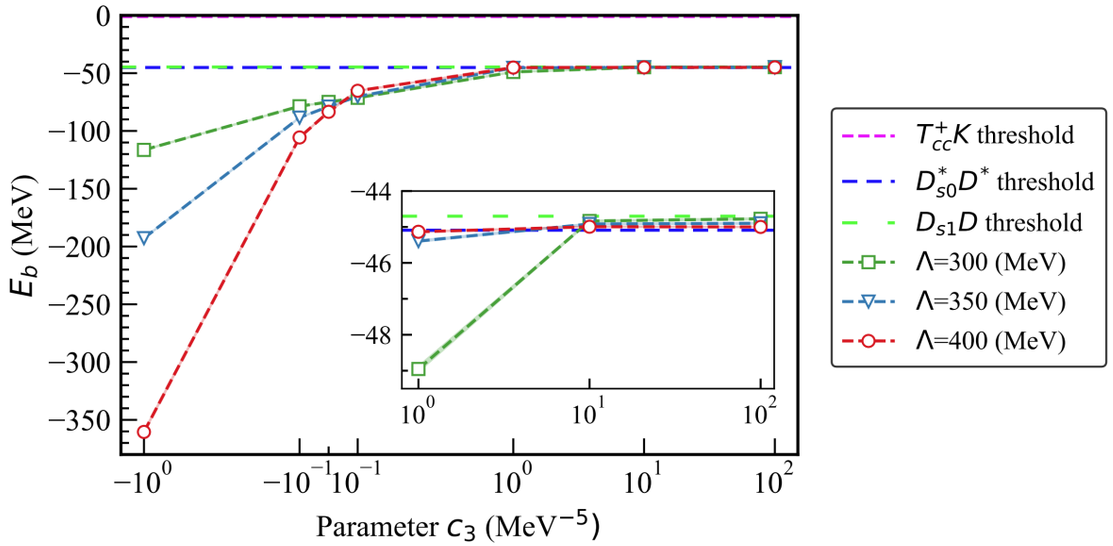


- Extrapolate to infinite volume

Meng et al., PRD98(2018)014508

$$\frac{\Delta E}{E_T} = -(\kappa L)^{-3/2}\sum_{i=1}^{3} C_i \exp\left(-\mu_i \kappa L\right)$$

- Switch off three-body force, the result is consistent with that in

Ma et al., CPC43(2019)014102

# Three-body system on the lattice in 2024

The first excited states

- No experimental data ⇒ binding energy with $\Lambda = 400$ MeV as input
- The parameter $c_3$ at various cubic

| $\Lambda$ (MeV) | Parameter | $L$ | | | | | | State |
|---|---|---|---|---|---|---|---|---|
| | | 9 | 10 | 11 | 12 | 13 | 14 | |
| 400 | $c_3$ (MeV$^{-5}$) | 0.100 | 0.100 | 0.100 | 0.100 | 0.100 | 0.100 | Input |
| 350 | | 0.170 | 0.162 | 0.164 | 0.164 | 0.163 | 0.163 | Fitted |
| 300 | | 0.328 | 0.305 | 0.281 | 0.278 | 0.281 | 0.280 | Fitted |

Zhang et al., Phys.Rev.D111(2025)036002

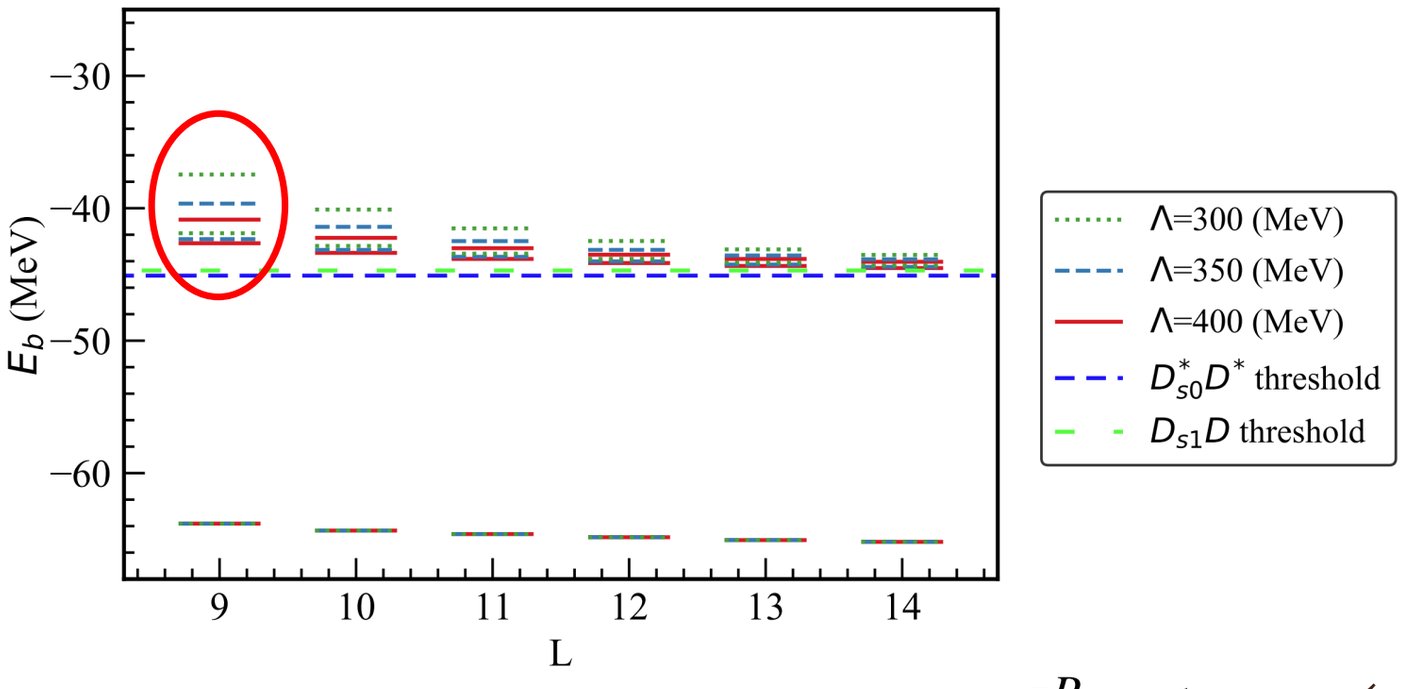


- $J^P = 1^-$ ⇐

- $E^{\text{excited}}_{\Lambda_1} - E^{\text{excited}}_{\Lambda_2}$ decreases
- $\rho$-type and $\lambda$-type excitation
- The standard angular momentum and parity projection technique is used

$$\left|\Psi_A\right\rangle = \frac{d_n}{24} \sum_{i=1}^{24} \chi_n\left(\Omega_i\right) R\left(\Omega_i\right) \left|\Psi_0\right\rangle$$

Lu et al., PRD90(2014)034507

# Three-body system on the lattice in 2024

$$\frac{\Delta E}{E_T} = -(\kappa L)^{-3/2} \sum_{i=1}^{3} C_i \exp\left(-\mu_i \kappa L\right)$$

Does this extrapolation formula also work for long-rang interaction?

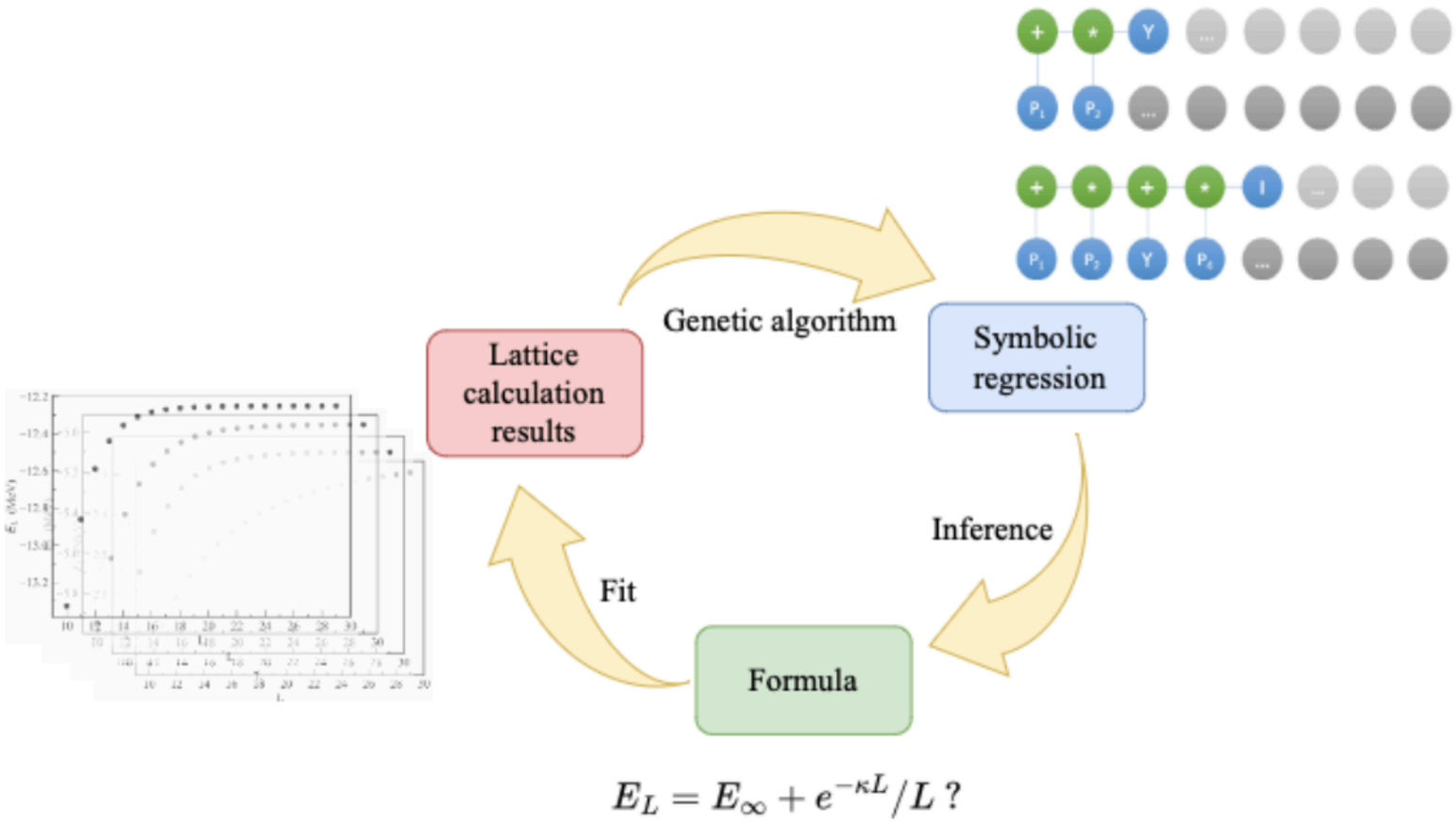


$$E_L = E_\infty + e^{-\kappa L}/L\,?$$

# Three-body system on the lattice in 2024

## 产生样本数据

- 短程相互作用 (两全同粒子 $m = 1969\text{MeV}$)

$$H = \sum_{i=1}^{2} \frac{\boldsymbol{p}_i^{\,2}}{2m_i} + f(\boldsymbol{p_1}, \boldsymbol{p_2})V(p)$$

$$f(\boldsymbol{p_1}, \boldsymbol{p_2}) = \prod_{i=1}^{2} g_\Lambda(\boldsymbol{p_i}) g_\Lambda(\boldsymbol{p_i'}) \qquad V(\boldsymbol{r}) = -C_0 \delta^3(\boldsymbol{r})$$

$g_\Lambda(\boldsymbol{p}) = \exp(-\boldsymbol{p}^6/2\Lambda^6)$

单粒子正规化　　接触项

- 长程相互作用(两全同粒子 $m = 1969\text{MeV}$)

$$V(\boldsymbol{r}) = -C_{01}\delta^3(\boldsymbol{r}) - C_{02}\frac{e^{-\mu r}}{r} \qquad C_{01} = C_{02}$$

$$f(\boldsymbol{p_1}, \boldsymbol{p_2}) = \prod_{i=1}^{2} g_\Lambda(\boldsymbol{p_i}) g_\Lambda(\boldsymbol{p_i'}) \quad \bar{f}(\boldsymbol{q}) = exp(-(\boldsymbol{q}^2 + \mu^2)/\Lambda^2)$$

单粒子正规化　　力程参数 $\mu = 20\text{MeV}$

# Three-body system on the lattice in 2024

## 符号回归

- PySR 模型对符号表达式(运算符、输入变量和常量项的符号)的空间进行采样
- 使用Loss和Score两个指标评估演化结果

$$\text{Loss} = \sum_{i=1}^{N} (E_{\text{PySR}}(L_i) - E_L(L_i))^2/N \qquad \text{Score} = -\frac{\Delta \ln(\text{Loss})}{\Delta C}$$

Loss即均方差函数，描述表达式与数据的符合程度，Score描述Loss与公式复杂程度的偏导。

| Times | Complexity | Loss | Score | Equation |
|---|---|---|---|---|
| 1 | 1 | 5.818 | 0.000 | $L$ |
| 2 | 2 | 0.014 | 6.016 | $-2.312$ |
| 3 | 4 | 0.010 | 0.180 | $L - 2.410$ |
| 4 | 5 | 0.007 | 0.396 | $-2.549\exp(L)$ |
| 5 | 6 | 0.005 | 0.220 | $-3.144\exp(\sqrt{L})$ |
| 6 | 7 | 0.003 | 0.653 | $(-0.028/L) - 1.992$ |
| 7 | 8 | 0.003 | 0.000 | $(-0.028/L) - 1.992$ |
| 8 | 9 | 0.001 | 0.682 | $-0.001/L^2 - 2.148$ |
| 9 | 10 | $3.679 \times 10^{-4}$ | 1.341 | $(\sqrt{L} - 0.171)/L - 3.696$ |
| 10 | 11 | $1.831 \times 10^{-6}$ | 5.302 | $-29.889\exp(-83.458L) - 2.245$ |
| 11 | 12 | $1.826 \times 10^{-6}$ | 0.003 | $-\exp(-83.388L + 3.393) - 2.245$ |
| 12 | 13 | $6.333 \times 10^{-7}$ | 1.059 | $\mathbf{-0.629\exp(-66.049L)/L - 2.244}$ |
| 13 | 14 | $6.292 \times 10^{-7}$ | 0.006 | $-0.628\exp(-66.022L)/L - 2.244$ |

短程势情况下，PySR演化过程。

# The power law of FV energy shift in 2025

## The result of short-range interaction

- Box size $10 \sim 30$ fm

$$E_L = C_1 + C_2 e^{-C_3 L}/L^2 \quad \text{(A)}$$

$$E_L = C_1 + C_2 e^{-C_3 L}/L \quad \text{(B)}$$

$$E_L = C_1 + C_2 e^{-C_3 L} \quad \text{(C)}$$

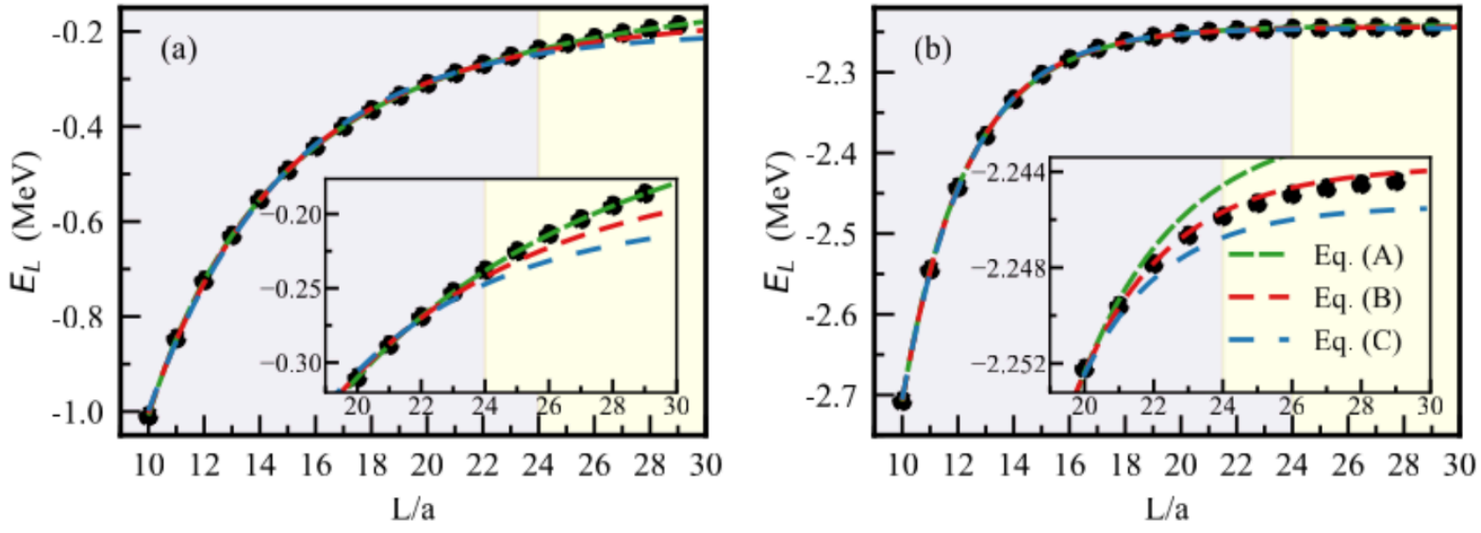


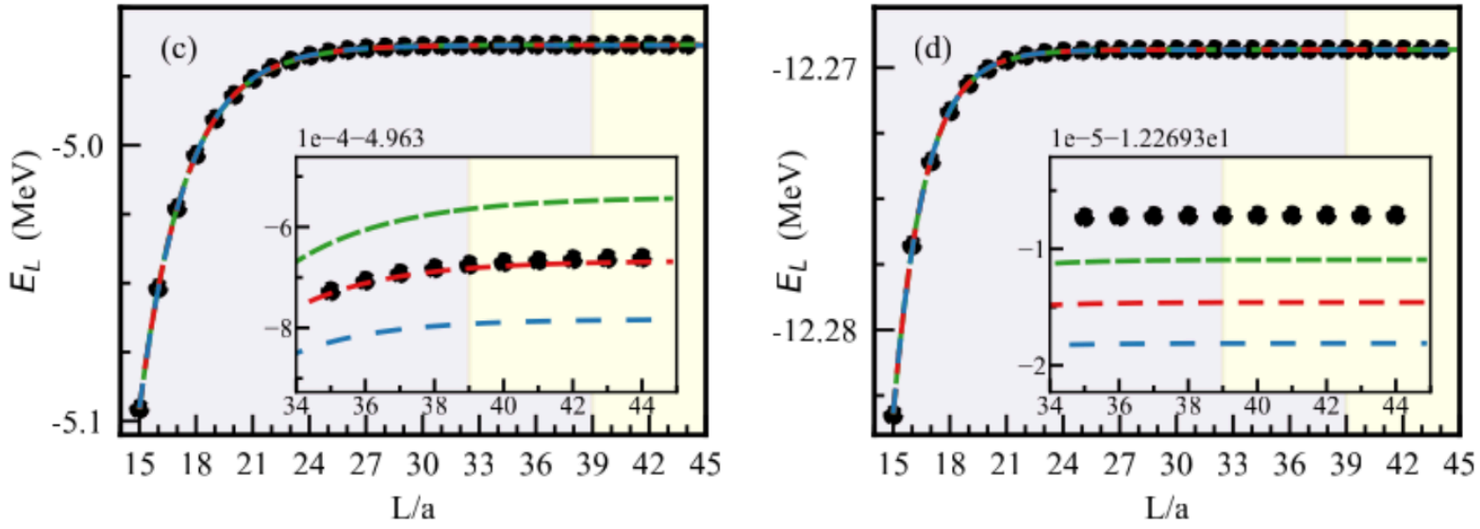


- The value of $C_3$ is exactly the binding momentum

- Recover the formula of short-range interaction successfully

# The power law of FV energy shift in 2025

## The result of long-range interaction

- Box size $10 \sim 30$ fm

$$E_L = C_1 + C_2 e^{-C_3 L}/L \quad \text{(A)}$$

$$E_L = C_1 + C_2 e^{-C_3 L} \quad \text{(B)}$$

$$E_L = C_1 + C_2 e^{-C_3 L} L \quad \text{(C)}$$

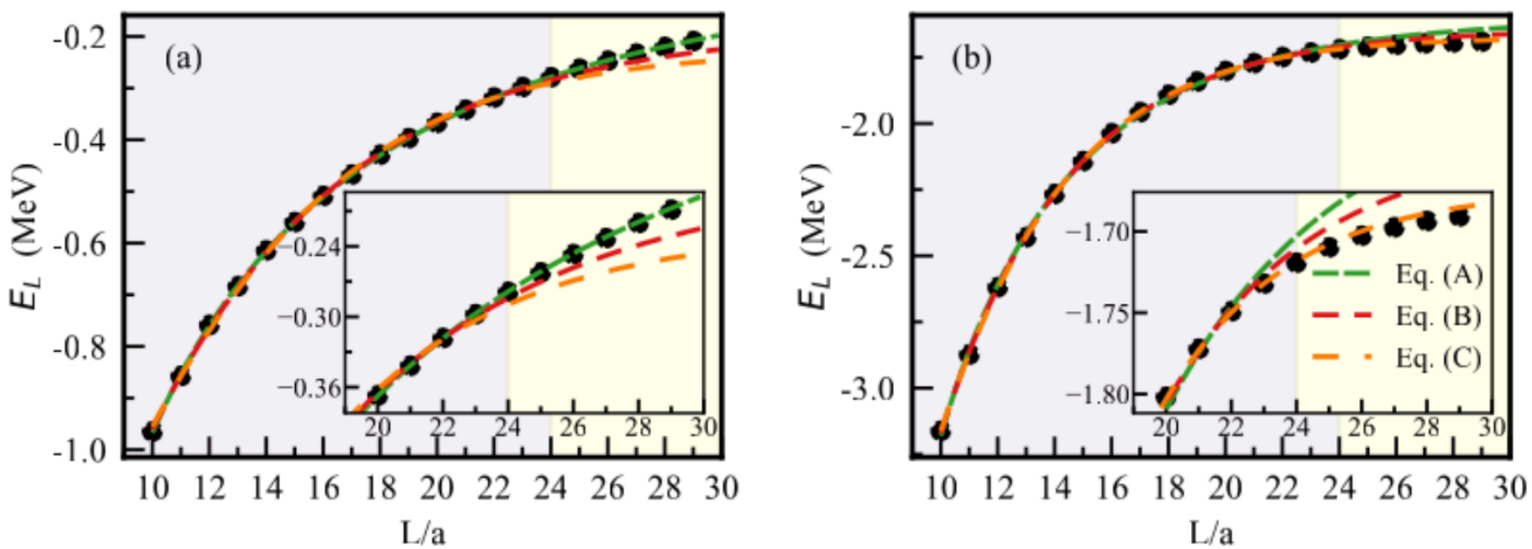


- The power of $L$ increases 2 for 10 fm range interaction

- The range parameter is set $\mu = 20$ MeV
- The power depends on the range of the force $E_L = C_1 + C_2 e^{-C_3 L} L^n$

# Three-body system

## 长程相互作用演化结果

- 格子体积10 ~ 30 fm
- 长程力力程从20逐渐减小到 0.25 fm

$$E_L = C_1 + C_2 e^{-C_3 L} L^n$$

- L的幂次n从2.5逐渐减少到 -1
- 力程从长程减小为短程后，再次重现Lüscher公式

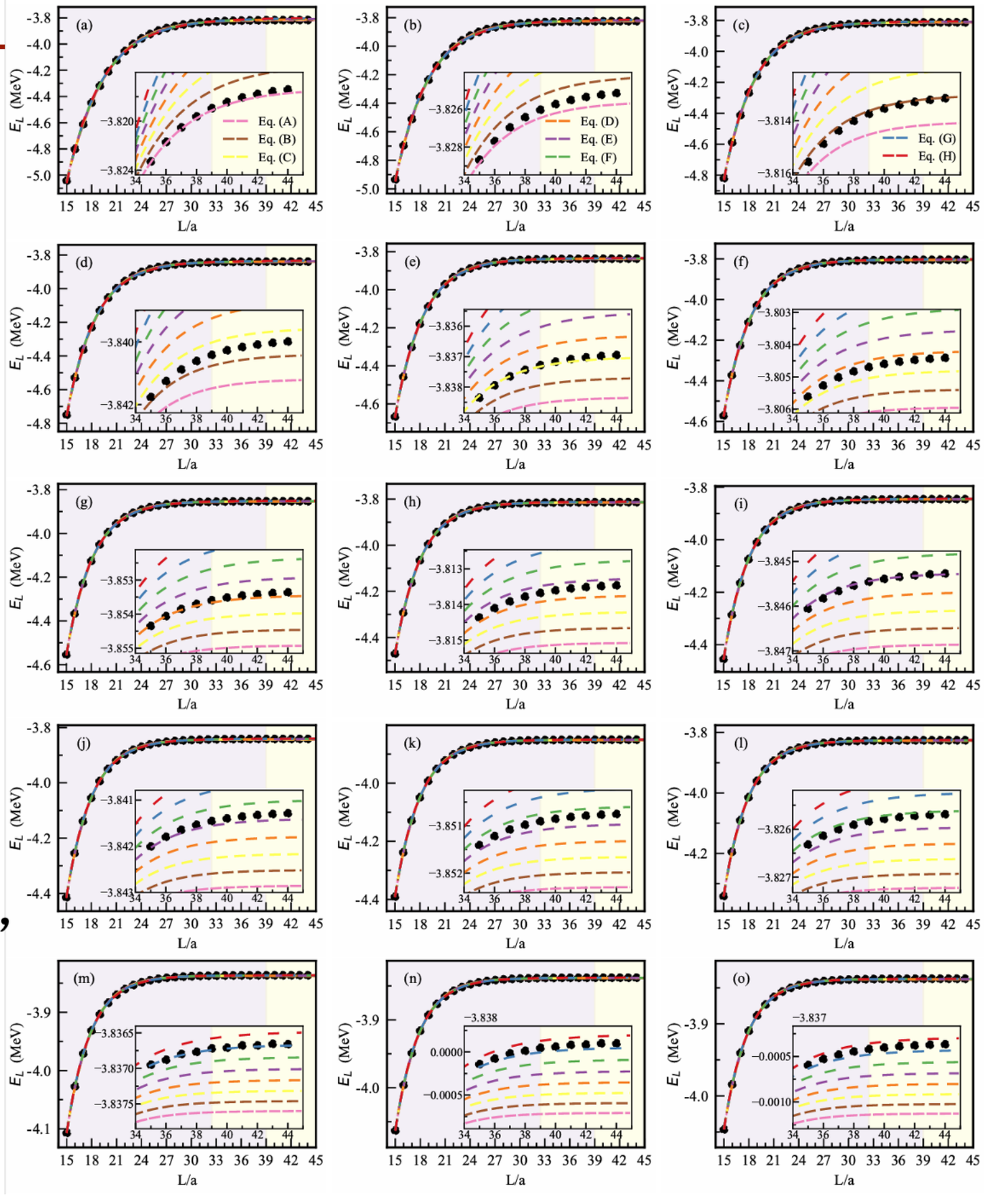

# The power law of FV energy shift in 2025

## The n and $C_3$ value

$\mu = 10, 20, \ldots, 120, 400, 600, 800\text{MeV}$

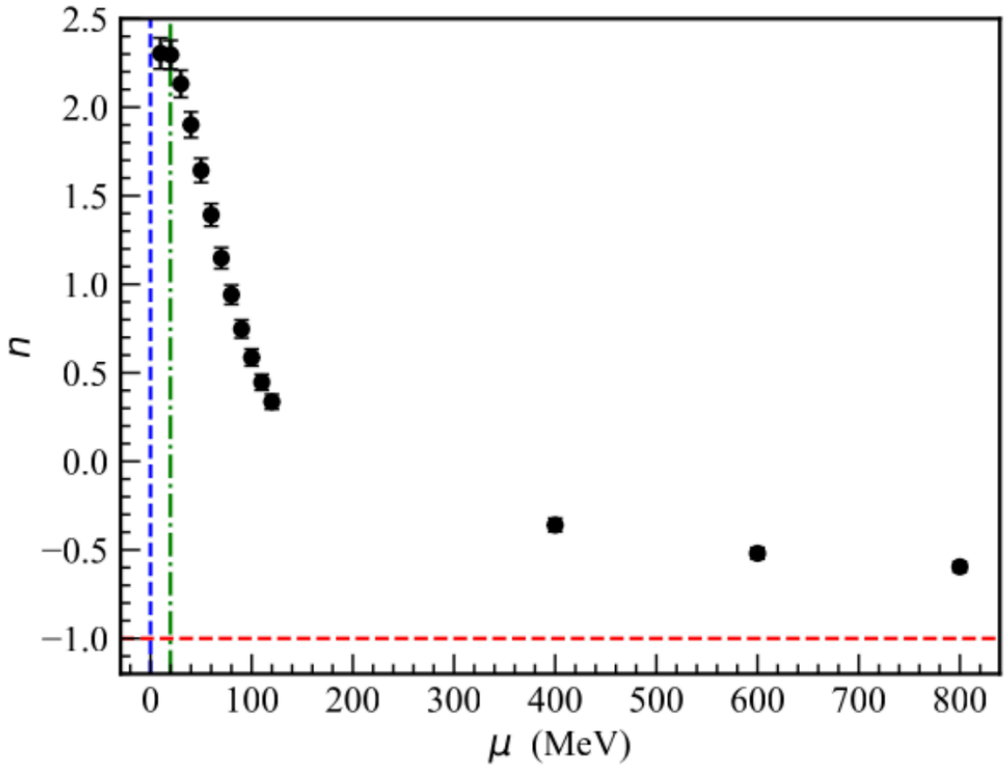


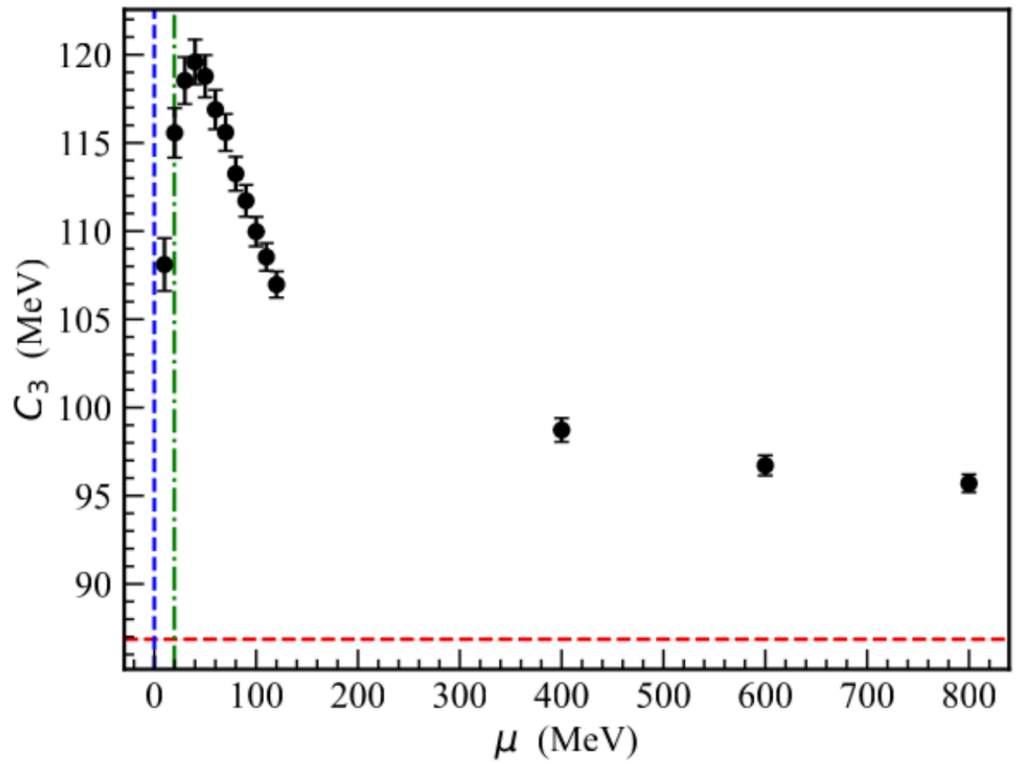


- $n = -1$ $\quad E_L = C_1 + C_2 e^{-C_3 L}/L$ $\quad$ - $\kappa_B$
- $\mu = 0$ $\quad$ - $\mu = 0$
- $\hbar c/10$ fm $\sim$ 20 MeV $\quad$ - $\hbar c/10$ fm $\sim$ 20 MeV

- The regressed formula recovers the short-range limit and indicates the long-range tendency

# The power law of FV energy shift in 2025

## The n and $C_3$ value

$\mu = 10, 20, \ldots, 120, 400, 600, 800$MeV

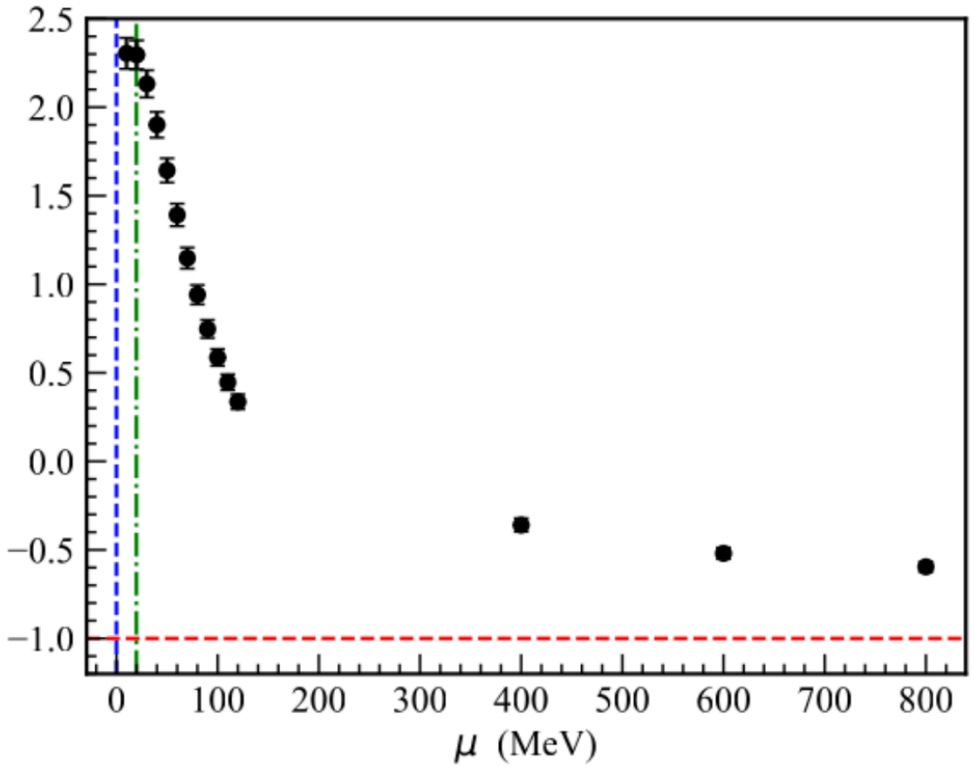


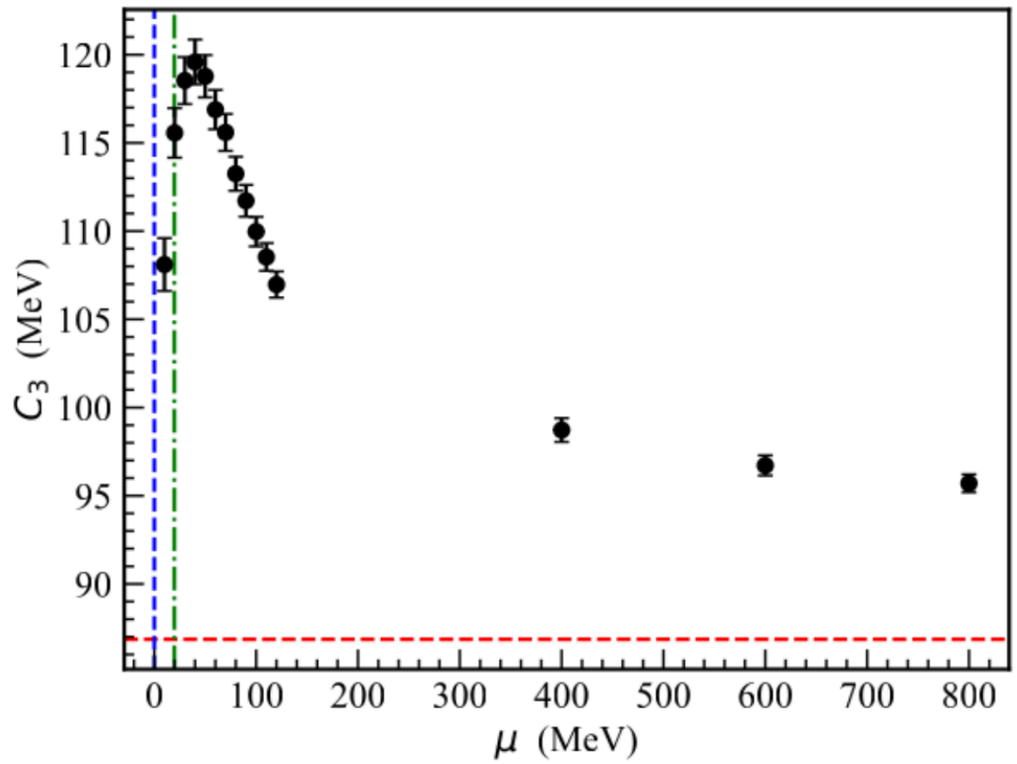


- $n = -1$ $\quad E_L = C_1 + C_2 e^{-C_3 L}/L$
- $\mu = 0$
- $\hbar c/10$ fm $\sim 20$ MeV

- $\kappa_B$
- $\mu = 0$
- $\hbar c/10$ fm $\sim 20$ MeV

The ML can extract unknown formula!

# Summary and outlook

2022 One-channel analysis

ML can do as good as normal fitting approach

2023 Multi-channel analysis ⇒ ML can extract more information

ML can extract more information than normal fitting approach

2025 Power law of FV energy shift ⇒ ML can extract unknown formula

Avoid model dependence.

XXXX ……

Thank you very much!